Energy sustainability and the water sector: systems modelling approaches for decision-making



Aman Majid

New College

University of Oxford

A thesis submitted for the degree of

Doctor of Philosophy

2021

‘‘Those clouds will come again,
but these rains will never be the same”

—*Nusrat Fateh Ali Khan*

Abstract

Water managers face enormous challenges in securing future supplies of water under the uncertainty of climate change and population growth. Energy sustainability is an increasingly important factor in the planning and management of water resources. Electricity use in the water and wastewater sectors has been growing at unprecedented rates. Left unchecked, this could compromise both the affordability and sustainability of the sector. At the same time, a number of promising options exist to the industry to enhance its energy efficiency and also reduce its reliance on the energy grid, though there are few analyses of the costs and risks associated with these opportunities at the moment. Water managers need reliable decision-making frameworks and tools to understand the complex interactions between water and energy systems. Such methodological advances will be important for the sustainable planning and development of the water industry.

The aim of this thesis is to introduce novel modelling techniques and frameworks that can capture the linkages between water and energy systems, for the purpose of facilitating transitions toward a more reliable, resilient, and energy sustainable water industry. Specifically, this thesis presents analytical approaches to: (1) understand the temporal evolution and drivers of electricity consumption in water-related systems; (2) model integrated water, wastewater, and energy networks; (3) model and study the costs, risks, and benefits of operational changes at high temporal resolution; and (4) map pathways to energy sustainability in the water sector under deeply uncertain futures.

The tools and frameworks developed in this thesis are applied to study the water system in the Thames basin, a region considered to be 'seriously water stressed'

and encompassing the mega-city of London. Results from the case-study demonstrate that water-related energy use has been rising sharply in the region (10.8% per year) and this is driven by expansions in operational capacity for larger populations, as well as local climate mitigation efforts. Yet, a number of opportunities to curtail rising energy costs are also available to the local utility. Results from this thesis demonstrate that participation in energy demand-response programmes has the potential to substantially lower energy costs by up to £5.2 million per year. Further, the utility can also expand on its energy self-generation capacity using a combination of biogas, solar, and wind generation, to decrease their reliance on the local energy system and realise net-zero carbon targets.

Keywords: water-energy nexus, water resources management, demand-side response, optimisation, systems analysis, systems modelling

Declaration of Funding

This doctoral research project was principally funded by the NERC-Oxford DTP programme (ref: DTP1 NE/L002612/1) and EDF Energy. I am extremely grateful for their financial support. Thanks are also due to Victoria Forth and Claudia Azevedo for coordinating the training programme and their continuous student support over the years. I also wish to thank Anes Dallagi from EDF Energy.

This research was also supported in part by the European Union's Horizon 2020 research and innovation programme under the Marie Skłodowska-Curie grant agreement No. 681228. This funding was used to support the collaboration between the University of Oxford and University of Auckland. Thank you to Dr Jean-François Auger for supporting this initiative.

Apportion of Credit

The research presented in this thesis was made possible thanks to the collaboration of a number of individuals. Below is a list of significant contributions:

- Dr Iliana Cardenes provided the data presented in Chapter 2.
- Dr Tony Downward assisted in the development of the software presented in Chapter 3.
- Professor Kobus van Zyl provided the hourly-resolution water demand data presented in Chapter 4.
- Dr Mohammad Mortazavi-Naeini helped create the WATHNET model used in Chapter 5.

List of Publications

This thesis is comprised of work that has been published in or submitted to the following peer-reviewed journals:

- **Majid, A.**, Mortazavi-Neini, M., and Hall. J.W. Efficient pathways to zero-carbon energy use by water supply utilities: an example from London, UK. *Environmental Research Letters*, 16(10), p.105010, DOI:10.1088/1748-9326/ac2931.
- **Majid, A.**, van Zyl, K., and Hall, J.W. Potential for demand-response in urban water systems: the influence of temporal variability and price tariffs. *Applied Energy*, 305, p.117808, DOI:10.1016/j.apenergy.2021.117808.
- **Majid, A.**, Downward, T., and Hall. J.W. InfraSim: An open-source water, wastewater, and electricity simulation model, with application to London, UK. *Submitted to Environmental Modeling & Software*.
- **Majid, A.**, Cardenes, I., Zorn, C., Russell, T., Colquhoun, K., Bañares-Alcantara, R., and Hall, J.W. (2020) An analysis of electricity consumption patterns in the water and wastewater sectors in South East England, UK. *Water*, 12(1), DOI:10.3390/w12010225.

Other publications that are partly related to the work in this thesis are:

- Cardenes, I., Hall, J.W., Eyre, N., **Majid, A.**, and Jarvis, S. (2020) Quantifying the energy consumption and greenhouse gas emissions of changing wastewater quality standards. *Water Science and Technology*, 2(1), DOI:10.2166/wst.2020.228.
- **Majid, A.** (2018) Simulating multi-sector systems using the multi-commodity flow algorithm. Final Report, *IIASA Young Summer Scientist Programme*, Laxenburg, Austria.

Acknowledgements

I wish to thank my supervisor, Professor Jim Hall. I learned a huge amount under his tutelage. He opened doors to many new opportunities, provided invaluable academic advice, and helped me to ask better questions. I will be forever grateful for the opportunity to work with him. I also wish to thank my co-supervisor, Dr. Rene Bañares Alcántara, who was always on-hand for support—academic and personal—and also got me involved in teaching.

I also want to thank my friends and colleagues at the Environmental Change Institute, who were always at hand to develop ideas and fix computer code, but also made the office a fun and productive place to be.

Through my D.Phil. studies, I had the honour of spending a summer at the International Institute for Applied Systems Analysis (IIASA) in Austria. Colleagues there helped formulate many of the ideas in this thesis, and I am most grateful for the lifelong friendships I formed with my fellow YSSPs. I also visited the Department of Civil Engineering at the University of Auckland, and I owe a great intellectual debt to Dr Tony Downward, Professor Kobus van Zyl, and Professor Michael O'Sullivan there.

Outside of work, I met and made friends with some truly remarkable people at Oxford – too many to name individually. My time at the university was immeasurably better shared with all of them.

Finally and most significantly, I want to say *bohot shukriya* to my parents. Several years ago now, they made the life-changing decision to move to England, away from their family and friends, all so that my brother and I could get a better education. This degree and the opportunities that await were all made possible because of their sacrifices, and I am forever indebted to them for that.

Aman Majid

Newcastle upon Tyne, 2021

Contents

Acronyms **xv**

1 Introduction **1**
1.1 Aims and objectives 4
1.2 Thesis overview 4

References **8**

2 Understanding water-related energy use **12**
2.1 Introduction 13
2.2 Thames basin 15
2.3 Methodology 17
2.3.1 Electricity data 17
2.3.2 Time series analysis 18
2.3.3 Calculating energy-intensity 20
2.4 Results and Discussion 21
2.4.1 Temporal evolution of electricity use 21
2.4.2 Electricity use by function 25
2.4.3 System energy-intensity 28
2.5 Conclusions 31

References **34**

3 Integrated modelling of water-energy systems **38**
3.1 Introduction 39
3.1.1 Relationship of urban water systems with energy 39
3.1.2 Integrated water, wastewater, energy models 41
3.2 Multi-commodity flow 44
3.2.1 General formulation 45
3.3 Model application 47
3.3.1 System description: Thames basin 48
3.3.2 Model framework 50

3.3.2.1 Geospatial database . . . 50
3.3.2.2 Simulation model . . . 52
3.3.2.3 Nodal flow data . . . 52
3.3.2.4 Outputs . . . 53
3.3.2.5 Setup and requirements . . . 53
3.4 Examples and Benchmarks . . . 54
3.4.1 Model run . . . 54
3.4.2 Benchmarking . . . 54
3.4.3 Computational efficiency . . . 58
3.4.4 Future extensions and limitations . . . 59
3.5 Conclusions . . . 61

References **62**

4 Case-study: energy flexibility and water **68**
4.1 Introduction . . . 69
4.1.1 Demand-side response . . . 69
4.1.2 Flexible operations in the water sector . . . 70
4.1.3 Paper scope and contribution . . . 74
4.2 Mathematical framework . . . 75
4.2.1 Simulation model overview . . . 75
4.2.2 General formulation . . . 76
4.2.2.1 Objective function . . . 77
4.2.2.2 Pumping constraints . . . 77
4.2.2.3 Conservation constraints . . . 78
4.2.2.4 Impounding reservoir control . . . 79
4.2.2.5 Service reservoir control . . . 79
4.2.3 Sensitivity analysis . . . 80
4.2.4 Software carpentry . . . 81
4.3 Case-study: Thames basin, England . . . 81
4.3.1 System description . . . 81
4.3.2 Electricity prices . . . 84
4.3.3 Water demands . . . 85
4.3.4 Scenarios tested . . . 86
4.3.5 Computing flexibility . . . 87
4.3.6 Model computational requirements . . . 87
4.4 Results and Discussion . . . 88
4.4.1 Optimal pumping schedules . . . 88
4.4.2 Temporal analysis of flexibility . . . 91
4.4.3 Global sensitivity analysis . . . 93
4.4.4 Relating water storage and flexibility . . . 96
4.4.5 Future extensions . . . 98
4.5 Conclusions . . . 100

References **102**

5 Case-study: long-term planning **109**
5.1 Introduction . . . 110
5.2 Case-study . . . 112
5.2.1 Study Area . . . 112
5.3 Methods . . . 115
5.3.1 Scenario generation . . . 117
5.3.2 Simulation model . . . 119
5.3.3 Decision module . . . 121
5.3.4 Experiments conducted . . . 122
5.3.5 Post-optimisation analysis . . . 123
5.4 Results . . . 124
5.4.1 Trade-off between water security, cost, and energy sustainability . . . 124
5.4.2 Post-optimisation analysis . . . 127
5.5 Discussion . . . 129

References **133**

6 Conclusions **143**
6.1 Thesis summary . . . 143
6.2 Conclusions . . . 145
6.3 Practical recommendations . . . 147
6.4 Directions for future work . . . 147

References **150**

A Additional materials for Chapter 2 **153**
A.1 Cost-benefit analysis of leakage reduction . . . 153

B Additional materials for Chapter 5 **154**
B.1 weather@home scenarios . . . 154
B.2 Water demands . . . 154
B.3 Simulation model setup . . . 155
B.3.1 Network linear programme . . . 155
B.3.2 WATHNET Model . . . 157
B.3.3 Renewable energy modelling . . . 159
B.4 Decision module setup . . . 161
B.4.1 Objectives . . . 161
B.4.2 ϵ–MOEA Setup . . . 163
B.5 Results . . . 164
B.5.1 Computing true Pareto frontier . . . 164
B.5.2 Non-dominated solution sets . . . 165

References **167**

Glossary **169**

List of Figures

1.1 A road map showing the contents and flow of this thesis. Dashed boxes show indicate research and results chapters that are based on papers. 5

2.1 Schematic representation of the water supply chain (blue rectangles) and the most energy consumptive processes in each step (white rectangles). Adapted from Rothausen et al. (2011). 14

2.2 Map of the Thames Water Utilities Ltd. area showing the water supply catchments (black boundaries) and the wastewater resource zone (dotted black line). Elevation is shown in the background. 18

2.3 Stacked area chart of electricity consumption (GWh) between 2009 and 2014 categorised by functional units. 22

2.4 Decomposition of electricity consumption (GWh) metrics. The panel plot shows (a) observed time series f, (b) trend α, (c) seasonal phase β, and (d) random component γ. 24

2.5 Derived trend components (α) for each functional category: water networks, water treatment, wastewater networks, and wastewater treatment. Shown as relative change (%) using the first term in the time series as the base value. 27

2.6 Water-related energy use (kWh per person per day) against water use (L per person per day) in the TWUL system in 2012, compared against other regions in the world (grey). The dotted lines are plotted for reference and indicate 0.5–2.0 kWh/m^3 energy intensities. This figure has been adapted from Lam et al. (2017) and reproduced with permission. 29

2.7 Curve expressing the relationship between capital cost (£ millions), leakage reductions (MLD, and reductions in operational expenditures due to electricity consumption (£ 1000s per day) for the Thames Water Utilities Ltd. system. The dashed red lines show the company's leakage reduction targets to 2020 (Hall et al. 2019) . 30

3.1 Influences and interdependencies represented in InfraSim 40

3.2 Map of the Thames basin in Southern England with a schematic representation of the regional water, wastewater, and energy system as modelled in InfraSim.Thames. 47

3.3 A schematic showing the methodological framework of InfraSim. 49

3.4 Sample Python code used to run the InfraSim.Thames model. 55

3.5 Simulated reservoir storage volumes from InfraSim.Thames compared with previously published data (Mortazavi-Naeini et al. 2019). Shown also are calculated values for the coefficient of determination ($R^2 = 0.95$) and the Nash-Sutcliffe coefficient (NSC $= 0.90$). 56

3.6 Panel plots showing annual (a) electricity production from the water and wastewater utilities in the Thames system, (b) energy demand for water and wastewater processes, and (c) energy demand for water-related services at the consumer level. All energy use statistics are given in GWh. 57

3.7 Linear regression between the total number of constraints and decision variables in the InfraSim.Thames model and the time (seconds) taken for the solver to converge to a solution. The results presented here were derived using a laptop PC with an Quad-Core i5 processor at 2 GHz and 16 GB of memory. 58

4.1 An illustration of a typical urban water supply system. The direction of flow is from left to right. 71

4.2 Thames basin storage reservoir control curve (Thames Water 2014). 79

4.3 Schematic of a simplified network model of the water supply system in the River Thames basin in South East England. 82

4.4 Electricity price and water demand data. Panel plots (a) and (c) show time series of prices and demands, respectively. Panel plots (b) and (d) show hourly medians of the price and water demands, where the shaded area shows the minimum and maximum observation for each hour. 83

4.5 A two-day sample of hydraulic behaviour in a system operating under the risk-neutral (RN) reservoir control strategy. The panel plots show: (a) the water demand, (b) RTP and TOU prices, (c) operational storage volume under the RTP and TOU prices, and (d) pumping rates under RTP and TOU prices. In plots b–d, RTP and TOU prices are shown in red and blue, respectively. 88

4.6 Median load shifted per month under each scenario. Shaded regions represent the 75% confidence interval. 91

4.7 Results from the global sensitivity analysis showing (a) the distribution of annual flexibility under the time-of-use and real-time price tariffs relative to the baseline scenario and (b) the relative influence (%) on the flexibility from the four parameters listed. 94

4.8 Relationship between reservoir capacity and load shifted, where (a) shows the cumulative distribution function (CDF) of $\mathbf{F}^* = \mathbf{F}/V$. and (b) a linear regression between the two parameters under the RN and RA scenarios. 96

5.1 Map of the Thames basin in south England. The nodes show major water storage reservoirs and options in blue and red, respectively. Red arrows indicate proposed water transfer schemes by means of new pipelines and inter-basin transfers. . . . 113

5.2 Illustration of the three-part integrated water-energy modelling framework. In the first part, stakeholders define future scenarios in the climate and local water system, as well as infrastructure alternative options. Next, a water-energy model exhaustively simulates various option combinations under the scenario set, where spatio-temporal dynamics of energy are tracked. Finally, a risk profile is derived for stakeholders to assess potential pathways to achieve their targets. 116

5.3 Schematic representation of the simulation model representing the energy prosuming water utility. The box and arrows shown in grey represent the processes not captured by our model. 120

5.4 Pareto frontiers (PFs) fitted onto the non-dominated solutions derived under the NF climate scenario for the IMP, BAL, and PRO energy strategies. Dashed lines are linearly interpolated curves representing the marginal cost of increasing self-generation capacity between 0–100%. 125

5.5 Non-dominated Pareto optimal solutions derived from the BL-BAL and NF-BAL experiments. The highlighted points (A–F) show the six investment plans chosen for post-optimisation analysis. 126

5.6 Composition of investment plans A–F showing the capacities of water (options 1–10 in ML) and energy (options 11–13 in MW) infrastructure implemented. . . . 128

5.7 Parallel coordinates plot showing results from the simulation of plans (a) A–C under the NF climate scenarios and (b) D–F under the BL climate scenarios. Light grey lines show results simulation results for each plan under each scenarios Ω, whereas the coloured lines show mean values computed over all scenarios. 129

B.1 Flow duration curves from the baseline and near-future scenarios. 155

B.2 Intra-annual demand curve (Thames Water 2014). 156

B.3 Schematic of the TWUL model (TWmod) as modelled within the WATHNET. The black boundaries show the spatial domain of TWUL's water resource zones. TWmod aggregates operations within the TWUL system by water resource zones. 158

B.4 Lower Thames reservoir storage control curve (Thames Water 2014). 162

B.5 Non-dominated Pareto optimal solutions (blue) along with the complete dominated solution set (grey) for all six experiments: BL-IMP, BL-BAL, BL-PRO, NF-IMP, NF-BAL, and NF-PRO. 166

Acronyms

ϵ–MOEA ϵ dominance multi-objective optimisation. x, 121, 122, 163, 164

BAL Balanced energy strategy. xiv, 122–128, 165, 166

BAS Baseline scenario. 84, 86, 87, 89, 90

BL Baseline. xiv, 117, 118, 122, 123, 125–127, 129, 163, 165, 166

CSO Combined sewer overflows. 26

DSR Demand-side response. 6, 69–76, 90, 92, 93, 95, 97–101, 131, 144, 148

E&W England and Wales. 13–15, 17

FiT Feed-in-tariff. 118, 121

IMP Importer energy strategy. xiv, 121–125, 165, 166

LP Linear programming. 76, 77, 81

MLD Megalitres per day. xii, 25, 26, 30, 31

MORDM Multi-objective robust decision making. 115, 116, 144

NF Near-future. xiv, 117, 118, 122–127, 129, 163, 165, 166

PF Pareto frontier. xiv, 124–126

PRO Prosumer energy strategy. xiv, 122–125, 165, 166

RA Risk averse. xiii, 86, 87, 89–92, 96, 97

RCP Representative concentration pathway. 117

RES Renewable energy system. 110, 111, 122–125, 130, 131, 148

RN Risk neutral. xiii, 86–90, 92, 96, 97

RTP Real-time electricity price tariffs. xiii, 73, 74, 85, 86, 88–90, 92, 93, 99

STL Seasonal and Trend decomposition method using Loess. 19

SWA Slough, Wycombe, and Aylesbury. 17, 26

SWOX Swindon and Oxford. 17, 26, 28, 119

TOU Time-of-use electricity price tariffs. xiii, 72–74, 84–86, 88–90, 92, 93, 99

TWUL Thames Water Utilities Ltd.. xii, xiv, 6, 13–17, 21, 23–26, 28–32, 51, 112–115, 118–122, 143–145, 148, 153, 154, 157–161

W&WW water and wastewater. 1–4, 13–15, 38–41, 43, 48, 143, 144, 146–149

WRZ Water resource zone. 16, 17, 119

Chapter 1

Introduction

Water and wastewater infrastructure sustain some of civilisation's most basic needs. This industry, known as the water and wastewater (W&WW) sector, is responsible for round the clock supplies of clean water, as well as the handling and treatment of post-use wastewater effluents. Substantial amounts of electricity is required to drive operations throughout these complex infrastructure networks. For instance, estimates from England and Wales suggest around 2–5% of a region's energy demand is attributed to W&WW operations (Rothausen et al. 2011). Moreover, energy consumption within the sector is both the primary source of greenhouse gas emissions from the industry and comprises the dominant portion of the total operational costs for utilities (Escriva-Bou et al. 2018). As such, W&WW operations are inherently linked to energy (Kenway et al. 2011).

The modern W&WW sector faces a number of major challenges. Climate change will cause greater variability in natural water resources, especially that of public water supply, and also increase the frequency of events such as droughts (Environment Agency 2008; Vörösmarty et al. 2000). At the same time, rapid urbanisation and population growth are swiftly increasing water demands. Meanwhile, the sector must also reduce its impact on the environment. For instance, increasing stringency in wastewater treatment standards have significantly increased operational costs (Baleta et al. 2012; Cardenes et al. 2020).

Tackling such issues requires the continuously changing W&WW processes. Nowadays, the sector is increasingly adopting alternative technologies, particularly in water supply. For instance, the use of desalination and effluent reuse, which have historically been underutilised due to high costs, are becoming more prominent across the world (Elimelech et al. 2011). Such factors have led to a commensurate acceleration of electricity use in the W&WW industry. Water-related energy is becoming a growing concern across the world. Careful planning must be undertaken to ensure W&WW services remain both affordable and sustainable in the long-term.

Planning is an essential part of the W&WW sectors. Utilities regularly produce detailed plans of future interventions and management practices to ensure future demands for services are secured. Yet, water and wastewater systems have historically been managed and planned independently despite being highly interconnected systems. Separate institutions operate and study each respective system with little to no collaboration between one another, which has led to siloed thinking and operational practices (Farid et al. 2016). Furthermore, the interconnection of W&WW to energy remains poorly understood. These practices have developed systematic inefficiencies, where interventions in one area of the system yield problems in another (Konadu et al. 2015). It is now widely recognised that such approaches are no longer valid (Scanlon et al. 2017). Instead, these industries need to be viewed as interconnected systems-of-systems with cause-and-effect feedbacks (Hall et al. 2014).

The use of computer models and decision frameworks have long underpinned planning exercises (Loucks et al. 2017). More recently, integrated models and frameworks have come to accepted as essential methodologies for incorporating *systems-thinking* into water, wastewater, and energy systems (Liu et al. 2020). This modelling approach seeks to integrate interactions between two or more sectors and hence capture feedback loops. For example, Khan et al. (2018) modelled energy and water systems at the national level in Spain to devise cross-sector infrastructure planning strategies. This seminal work demonstrated that managing the two sectors together could yield substantial economic savings and avoid undue environmental im-

pacts (*e.g.* carbon emissions). Yet, integrated approaches remain very much in their infancy. Moreover, the vast majority of literature to date has focussed on understanding the influence of water-related process (*e.g.* hydrological variability) on the energy sector. Meanwhile, the link of W&WW systems to energy remains substantially understudied (Wu et al. 2020). There are few planning tools or models available to decision-makers in the W&WW sector that can aid their understanding of the energy-related challenges and opportunities in the context of change and uncertainty.

This thesis contributes to advancing this knowledge frontier. *How is electricity use in the W&WW sector evolving over time? What are the main risks and opportunities related to water-related energy? How can planning models be improved or developed to manage these risks and identify the potential of such opportunities? How can decision-makers navigate the trade-offs between water and energy in the context of deeply uncertain futures?* These are the sorts of questions this thesis seeks to address.

The work presented here builds upon recent innovations in integrated-modelling approaches (e.g. Hall et al. 2014; Ishimatsu 2013; Khan et al. 2018; Parkinson et al. 2018) to devise planning tools and frameworks that capture the interactions of W&WW processes to energy. The work presented here differs from the previous efforts in that it focuses at a utility-scale rather than national or global levels. To do so, this thesis advances techniques in utility-scale simulation modelling, which have been used in W&WW planning for decades (e.g. Kuczera 1992; Wurbs 1993). Finally, recent advances in multi-objective robust decision-making under uncertainty (e.g. Kasprzyk et al. 2013a; Kasprzyk et al. 2013b) are combined with integrated modelling approaches, which brings the context of deeply uncertain futures into the decision framework.

The tools and methods developed here are demonstrated on the W&WW system within the Thames basin in southern England. This was chosen as the focal area as the regional system is regarded as 'severely water stressed' and faces chronic pressures from climate and population change. Moreover, the local W&WW system is highly energy-intensive and regional decision-

makers are making concerted efforts to better understand its water-related energy risks and opportunities. Though the work presented here is stylised for the Thames system, the insights are applicable to other regions and the models and tools can be adopted elsewhere.

1.1 Aims and objectives

The purpose of this thesis is to provide new tools and frameworks to better capture interactions in energy-water systems planning at a regional scale, in particular from the perspective of W&WW utilities. The methodological advances developed here aim to provide policy insights and develop decisions that are cost-effective and sustainable. To achieve this aim, a modular approach was adopted to identify the following objectives:

(i) Understand water-related energy use in the Thames basin.

(ii) Advance current modelling techniques to incorporate *systems-thinking* into regional W&WW planning.

(iii) Demonstrate the developed models and tools across multiple temporal scales.

(iv) Progress our understanding of the trade-offs between W&WW service security and energy sustainability.

1.2 Thesis overview

The contents of this thesis can be divided into six main chapters, four of which are research and results chapters (Figure 1.1). The first chapter will introduce the Thames basin—the case-study region of this thesis. Here, the local water and wastewater system is introduced, as well

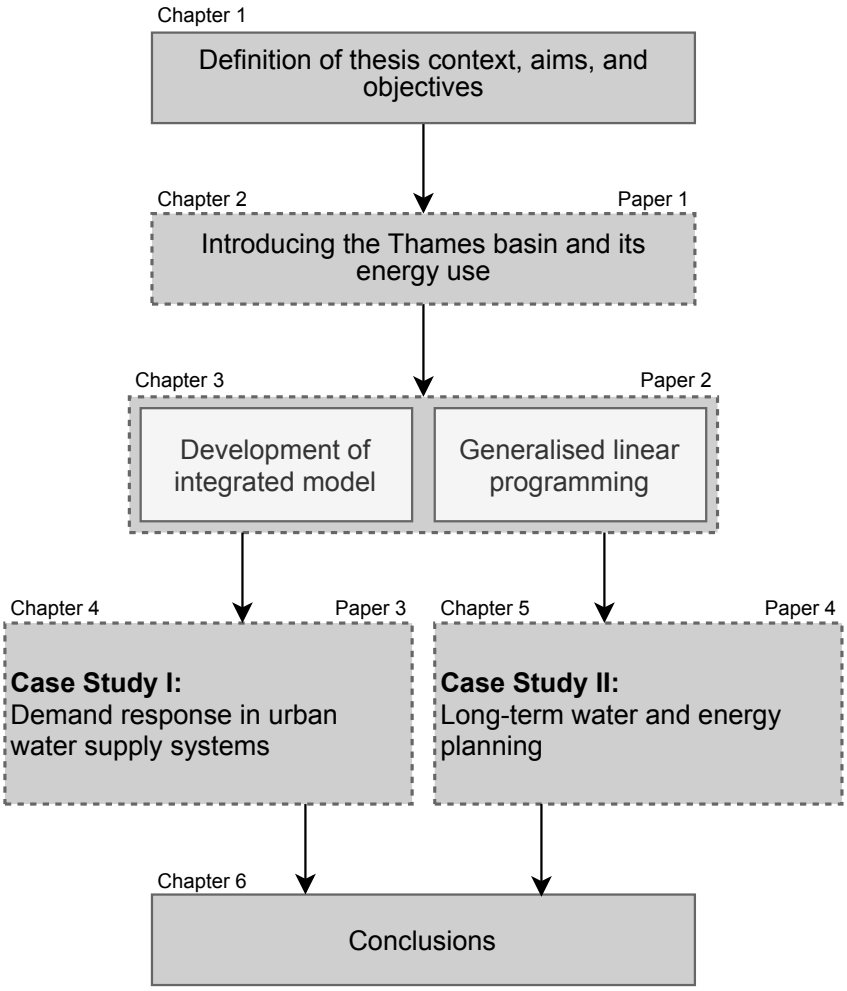


Figure 1.1: A road map showing the contents and flow of this thesis. Dashed boxes show indicate research and results chapters that are based on papers.

as a temporal analysis of its electricity use. This novel empirical study reveals that water-related energy is rising sharply in the Thames basin. Moreover, region water-related energy use is contextualised in the context of similarly developed OECD nations. The data and insights presented in this chapter inform the modelling work in subsequent chapters.

In Chapter 3, simulation models are firstly discussed as these are central to the decision methods developed in this thesis. Next, the InfraSim model is introduced, which is an open-source software that can be used to simulate water, wastewater, and electricity systems-of-systems to inform planning and management. InfraSim is used in later chapters. Chapter 3

shows that the model developed can simulate the TWUL system in a computationally efficient manner. Moreover, it is demonstrated that the model shows good agreement with previously reported data. It is argued that InfraSim is a valuable contribution to the field given that its free for academic purposes.

Chapter 4 applies InfraSim to study the potential for demand-side response (DSR) in the TWUL system. DSR is often touted as a significant opportunity for the water sector to lower its energy-related operational expenditures whilst alleviating peak-demand effects on the energy grid (Kirchem et al. 2020). Yet, there exist very few studies quantifying such benefits under the strict operational rules of water supply networks and temporal variability of water demands. This study aims to address this knowledge gap. Here, it is shown that up to 20.1% of TWUL's annual energy demand can be shifted to periods with relatively lower electricity prices, which could theoretically lower electricity costs by £5.6 million per annum. Yet, the demand shifting potential is shown to be highly variable and hence financial returns are volatile. In conducting this study at the hourly temporal resolution, InfraSim's capability at high temporal resolution is demonstrated.

The final research chapter adopts a long-term planning perspective. Here, pathways to realising TWUL's energy sustainability targets to 2030 are studied. A multi-objective framework is presented that facilitates decision-makers to navigate the trade-offs between cost, water security, and energy sustainability, under deep uncertainties in future conditions such as climate change and population growth. Chapter 5 demonstrates that achieving energy sustainability entails significant costs. However, balancing trade-offs can yield investment pathways that can minimise future water risks whilst managing overall electricity use using a combination of efficiency, self-generating via locally installed renewable energy, and purchasing green credits from the grid.

Finally, the thesis closes with a conclusions chapters where I discuss the main research, practical, and policy implications of the work conducted here. A glossary and list of acronyms is provided at the end of this document for the convenience reader. Each chapter in this thesis

is self-contained. As such, each chapter has its own references and mathematical notations are defined uniquely within. Note that the words energy and electricity are used interchangeably throughout this thesis. However, this is always referring to electricity (units: kWh) unless stated otherwise.

This thesis was produced following the paper route as outlined by the rules of the School of Geography and Environment at the University of Oxford. As such, Chapters 2–5 are based on papers that have been published in or submitted to peer-reviewed journals (Majid et al. 2020; Majid et al. 2021; Majid et al. 2022) (see list of publications in the front matter). These chapters are generally identical to the paper form, though minor changes have been made to improve cohesion between chapters.

References

Baleta, H., & Mcdonnell, R. (2012). Water quality standards or carbon reduction: Is there a balance? *Area*. https://doi.org/10.1111/j.1475-4762.2011.01066.x

Cardenes, I., Hall, J. W., Eyre, N., Majid, A., & Jarvis, S. (2020). Quantifying the energy consumption and greenhouse gas emissions of changing wastewater quality standards. *Water Science and Technology*, *2*, 1–10. https://doi.org/10.2166/wst.2020.228

Elimelech, M., & Phillip, W. A. (2011). The future of seawater desalination: Energy, technology, and the environment. *Science*, *333*(6043), 712–717. https://doi.org/10.1126/science.1200488

Environment Agency. (2008). *International comparisons of domestic per capita consumption* (tech. rep.).

Escriva-Bou, A., Lund, J. R., & Pulido-Velazquez, M. (2018). Saving Energy From Urban Water Demand Management. *Water Resources Research*, *54*(7), 4265–4276. https://doi.org/10.1029/2017WR021448

Farid, A. M., Lubega, W. N., & Hickman, W. W. (2016). Opportunities for energy-water nexus management in the Middle East & North Africa. *Elementa*, *4*, 1–17. https://doi.org/10.12952/journal.elementa.000134

Hall, J. W., Henriques, J. J., Hickford, A. J., Nicholls, R. J., Baruah, P., Birkin, M., Chaudry, M., Curtis, T. P., Eyre, N., Jones, C., Kilsby, C. G., Leathard, A., Lorenz, A., Malleson, N., McLeod, F., Powrie, W., Preston, J., Rai, N., Street, R., … Watson, J. W. (2014). Assess-

ing the long-term performance of cross-sectoral strategies for national infrastructure. *Journal of Infrastructure Systems*. https://doi.org/10.1061/(ASCE)IS.1943-555X.0000196

Ishimatsu, T. (2013). Generalized Multi-Commodity Network Flows: Case Studies in Space Logistics and Complex Infrastructure Systems. *Massachusetts Institute of Technology*, (2004).

Kasprzyk, J. R., Nataraj, S., Reed, P. M., & Lempert, R. J. (2013a). Many objective robust decision making for complex environmental systems undergoing change. *Environmental Modelling and Software*, *42*, 55–71. https://doi.org/10.1016/j.envsoft.2012.12.007

Kasprzyk, J. R., Nataraj, S., Reed, P. M., & Lempert, R. J. (2013b). Many objective robust decision making for complex environmental systems undergoing change. *Environmental Modelling & Software*, *42*, 55–71. https://doi.org/10.1016/J.ENVSOFT.2012.12.007

Kenway, S. J., Lant, P. A., Priestley, A., & Daniels, P. (2011). The connection between water and energy in cities: A review. https://doi.org/10.2166/wst.2011.070

Khan, Z., Linares, P., Rutten, M., Parkinson, S., Johnson, N., & García-gonzález, J. (2018). Spatial and temporal synchronization of water and energy systems : Towards a single integrated optimization model for long-term resource planning. *Applied Energy*, *210*, 499–517. https://doi.org/10.1016/j.apenergy.2017.05.003

Kirchem, D., Lynch, M., Bertsch, V., & Casey, E. (2020). Modelling demand response with process models and energy systems models: Potential applications for wastewater treatment within the energy-water nexus. *Applied Energy*, *260*(December 2019), 114321. https://doi.org/10.1016/j.apenergy.2019.114321

Konadu, D., Fenner, R., Richards, K., & Allwood, J. (2015). *UK water-energy nexus under climate change* (tech. rep.). wholeSEM. Cambridge.

Kuczera, G. (1992). Water supply headworks simulation using network linear programming. *Advances in Engineering Software*. https://doi.org/10.1016/0965-9978(92)90084-S

Liu, L., Lopez, E., Dueñas-Osorio, L., Stadler, L., Xie, Y., Alvarez, P. J., & Li, Q. (2020). The importance of system configuration for distributed direct potable water reuse. *Nature Sustainability*. https://doi.org/10.1038/s41893-020-0518-5

Loucks, D. P., van Beek, E., Stedinger, J. R., Dijkman, J. P., & Villars, M. T. (2017). *Water Resources Systems Planning and Management and Applications: An Introduction to Methods, Models and Applications* (Vol. 51). https://doi.org/92-3-103998-9

Majid, A., Cardenes, I., Zorn, C., Russell, T., Colquhoun, K., Bañares-Alcantara, R., & Hall, J. W. (2020). An Analysis of Electricity Consumption Patterns in the Water and Wastewater Sectors in South East England, UK. *Water*, *12*(1), 225. https://doi.org/10.3390/w12010225

Majid, A., Mortazavi-Naeini, M., & Hall, J. W. (2021). Efficient pathways to zero-carbon energy use by water supply utilities: an example from London, UK. *Environmental Research Letters*, *16*(10), 105010. https://doi.org/10.1088/1748-9326/ac2931

Majid, A., van Zyl, J. E., & Hall, J. W. (2022). The influence of temporal variability and reservoir management on demand-response in the water sector. *Applied Energy*, *305*. https://doi.org/10.1016/j.apenergy.2021.117808

Parkinson, S. C., Makowski, M., Krey, V., Sedraoui, K., Almasoud, A. H., & Djilali, N. (2018). A multi-criteria model analysis framework for assessing integrated water-energy system transformation pathways. *Applied Energy*, *210*, 477–486. https://doi.org/10.1016/j.apenergy.2016.12.142

Rothausen, S. G., & Conway, D. (2011). Greenhouse-gas emissions from energy use in the water sector. Nature Publishing Group. https://doi.org/10.1038/nclimate1147

Scanlon, B. R., Ruddell, B. L., Reed, P. M., Hook, R. I., Zheng, C., Tidwell, V. C., & Siebert, S. (2017). The food-energy-water nexus: Transforming science for society. https://doi.org/10.1002/2017WR020889

Vörösmarty, C. J., Green, P., Salisbury, J., & Lammers, R. B. (2000). Global water resources: Vulnerability from climate change and population growth. *Science*. https://doi.org/10.1126/science.289.5477.284

Wu, W., Maier, H. R., Dandy, G. C., Arora, M., & Castelletti, A. (2020). The changing nature of the water–energy nexus in urban water supply systems: a critical review of changes and responses. *Journal of Water and Climate Change*, 1–28. https://doi.org/10.2166/wcc.2020.276

Wurbs, R. A. (1993). Reservoir-system simulation and optimization models. *Journal of Water Resources Planning and Management, 119*(4), 455–472.

Chapter 2

Understanding water-related energy use

Abstract

Water and wastewater systems are known to be energy-intensive. Yet, there exist significant geographical variation in water-related energy use due to the inherent heterogeneity in infrastructure systems. There currently exist no analyses of water-related energy in the Thames basin and this poses a stumbling block to devising regional energy management policies. In this chapter, high-quality telemetry data of energy use by water and wastewater systems in the Thames basin are analysed. The analysis breaks down energy use into individual operations and presents a statistical approach for handling seasonal and random cycles in the data. Further, novel energy-intensity metrics (kWh/m^3) are derived and compared against water systems in other parts of the world, allowing us to gauge to energy-intensity of the TWUL system. Results showed that sectoral energy use grew sharply at around 10.8% per year in just five years. This was associated with the company's response to growing demands and increased storm water flooding. Energy-intensity for the utility's service zone was measured in a range between 0.46–0.92 kWh/m^3. Plans to improve the efficiency of the system could yield benefits in lower energy-intensity, but the overall energy saving would be temporary as external pressures from population and climate change drive water and energy use.

2.1 Introduction

Water and wastewater systems in the Thames basin can be highly energy-intensive. Driven by the rising cost of electricity, as well as the greenhouse gas footprint associated with energy use, the local utility (TWUL) has recognised energy as a significant cost that needs to be managed. As a result, TWUL is making concerted efforts to manage its energy use and hence lower its carbon impacts. Yet, despite a rapidly changing landscape of water-related energy in the TWUL system, there are currently no studies that have analysed the energy-intensiveness of this system. This chapter aims to address this knowledge gap.

W&WW systems play a central part of urban infrastructure networks. The sector is comprised of complex systems that are responsible for abstracting, storing, treating, and distributing water over, often over hundreds of kilometers. As shown in Figure 2.1, electricity is needed throughout this chain of operations. Since the characteristics of W&WW systems differ hugely between regions, based on the local water demands, climate, and geography, the amount of electricity needed in each function within the supply chain can be significantly different between regions (Perrone et al. 2011). However, these systems are usually very energy-intensive as they can consume up to 7% of a city's total energy use (Wakeel et al. 2016). A number of recent papers have focused on understanding the energy-influence of water at a regional level (e.g. Kenway et al. 2011). One of the main lessons from this body of literature is that such case-studies are fundamental to both understand local water-related energy, as well as design effective management strategies (Kenway et al. 2019).

Though data on the energy-intensiveness of the water and wastewater sector of England and Wales (E&W) is extremely scarce, it is known that the landscape of water-related energy is changing swiftly. The W&WW sector reportedly consumes around 2–5% of the national energy supply (Nair et al. 2014), making it the fourth most energy-intensive industry (Veolia 2019). Moreover, electricity use in the W&WW sector of E&W grew by over 10% in the 8 years between 2002 and 2010 (Watson et al. 2013). The drivers of this growth are not exactly

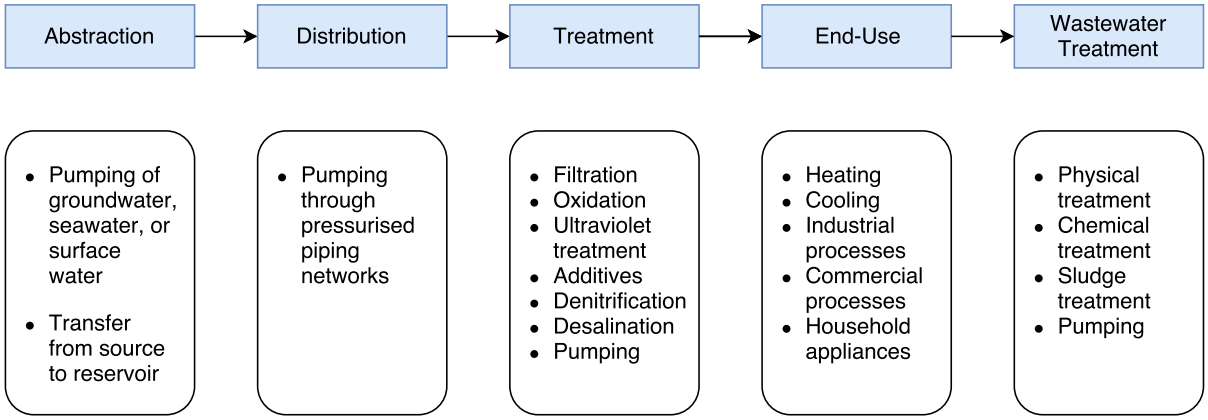


Figure 2.1: Schematic representation of the water supply chain (blue rectangles) and the most energy consumptive processes in each step (white rectangles). Adapted from Rothausen et al. (2011).

known but are likely attributed to changing water quality standards given the amount of water supplied remained largely the same (Cardenes et al. 2020). W&WW managers have acted quickly to manage energy costs in response to these patterns. Operational assets are being optimised and upgraded to better manage energy demands (Veolia 2019). Several utilities in E&W have already implemented local installations of solar and wind energy generation, and many are also generating biogas from sewage sludge at wastewater treatment plants. For instance, TWUL self-generate around 23% of their total electricity consumption (Thames Water 2019b).

There is, therefore, a clear momentum to better understand and control electricity use in the W&WW industries of E&W. However, for the moment the literature is lacking, in that there is very little published of data on a regional scale. Such works form a vital pre-requisite to the effective design of energy management strategies (Kenway et al. 2015; Renouf et al. 2018). For example, the work of Klein et al. (2005) in California led to a proliferation in local studies, which led to the implementation of energy management strategies in the W&WW sector. Recent estimates show these operational changes reduced sectoral energy use by around 1830 GWh in only 2-3 years (Spang et al. 2015; Spang et al. 2018).

This chapter presents a novel regional case-study to report the energy-influence of a W&WW system based in E&W. Specifically, an analysis of data from TWUL is presented. TWUL is the largest water and wastewater utility in E&W and is also responsible for serving one of the largest mega-cities in the world, London. Using five years of monthly resolution data on TWUL's electricity consumption, this study seeks to: (1) produce the first W&WW related energy metrics in the context of the E&W, (2) present a statistical method to separate the trend, seasonal effect, and random component from the electricity use time series and (3) compare and contrast W&WW electricity use in this study against those from other parts of the world.

In this chapter, the TWUL system is firstly presented and its main energy-related challenges are described. Next, the telemetry data obtained from TWUL, as well as its processing and analysis, are described. Then, a temporal analysis of electricity consumption in the TWUL system is presented, where it is demonstrated that regional energy use has been increasing sharply.

2.2 Thames basin

The Thames basin area covers approximately 16,200 km^2 (Thames Water 2014). Within the entire region, TWUL is the largest water utility out of four and the only wastewater utility. The company is also the largest water and wastewater utility company in the E&W and has a customer base of 10 million and 15 million persons in water supply and wastewater respectively (Thames Water 2019b). TWUL is privately owned and has an annual turnover of around £2 billion. It should be recognised that there are three other water supply companies within the region shown in Figure 2.2 but these utilities are not studied in this thesis.

Water resources are sourced from a combination of groundwater and surface water (Thames Water 2014). Drinking water is supplied to customers through around 32,000 km

of water mains, 97 water treatment works, 26 raw water service reservoirs, 308 clean water pumping stations, and 235 clean water service reservoirs (Thames Water 2019b). As with most of the UK, a combined system conveys both sewage and urban stormwater runoff through the same sewer network. Post-use wastewater and stormwater drainage is captured and transferred through 109,000 km of sewerage mains and 4,780 wastewater pumping stations, which is eventually treated at one of 351 wastewater treatment works in the area (Thames Water 2019b). After employee costs, electricity represents the largest operational expense for TWUL at approximately £130 million per year, which represents around 14% of the total operational cost. Of this total sum, around 42% and 39% can be apportioned to the water and wastewater system respectively. Given the significance of the electricity expenditure, there have been concerted efforts from the utility to better understand opportunities for efficiency gains. During the 2017-18 business period, TWUL reportedly self-generated a fifth of their total electricity demand, which is equivalent to 293 GWh and £30 million in operational expenditures (Thames Water 2019b). As is the case for many water and wastewater utilities, there are a number of sources of inefficiencies across the ageing system such as old and inefficient pumping stations and treatment plants. However, leakages in the water supply system is widely recognised as the major inefficiency, reported to be around 26% of the total output from water treatment plants (Thames Water 2017). The utility plans to reduce the overall leakage in the network by 15% in the period between 2020 and 2025 (Thames Water 2019b). Further, the process of replacing aging infrastructure and optimising process operations is continuous. At the demand-side, TWUL plans to install 300,000 smart meters by 2020 to manage overall demand (Thames Water 2014).

Figure 2.2 illustrates the Thames basin with the local elevation profile, as well as the major cities within the area. The TWUL water supply area is divided into six water resource zones (WRZs), which represent a standard geographical unit for water resources planning. Descriptive statistics of each WRZ can be found in Table 2.1. The UK Environment Agency define a WRZ as 'an area within which the abstraction and distribution of supply to meet demand is largely self-contained... so that all customers in the WRZ should experience the same risk

of supply failure and the same level of service for demand restrictions' (Environment Agency 2013). As it can be observed in Figure 2.2, the largest WRZ is the area encompassing Swindon and Oxford (SWOX), which is followed by the London WRZ encompassing the Greater London region. Both of these regions are largely reliant on river-based abstractions. The other four zones are Kennet Valley, Henley, SWA (comprising Slough, Wycombe, and Aylesbury), and Guildford. These WRZs are relatively smaller in area and are reliant on both groundwater and river abstractions.

2.3 Methodology

The main purpose of this study is to derive the first energy-intensity metrics for the water and wastewater systems in E&W. To do so, empirical electricity consumption data are analysed as follows: (i) evaluate time series to understand the trends in energy use and breakdown usage by functions in the supply-chain; (ii) each time series is then decomposed using an additive model to understand the long-term trends; and (iii) energy-intensity statistics are derived and compared against other regions in the world.

2.3.1 Electricity data

For this study, telemetry data provided by TWUL spanning between September 2009 and 2016 (60-months) were collected and analysed. The data were aggregated electricity consumption statistics at monthly time-resolution produced by a proprietary energy auditing system. The primary data (which were not made available for this study) were generated by asset-level electricity meters at half-hourly to daily resolution before being aggregated to the monthly timescales by the energy auditing system. The sample covered 395 sites in total, including: (1) 139 water pumping stations, (2) 112 wastewater pumping stations, (3) 98 wastewater treatment plants, (4) 40 water treatment plants, (5) 1 desalination plant, and (6) 5 other sites including

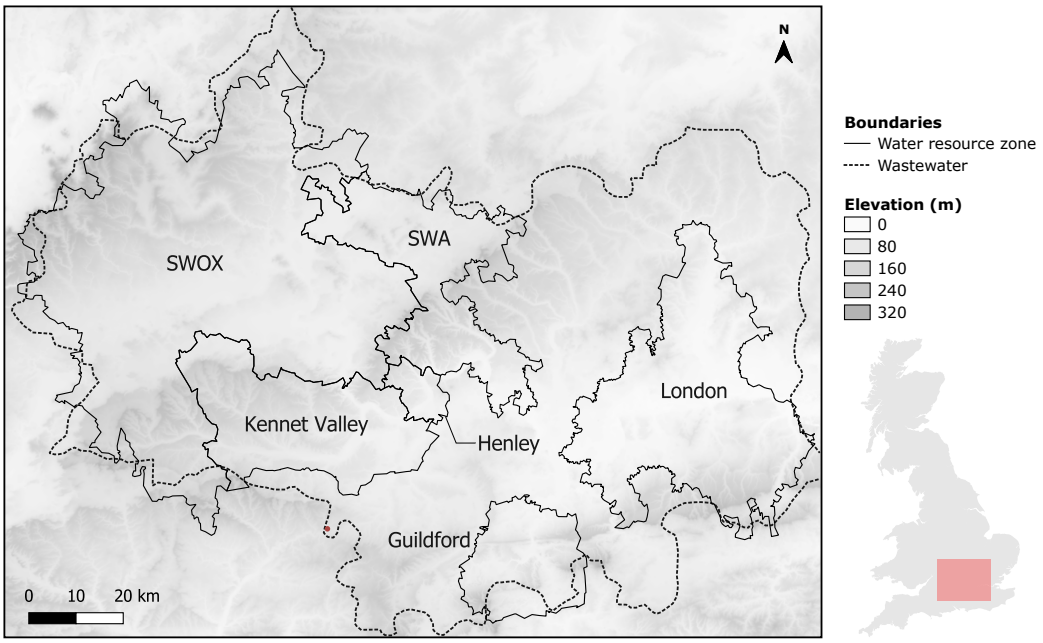


Figure 2.2: Map of the Thames Water Utilities Ltd. area showing the water supply catchments (black boundaries) and the wastewater resource zone (dotted black line). Elevation is shown in the background.

facilities, laboratories, and properties.

2.3.2 Time series analysis

Electricity consumption data (kWh/month) for each asset were aggregated by functional categories and converted into time series following a similar approach to previous studies (Spang et al. 2015). By functional categories, we are referring to following specific operations in the supply-chain: (1) wastwater treatment, (2) wastewater networks, (3) water treatment, (4) water networks, (5) desalination, and (6) other auxiliary functions. Time series of electricity use in water systems have previously been observed to exhibit strong seasonality driven by seasonal patterns in demand (Spang et al. 2015). The electricity consumption data will

also show an overall trend in accordance with, for instance, growth in water demands. Finally, abnormal fluctuations from the mean of the time series might also be observed caused by upsurges in demand during events such as major holidays and sporting events, amongst other factors including weather events. However, these cannot be captured within a long-term seasonal or trend component, and so can be considered as a statistically random component within the time series. Hence, to partition the influence of such factors on the overall electricity consumption, the Seasonal and Trend decomposition method using Loess (STL) developed by Cleveland et al. (1990) was used. This technique decomposes the time series f into three components such that:

$$f_t = \alpha_t + \beta_t + \gamma_t \tag{2.1}$$

where α represents the long-term trend in the time series, providing an understanding of the rate of change in the series. The β component captures the seasonal effects in the data, which in the case of water and wastewater flows could be linked to seasonal changes in demand and climate effects. Finally, γ represents a stochastic irregular (random) component that would represent one-off events that can result in unusual fluctuations in the time series. The STL procedure was used as it is a versatile and robust additive time series decomposition method and it has been successfully demonstrated in a significant number of different applications, which includes analysis of electricity consumption data (Makridakis et al. 1998). A sequence of smoothing operations are applied using locally-weighted polynomial regressions. Whilst STL can handle changes in seasonality in time, it was assumed that the seasonal phase in each of the time series was constant given the relatively short timescale of the data. The STL technique can handle multiple types of seasonality, allows the user to define the smoothness of the trend-cycle, and it is robust to outliers in its estimation of the trend and seasonal cycles (Makridakis et al. 1998). The trend in electricity consumption was then evaluated by applying a least-squares regression model on the α component and the slope (first-order derivative) was computed, which allows us to understand whether consumption was changing in time.

All rates of change reported in this work are obtained from the gradient estimation from the least-squares regression model, where the uncertainty is taken as the standard-error in the model.

2.3.3 Calculating energy-intensity

Energy-intensity ϵ, measured as the unit energy use per unit of water demand or wastewater treated (kWh/ML), is a common metric used globally for assessing the energy intensiveness of a water system (Kenway et al. 2011). Previous works have tended to present ϵ metrics per functional category in a water or wastewater system. However, since time series data on water flows through each of the 395 sites analysed in this work were not available, the energy-intensity metrics for each site or by functional units could not be calculated. Therefore, ϵ metrics in this work are computed for each of the six water resource zones in the Thames basin, which are presented in Figure 2.2. For each water resource zone, ϵ was calculated as:

$$\epsilon_z = \frac{\varphi_z}{\zeta_z} \tag{2.2}$$

where φ is the electricity consumption per capita (kWh/person), ζ is the water use per capita (m^3/person), and z denotes the specific water resource zone. The per capita use of water and energy are calculated respectively as:

$$\varphi_z = \frac{\sum_{t=1}^{n} f_{t,z}}{P_z} \tag{2.3}$$

$$\zeta_z = \frac{\sum_{t=1}^{n} w_{t,z}}{P_z} \tag{2.4}$$

where f is a time series of electricity consumption (kWh) of a specific water resource zone z, ω represents the total water used across the water resource zone within the same time period (m^3), and P is the total population (number of persons). Values for the total water used ω and population P in each water resource zone were obtained from Thames Water (2014) and originally estimated from internal TWUL modelling based on metering data. The total water use equivalent is the total quantity of water produced, which is the sum of residential and non-household demand, as well as system leakages. These data are summarised in Table 2.1. The derived metrics for energy-intensity were then compared locally to understand regional spatial variations. It is noted that this investigation did not consider wastewater energy-intensity as the required data for wastewater flows were not available.

2.4 Results and Discussion

2.4.1 Temporal evolution of electricity use

Figure 2.3 shows the time series of total electricity consumption f_t across the TWUL system between September 2009 and 2014 per functional category. Across the 60-month time-period, the total electricity use in the system was 4426 GWh, equivalent to 870 GWh/year. In descending order, the main contributors to the total energy consumption over the study period were observed to be water networks (33%), wastewater treatment (32%), water treatment (24%), wastewater networks (6%), and desalination (2%). The remainder of consumption (1%) was in other operations such as laboratories, properties, and maintenance work, and is not discussed any further in this work due to the negligible overall contribution of this category. The total number of assets in the TWUL system exceed the quantity of assets that were considered in this chapter. However, the sites not analysed are relatively small facilities and their energy consumption is negligible in comparison.

In observing the temporal evolution of the total electricity consumption, a consistent in-

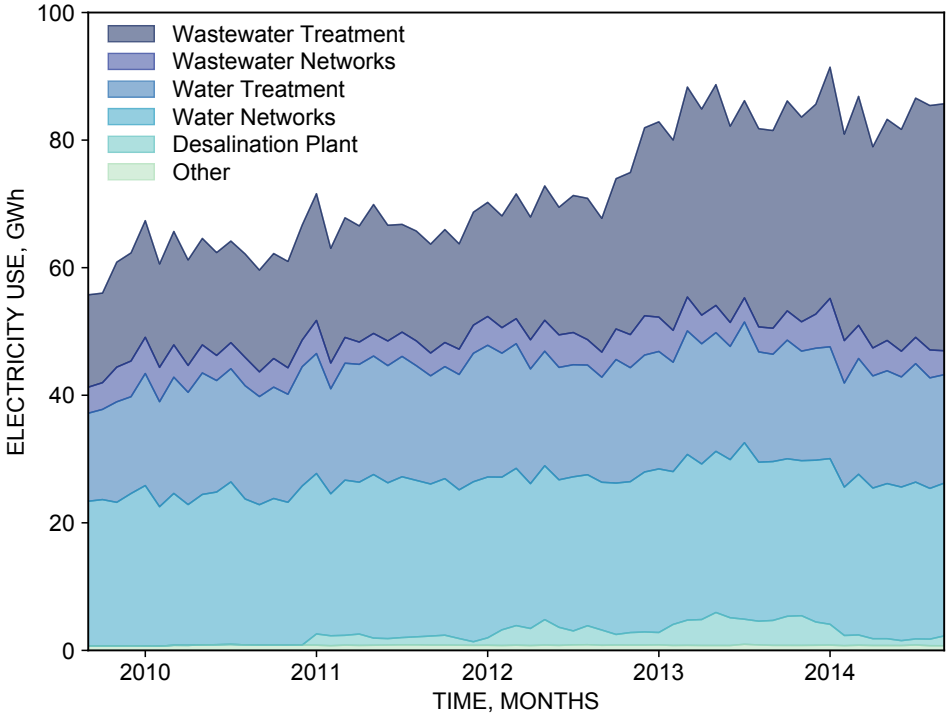


Figure 2.3: Stacked area chart of electricity consumption (GWh) between 2009 and 2014 categorised by functional units.

creasing trend in electricity usage is evident across the system during the study period. Between the first and last time-period, monthly electricity consumption grew from 56 GWh to 86 GWh. In Figure 2.4, the observed time series f, trend α, seasonal phase β, and random component γ are shown in each of the panel plots. In order to ensure the model has adequately captured each phase, the γ-phase was further analysed, where a random distribution was observed with no autocorrelation. The mean contribution from seasonality β and random effects γ were observed as minor components of the time series f at 0.10% and 0.12% respectively. Given the relatively short timescale of the case-study, it was assumed that the seasonal cycle remained constant in the analysis, but this assumption could lead to erroneous representation of the seasonal phase. Future studies that employ this method should calibrate the model to better capture the seasonal cycle, particularly if the influence of climate change on energy-use in water and wastewater operations is an important aspect of the study. The random component of the model shows a generally consistent pattern between 2010–2013, after which more

variability is exhibited, which suggests that an exceptional event might have occurred that could have led to an increase from usual levels of electricity use.

Once the time series has been adjusted for seasonality and random effects, a strong growth is observed in the long-term trend component α during the study period, with an equivalent rate of change of 6.7$\pm$0.3 GWh/year (10.8$\pm$0.4% per year). The rate was estimated by fitting a linear regression model to α and computing the slope of the model, where the error is assumed as the standard error in the model estimation. More recent statistics from TWUL public reports suggest this growth continued: total electricity consumption across the network was reported to be 941 GWh in 2017–18 (Thames Water 2019a). This later reported consumption exceeds the expected value if we were to extrapolate using the rate of change observed over the time slice of the data in this study. This might be attributed to a number of factors including: (i) a significant increase of pumping into reservoirs to meet a sudden increase in summer demand, (ii) an unexpected cold wave and increased pipe bursts in February 2018, and (iii) the exceptionally hot and dry summer of 2018.

Figure 2.5 shows the derived trend components from the time series decomposition of each functional category, which have been plotted as the relative change (%) using the first value in the time series as the base value. Here, a strong growth in the electricity requirements for wastewater treatment can be observed. Between 2010 and 2012, electricity use in wastewater treatment works grew by approximately 10%, after which it increased dramatically by around 110% to the end of the time series. After conferring with operations managers from TWUL, it was gleaned that this sudden growth can be attributed to major modifications in five of the utility's largest wastewater treatment works, where the following unit operations were added: (1) 12 aeration plants, (2) 2 picket fence thickeners, (3) 2 activated sludge thickeners, (4) 24 final settlement tanks, (5) 5 primary settlement tanks, and (6) 2 inlet pumps. Furthermore, exceptional levels of flooding within this period resulted in larger than normal volumes of stormwater entering the sewer system, which led to additional levels of associated pumping. Across the other functional categories (*i.e.* water networks, water treatment, and wastewater

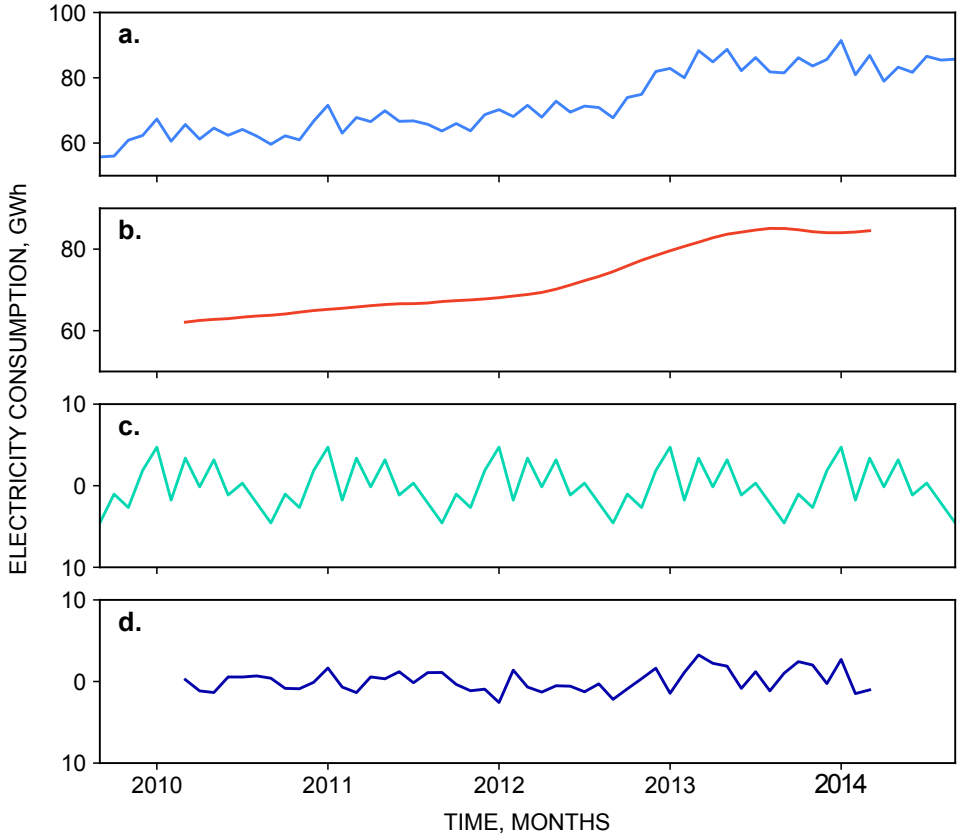


Figure 2.4: Decomposition of electricity consumption (GWh) metrics. The panel plot shows (a) observed time series f, (b) trend α, (c) seasonal phase β, and (d) random component γ.

networks), no statistically significant trend in the relative energy consumption was observed. Hence, it is likely the increases in electricity consumption observed across the TWUL system mainly attributed to the modifications in wastewater treatment operations, as well as increased volume of wastewater pumping induced by flooding.

Some of the increasing trends in electricity use can also be attributed to the commissioning of the Beckton Desalination Plant, which is first desalination facility in the United Kingdom and became fully operational in late 2010. The plant was designed to treat brackish water, which has a lower saline content than seawater, and hence requires less treatment. Beckton is only used at times of drought. Whilst desalination is typically synonymous with high electricity consumption—*e.g.* Sydney's desalination plant consumed 257.7 GWh of electricity in

2010 (Radcliffe 2018)—the single desalination plant in the Thames basin is not used frequently. The Beckton Desalination Plant has on average only processed around 23% of its capacity (150 MLD) since it came online, and yet a notable electricity footprint can be observed associated with its use in Figure 2.3 between 2011 and 2014, contributing around 2% to the total electricity use. The energy-intensity of the plant was estimated as 2.26 kWh/m^3, which is within the upper-range of 1.0–2.5 kWh/m^3 reported for brackish water RO in previous studies (Stokes et al. 2006). As water scarcity pressures enhance in the future, the use of the Beckton Desalination Plant could potentially increase if other water resource options with lower energy needs are not developed, which would translate into a higher water-related electricity footprint. Outside of the Thames basin, there are suggestions that additional desalination plants might be required in the UK (Ives et al. 2018), which would enhance the electricity footprint of water supply across the country, though the feasibility of desalination as a solution elsewhere in England and Wales remains uncertain.

2.4.2 Electricity use by function

The three most electricity-consumptive functions in the TWUL system were observed to be water networks (33%), wastewater treatment (32%), and water treatment (24%). In water supply networks, electricity consumption is primarily a function of water demands, as well as network conditions with respect to hydraulic properties of the pipe (*i.e.* velocity, pressure head, frictional losses, etc.), asset age, and topography. Post-treatment leakages within the TWUL system are currently reported to be 26% of the total demand and the company is targeting to reduce this number by 15% in the period between 2020-2025 (Thames Water 2019b). This would theoretically result in decreased electricity consumption within the water distribution network as sources of water losses are removed and older assets are replaced. In addition, reducing losses in the water network would also lower the throughput needed in water treatment plants, and so reduce the associated electricity use. Though any benefits that are potentially realised here would be offset by population growth.

Table 2.1: Summary statistics related to the water supply system for each water resource zone (WRZ) as of 2014. Energy use and intensity were calculated in this work, whereas population and water demand were obtained from (Thames Water 2014). The final row shows a sum for the entire Thames Water system with the exception of the ϵ column, where a mean value is shown.

Water Resource Zone	Population [p]	Water Demand [MLD]	Energy Use [GWh per year]	ϵ [kWh/m^3]
Guildford	150,136	44.7	10.6	0.65
Henley	49,082	13.1	3.4	0.71
Kennet Valley	389,946	98.4	32.9	0.92
London	6,946,620	2048.1	389.2	0.52
SWA	507,627	135.7	31.4	0.63
SWOX	999,996	261.9	44.7	0.47
Thames Water	9,043,407	2602.0	512.2	0.65

Analysis from TWUL predicts an increase in overall water demands at a rate between 0.25–0.75% per year, which is associated with population growth scenarios (Thames Water 2014). However, plans to implement smart meters and relatively more water-efficient technologies such as modern dishwashers, washing machines, and low volume toilet cisterns will help to temporarily offset the increases in water demands by reducing per capita consumption (Thames Water 2014).

The most common method for sewage collection across England and Wales is through combined sewage systems, in which sewage from domestic, industrial, and commercial sources is combined with surface runoff, and distributed to local wastewater treatment plants. Combined sewer overflows (CSOs), which is when the total inflows into a combined sewer exceed its capacity causing the discharge of untreated wastewater into local water bodies, have been long recognised as an environmental and public health risk in the Thames basin, and indeed in other catchments across England and Wales (Mourato et al. 2005). As such, TWUL have targets to reduce overflow events in certain areas. One such project to deal with this issue is the Thames Tideway Tunnel—a 25 km long and 7.2 m diameter sewer that is being bored under the River Thames expected to be completed by 2024 at an estimated cost of £4.9 billion.

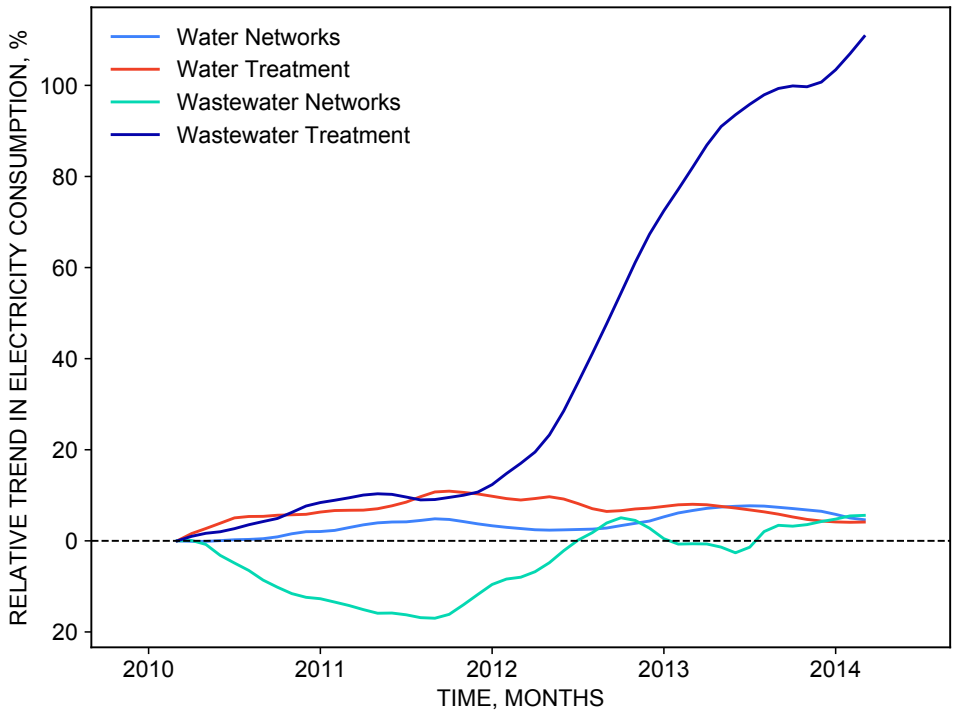


Figure 2.5: Derived trend components (α) for each functional category: water networks, water treatment, wastewater networks, and wastewater treatment. Shown as relative change (%) using the first term in the time series as the base value.

The sewer has been designed to reduce the frequency of overflow events from 50–60 to 3–4 per year, which will facilitate the UK Government to become compliant with the EU Urban Wastewater Treatment directive. This project will immediately yield significant public health, environmental, and aesthetic benefits as overflows events are reduced and more wastewater is directed to local treatment plants (Thomas et al. 2011). With more water being pumped out of the tunnel and increased inflows into wastewater treatment plants, the electricity use in the wastewater supply chain will increase as a result. It is important to track the energy influence such major implementations as this would form a useful planning guide for other similar projects globally.

2.4.3 System energy-intensity

Figure 2.6 shows water-related energy use (kWh per person per year) against water use (L per person per day) in the TWUL system (in colour) compared against other regions in the world (grey) for the study period. This chart shows data for water supply only and energy for water use at the household level is not included. Dashed lines in the plot, which indicate linear functions of energy-intensity between 0.5–2.0 kWh/m^3 have been shown for reference. The per capita water demands in the Thames basin are within the average range of the other cities reported. Whilst the observed energy-intensities are generally above the average of all the cities plotted (0.6 kWh/m^3), both SWOX and London, where the greatest populations are served, are both below this average value. Further, though the potential for differences in drinking water quality standards globally and hence treatment requirements are recognised, the energy-intensity values derived are higher than those calculated for similarly developed cites, such as Melbourne, Berlin, Sydney, and San Francisco. It should be noted, however, that the regions studied in this work are water resource zones, and so the spatial extents might vary in comparison to the other regions in the plot, which consider only the city-scale or are an aggregate of all encompassing water supply zones.

Factors that influence the energy-intensity of water-related energy use are known to include climate, topography, water use patterns, and operational efficiency (Lam et al. 2018). In addition, the initial raw water quality, as well as the required water quality parameters of the final product also influence the electricity requirements of the system. The energy-intensity values derived for the TWUL system can likely be explained by two factors: (i) the volume of pumping in the system and (ii) low system efficiency attributed to relatively high leakage rates. The TWUL system requires relatively high amounts of pumping to convey water between process operations, which is likely due to little topographical variation within water resource zones. Secondly, the energy intensiveness of the TWUL system could also be explained by system leakages, which are known to be relatively high across the network. Sections of the supply network are among the oldest in the world and date back to the Victorian

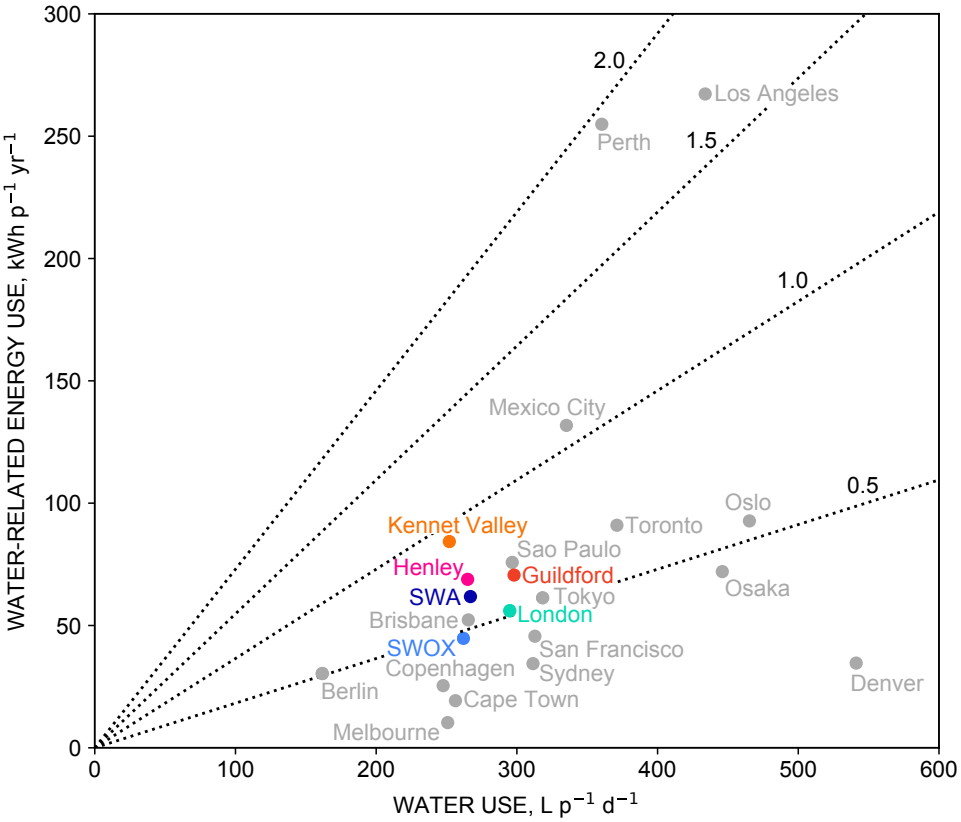


Figure 2.6: Water-related energy use (kWh per person per day) against water use (L per person per day) in the TWUL system in 2012, compared against other regions in the world (grey). The dotted lines are plotted for reference and indicate 0.5–2.0 kWh/m^3 energy intensities. This figure has been adapted from Lam et al. (2017) and reproduced with permission.

era. Further, recent network maintenance reviews revealed the annual asset replacement rates in the network are small-scale in comparison to other parts of the world (Thames Water 2017). Age of a network has been known to correlate with higher leakages in a water distribution network (Venkatesh 2012), which could explain the relatively high levels of leakages in the TWUL system. Leaks in the system are well-known to increase the energy consumption in a water system in two ways: (i) by increasing the need to abstract, treat, and output larger volumes of water into the distribution network and (ii) through greater dynamic losses that result from restoring equivalent service (Colombo et al. 2005). The utility has targets to reduce leakage rates by fixing or replacing assets within the network, which would yield savings in electricity consumption in the short-term.

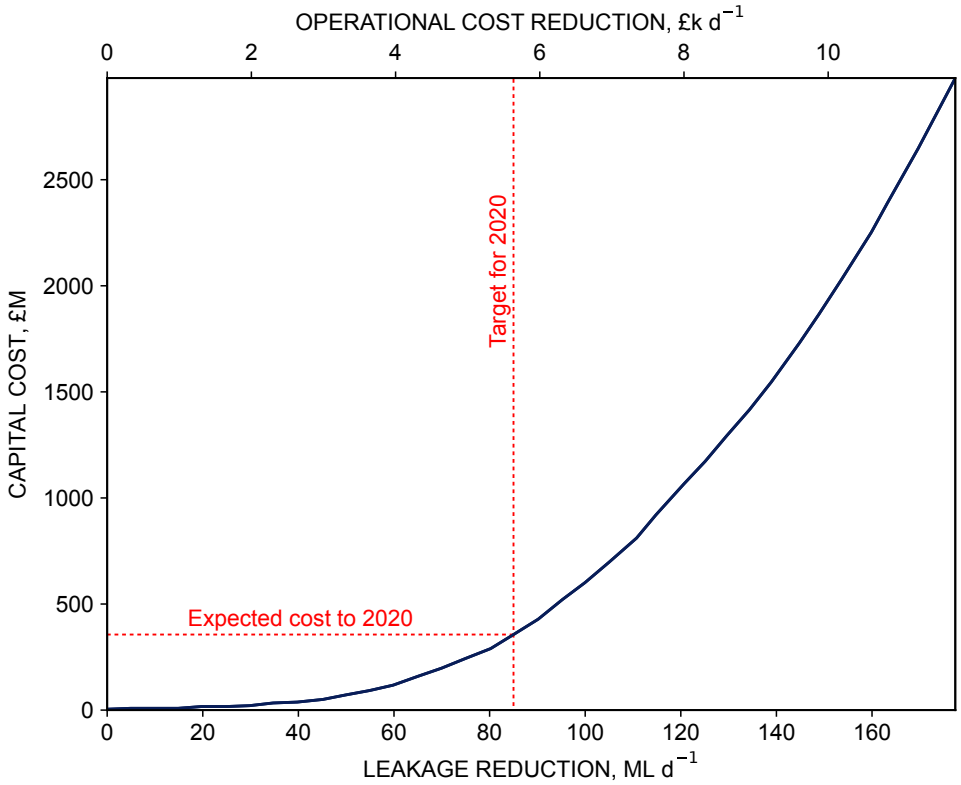


Figure 2.7: Curve expressing the relationship between capital cost (£ millions), leakage reductions (MLD, and reductions in operational expenditures due to electricity consumption (£ 1000s per day) for the Thames Water Utilities Ltd. system. The dashed red lines show the company's leakage reduction targets to 2020 (Hall et al. 2019)

Identifying and reducing leakage across the water distribution network has benefits towards an energy efficient system. However, this can come at a significant cost. Figure 2.7 shows the relationship between capital cost investments and leakage reductions, which is based on an analysis by TWUL (Hall et al. 2019). The curve assumes an exponential relationship between leakage reduction and capital cost, in that significant reductions could be realised cost-effectively in the first instance but the economic case decreases after a turning point. The dashed line in Figure 2.7 represents the targeted leakage reduction by the utility up to 2020: 85 MLD with an expected cost of around £340 million. For relative context, this volume of water could meet 96% of the daily demands of the Guildford, Henley, and Kennet Valley water resource zones (589,164 people) (Thames Water 2014). There are a number of benefits of reducing leakages that regulators and utilities in the UK have recognised, and

whilst energy savings are also acknowledged, they have not yet been quantified in terms of potential reductions in operational cost. That is, *what would be the unit cost saving for each unit of water leakage prevented?* Using the metrics for energy-intensity (kWh/m^3) derived in this work, this relationship has been expressed in terms of the energy cost savings that could be realised for every unit reduction in leakage (calculation shown in Appendix A.1). Should the utility reach its target, this could result in a theoretical reduction of 85 MLD, which is approximately equivalent to operational expenditures due to electricity consumption of ∼£2.1 million per year. This number accounts for around 2% of the total operational cost associated with importing grid electricity. However, there is a caveat to this theoretical value as it is derived in the absence of other external pressures such as population growth and demand changes in time. Discourse on the motivations for leakage reductions primarily focus on the environmental benefits of reduced water withdrawals from rivers, as well as the improvement in political and public perception, and less often focuses on the energy-related co-benefits.

2.5 Conclusions

Electricity consumption in the TWUL network increased consistently during the period 2009 to 2014, which was mainly driven by expansions in wastewater treatment works to achieve higher effluent water quality standards and periods of heavy rainfall that caused more storm water pumping and treatment. In addition, the operations of a new desalination plant also contributed to increasing patterns. As the utility continues to invest in more water supply technologies to meet increasing demands, as well as upgrade its sewer and wastewater treatment capacities, we can reasonably expect this growth in electricity consumption to continue. Some of this growth could be managed should the planned improvements to water infrastructure efficiency (*e.g.* leakage reductions) be realised. However, the temporary nature of these benefits should be recognised as external pressures such as stricter water quality standards and population growth would offset the potential benefits.

With regards to energy use in wastewater operations, regulatory changes require utilities to reduce overflow events in combined sewage networks. Whilst this will reduce the number of discharges of untreated wastewater into local water bodies, it will result in increased pumping of wastewater and larger volumes for wastewater plants to handle, that might increase the associated electricity usage. Though implementation of source control measures for storm water runoff in urban areas could potentially mitigate the energy consumption impacts. This highlights the fact that increasing stringency in mandatory effluent standard regulations will generally be associated with higher energy requirements.

When analysing the derived energy-intensity metrics for each water resource zone in the water utility's system, the energy efficiency of the water network was observed within the average range when compared with other similarly developed cities of the world. Given that TWUL has plans to improve the efficiency of their system through management schemes such as leakage reduction, the energy-intensity of the network and the operational cost associated with electricity could decrease in the short-term as a result, though the benefits would erode in time as a result external factors such as population growth. This study did not deal with the energy used for water provisions at the household level. However, it has been estimated that customers of TWUL use seven times more electricity for water-related services as compared to the utility's electricity use for their operations, which is also the case for many other regions across the world. It is therefore also important to target opportunities for water-related efficiency improvements at the consumer level. State-of-the-art frameworks used to understand and improve water-related energy use should be clearly separated to define energy use in industry from that at the household level.

Temporal studies of the energy influence of water-related operations are rare. Through this study, we have have seen that such studies can be useful in better understanding the energy-related characteristics of a water and wastewater systems. This is particularly important in relation to understanding long-term electricity consumption trends, which can reveal insights on the energy impacts of infrastructure and effectiveness of policy development, and

to understand the exogenous seasonal and random influence from the local environment. The information that can be gleaned from such analyses are an important basis for effective energy management programmes in water and wastewater operations.

References

Cardenes, I., Hall, J. W., Eyre, N., Majid, A., & Jarvis, S. (2020). Quantifying the energy consumption and greenhouse gas emissions of changing wastewater quality standards. *Water Science and Technology*, *2*, 1–10. https://doi.org/10.2166/wst.2020.228

Cleveland, R. B., Cleveland, W. S., McRae, J. E., & Terpenning, I. (1990). STL: A seasonal-trend decomposition procedure based on loess.

Colombo, A. F., & Karney, B. W. (2005). Impacts of leaks on energy consumption in pumped systems with storage. *Journal of Water Resources Planning and Management*, *131*(2), 146–155. https://doi.org/10.1061/(ASCE)0733-9496(2005)131:2(146)

Environment Agency. (2013). *Water stressed areas – final classification* (tech. rep. July). https://assets.publishing.service.gov.uk/government/uploads/system/uploads/attachment_data/file/244333/water-stressed-classification-2013.pdf

Hall, J. W., Mortazavi-naeini, M., Borgomeo, E., Baker, B., Gavin, H., Gough, M., Harou, J. J., Hunt, D., Lambert, C., Piper, B., Richardson, N., & Watts, G. (2019). Risk-based water resources planning in practice : a blueprint for the water industry in England, *0*, 1–14. https://doi.org/10.1111/wej.12479

Ives, M. C., Simpson, M., & Hall, J. W. (2018). Navigating the water trilemma: a strategic assessment of long-term national water resource management options for Great Britain. *Water and Environment Journal*, *32*(4), 546–555. https://doi.org/10.1111/wej.12352

Kenway, S. J., Lam, K. L., Stokes-draut, J., Twomey, K., Binks, A. N., Bors, J., Head, B., Olsson, G., & Mcmahon, J. E. (2019). Defining water-related energy for global comparison ,

clearer communication , and sharper policy. *Journal of Cleaner Production*, *236*, 117502. https://doi.org/10.1016/j.jclepro.2019.06.333

Kenway, S. J., & Lant, P. A. (2015). How Does Energy Efficiency Affect Urban Water Systems?, In *Global issues in water policy*. https://doi.org/10.1007/978-94-017-9801-3{_}28

Kenway, S. J., Lant, P. A., Priestley, A., & Daniels, P. (2011). The connection between water and energy in cities: A review. https://doi.org/10.2166/wst.2011.070

Klein, G., Krebs, M., Hall, V., O'Brien, T., & Blevins, B. B. (2005). *California's Water – Energy Relationship* (tech. rep.). https://doi.org/CEC-700-2005-011-SF

Lam, K. L., Lant, P. A., & Kenway, S. J. (2018). Energy implications of the millennium drought on urban water cycles in Southeast Australian cities. *Water Science and Technology: Water Supply*, *18*(1), 214–221. https://doi.org/10.2166/ws.2017.110

Lam, K. L., Kenway, S. J., & Lant, P. A. (2017). Energy use for water provision in cities. *Journal of Cleaner Production*, *143*, 699–709. https://doi.org/10.1016/j.jclepro.2016.12.056

Makridakis, S. G., Wheelwright, S. C., & Hyndman, R. J. (1998). *Forecasting : methods and applications*.

Mourato, S., Atkinson, G., Ozdemiroglu, E., Newcombe, J., & de Garis, Y. (2005). Does a cleaner thames pass an economic appraisal?: The value of reducing sewage overflows in the river thames. *Water International*. https://doi.org/10.1080/02508060508691858

Nair, S., George, B., Malano, H. M., Arora, M., & Nawarathna, B. (2014). Resources , Conservation and Recycling Water – energy – greenhouse gas nexus of urban water systems : Review of concepts , state-of-art and methods. *"Resources, Conservation & Recycling"*, *89*, 1–10. https://doi.org/10.1016/j.resconrec.2014.05.007

Perrone, D., Murphy, J., & Hornberger, G. M. (2011). Gaining perspective on the water-energy nexus at the community scale. *Environmental Science and Technology*, *45*(10), 4228–4234. https://doi.org/10.1021/es103230n

Radcliffe, J. C. (2018). The water energy nexus in Australia – The outcome of two crises. *Water-Energy Nexus*. https://doi.org/10.1016/j.wen.2018.07.003

Renouf, M. A., Kenway, S. J., Lam, K. L., Weber, T., Roux, E., Serrao-Neumann, S., Choy, D. L., & Morgan, E. A. (2018). Understanding urban water performance at the city-region scale using an urban water metabolism evaluation framework. *Water Research*. https://doi.org/10.1016/j.watres.2018.01.070

Rothausen, S. G., & Conway, D. (2011). Greenhouse-gas emissions from energy use in the water sector. Nature Publishing Group. https://doi.org/10.1038/nclimate1147

Spang, E. S., & Loge, F. J. (2015). A High-Resolution Approach to Mapping Energy Flows through Water Infrastructure Systems, *19*(4). https://doi.org/10.1111/jiec.12240

Spang, E. S., Holguin, A. J., & Loge, F. J. (2018). The estimated impact of California's urban water conservation mandate on electricity consumption and greenhouse gas emissions. *Environmental Research Letters*, *13*(1). https://doi.org/10.1088/1748-9326/aa9b89

Stokes, J., & Horvath, A. (2006). Life cycle energy assessment of alternative water supply systems. *International Journal of Life Cycle Assessment*, *11*(5), 335–343. https://doi.org/10.1065/lca2005.06.214

Thames Water. (2019a). *Building a better future* (tech. rep.). https://corporate.thameswater.co.uk/-/media/Site-Content/Thames-Water/Corporate/AboutUs/Investors/Annual-report/2019/2018-19-Annual-Report-and-Annual-Performance-Report.pdf

Thames Water. (2019b). Facts and figures. https://corporate.thameswater.co.uk/media/Facts-and-figures

Thames Water. (2017). *Thames Water Trunk Mains Forensic Review* (tech. rep.). Reading.

Thames Water. (2014). *Water Resources Management Plan 2014 (WRMP 14)* (tech. rep. June). Reading.

Thomas, G. B., & Crawford, D. (2011). London tideway tunnels: Tackling London's victorian legacy of combined sewer overflows. https://doi.org/10.2166/wst.2011.012

Venkatesh, G. (2012). Cost-benefit analysis - leakage reduction by rehabilitating old water pipelines: Case study of Oslo (Norway). *Urban Water Journal*. https://doi.org/10.1080/1573062X.2012.660960

Veolia. (2019). *H2O27: Future-Proofing UK Water* (tech. rep.). Veolia. London.

Wakeel, M., Chen, B., Hayat, T., Alsaedi, A., & Ahmad, B. (2016). Energy consumption for water use cycles in different countries: A review. https://doi.org/10.1016/j.apenergy.2016.06.114

Watson, J., & Rai, N. (2013). Governance interdependencies between the water & electricity sectors, 50. https://itrc.ouce.ox.ac.uk/wp-content/PDFs/Water-Energy-Case-study-for-publication-final.pdf

Chapter 3

Integrated modelling of water-energy systems

Abstract

Water and wastewater (W&WW) systems are becoming intertwined with energy networks. W&WW utilities are increasingly self-generating their energy demands and participating in demand-side energy market schemes. Yet, simulation models that inform planning in the W&WW sector hardly capture such interactions. This chapter describes InfraSim.Thames, an open-source software implementation of water, wastewater, and energy systems in the Thames basin, home to the city of London, UK. The model uses the dynamic multi-commodity network flow algorithm. From given inputs related to the regional hydrology, climate, water and energy demand curves, as well as spatial characteristics of the network, the model will compute dynamic supply-demand balances of multiple commodities (water, wastewater and electricity). InfraSim.Thames is shown to validate well against previously reported data. Further, model benchmarks show the optimisation is highly efficient computationally. The purpose of this implementation is to inform cross-sectoral planning and management within the region. Further, given that the implementation is open-source, cross-platform, and modular, the InfraSim framework can be adapted to study energy-water systems in other parts of the world.

3.1 Introduction

The need to integrate water, wastewater, and energy systems in natural resources and infrastructure planning models is now widely recognised (Scanlon et al. 2017). In terms of the utilities sector, water and wastewater (W&WW) systems consume substantial amounts of electricity, whereas energy systems are reliant on water for cooling processes (Rothausen et al. 2011). Improving our understanding of these inter-linkages may open the possibility for more efficienct and sustainable system operation (Khan et al. 2017; Khan et al. 2018). Whilst there has been a recent proliferation in the number of energy-water nexus modelling studies, the field remains very much in its infancy (L. Liu et al. 2020). Efforts to date have largely focused on modelling energy-water interactions at the global or national level, and much less attention has been given to regional systems modelling (Parkinson et al. 2018). Moreover, there is a significant literature gap when considering the relationship of W&WW utilities with energy systems (Wu et al. 2020). The need to understand this specific interaction is particularly important given the number of systems-level changes occurring in the W&WW sector. This paper aims to address this knowledge gap by introducing a novel water, wastewater, and energy simulation model.

3.1.1 Relationship of urban water systems with energy

Urban water networks are engineered systems responsible for abstracting, treating, and pumping water to household and non-household users. Post-use water effluents (wastewater) are then transported to treatment facilities via sewer networks before being discharged back into the environment. This entire supply chain can consume substantial amounts of electricity (Plappally et al. 2012). For instance, the water and wastewater sector of England and Wales consumes around 2–3% of the national electricity demand (Watson et al. 2013). Hence, the W&WW sector is inherently connected with the energy system.

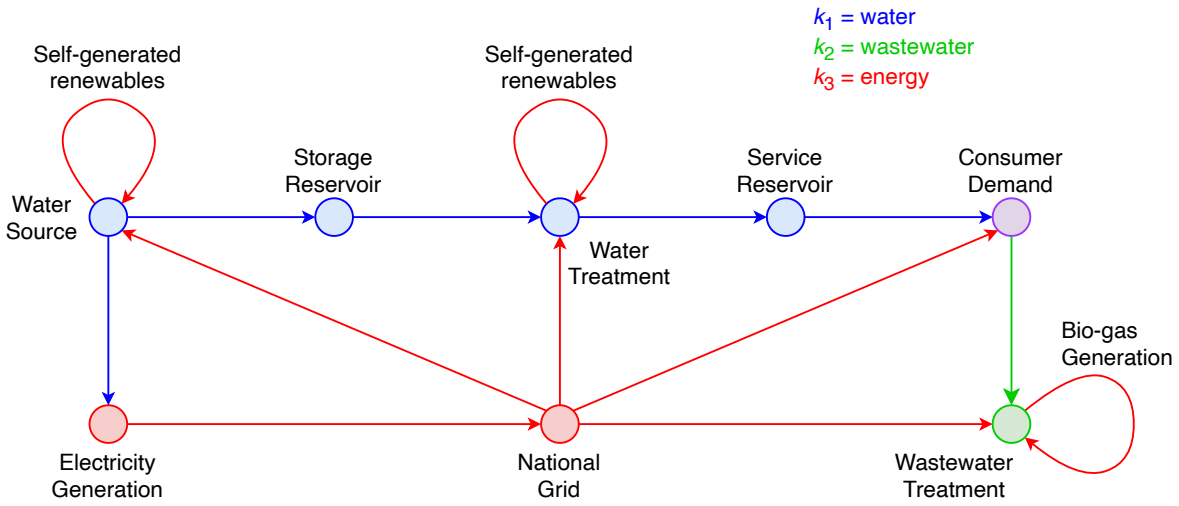


Figure 3.1: Influences and interdependencies represented in InfraSim

Major changes within the water, wastewater, and energy sectors are increasing the importance of cross-sectoral interdependencies. Recent studies have shown electricity use in the W&WW is rising sharply (Majid et al. 2020). This has pushed W&WW utilities to pursue energy management strategies as electricity usually represents the largest operational cost for companies (Escriva-Bou et al. 2018b). W&WW utilities are beginning to partially self-generate their energy needs by local installations of solar and wind systems, as well as producing bio-gas from sewage sludge. Such changes will see the W&WW sector interact in a wholly different way with local energy systems. For example, some W&WW utilities may reach a state of net-negative energy use (Gu et al. 2017), and hence be able to export electricity to the grid. Moreover, W&WW can exploit storage in their system to optimise electricity consumption to periods with relatively lower tariffs (known as demand-side response) (Kernan et al. 2017; Menke et al. 2016). Though not considered in this study, the reliance of the energy sector on water resources in the context of climate change and decarbonisation economies is also changing (Byers et al. 2020; Byers et al. 2014).

Figure 3.1 shows an illustration summarising the linkages between water, wastewater, and energy systems. The dynamic interdependencies between water, wastewater, and energy systems are seldom represented within simulation models. Hence, the propagation of exogenous

changes (e.g. climate and technological change) through these systems is not fully understood, strengthening the case for advancing cross-sector modelling techniques.

3.1.2 Integrated water, wastewater, energy models

This study is primarily concerned with better representing the interaction of W&WW utilities with energy systems, which as far as the authors are aware has not been modelled previously. Yet, there have been a number of recent studies that have introduced models linking energy-water systems—commonly referred to as *integrated models*—at varying spatial and temporal scales (see reviews by J. Liu et al. (2018), Khan et al. (2017), and Vakilifard et al. (2018)). Given that these previous implementations have influenced the work in this chapter, a brief overview of current modelling strategies is provided here.

As observed by Gonzalez et al. (2020), the manner in which models are linked can vary substantially due to the inherent complexities associated with the water and energy sectors. Broadly, linked models can be categorised as follows: (1) constraint-based models, (2) soft-linked models, and (3) hard-linked models.

Firstly, constraint-based models are those that connect a central model of a particular sector to parameters of another sector using constraints. The use of energy models with water-related constraints is a common example of this. For instance, Price et al. (2018) used highRes—a detailed model of the electricity network within Great Britain (GB)—to study the impact of cooling-water constraints on future GB power systems. Such a linkage method has been used in other energy systems planning studies (e.g. Byers et al. 2014). Another example is of water-centred models that introduce energy-related constraints into the model setup. For instance, Porse et al. (2020) introduced a simulation model of California's water and wastewater system, in which the energy use at each process stage was dynamically tracked and minimised. However, this framework did not incorporate energy infrastructure, and so the self-generation capacity of the regional water system through mechanisms such as pumped hydro was not

considered. Constraint-based modelling approaches are often preferred, since a longstanding and established model can be modified with relative ease to consider the influence of new parameters. Yet, such models only loosely relate sectors and are often predicated upon over-simplifications.

Due to the reductive nature of constraint-based model linkages, others have sought more sophisticated techniques to couple complex infrastructure simulations. A second approach is to form 'soft linkages' between models. Here, independent sectoral models are iteratively run, and the outputs from one model form the inputs for another. Hall et al. (2016) introduced a framework to run and connect large national-scale infrastructure systems models, which was applied in a series of studies applying soft-linkages between sectoral of electricity, gas, transport, water, and solid waste to inform high-level systems-of-systems decision making. Such linkage models can be advantageous, as the intricacies and uncertainties of cross-sectoral systems can be captured to yield more-robust decision frameworks. However, soft-linked models can require substantial resources, in terms of the amount of input needed from sector experts, as well as the computational resources required. Further, convergence or optimality cannot be assured since feedback loops may not be closed (Khan et al. 2017).

The final linkage approach adopted in multi-sector models uses 'hard-linkages', where models are formulated within the same software or code, generally sharing mathematical expressions (Khan et al. 2017). There have been a number of studies to date that have integrated water-energy systems using hard-linked model setups for planning purposes (Giudici et al. 2019; Gonzalez et al. 2020; Khan et al. 2018; Parkinson et al. 2018). Here, it has been shown that models based on constraint-based or soft linkages could yield sub-optimal management and investment plans for multi-sector systems when compared with frameworks based on hard-linkages. However, assimilating multi-sector data to achieve temporal and spatial uniformity in hard-linked models presents significant barriers for analysts (Khan et al. 2017).

It is important also to distinguish between *planning* models and *simulation* models. Planning models typically use optimisation to minimise or maximise an objective function (e.g.

capital cost) to compute the values of unknown decision variables (e.g. amount of additional energy capacity needed). Meanwhile, a simulation model considers the *what-if* of a planning problem—*e.g.* what may happen to a system if a particular scenario is assumed? (Loucks et al. 2017). The majority of literature to date on integrated modelling considers planning models (e.g. Byers et al. 2014; Khan et al. 2018; Parkinson et al. 2018; Price et al. 2018). Meanwhile, only a handful of studies to date have introduced simulation models (e.g. Giudici et al. 2019; Gonzalez et al. 2020). The latter are particularly important in the context of W&WW planning and management, where the use of simulation models dominates the decision-making frameworks to understand, for example, the resilience of the water system to exogenous changes in the climate.

Whilst there have been significant advances in integrated modelling in recent times, there remain significant knowledge gaps, particularly from the context of the W&WW sector. Firstly, despite being operationally connected, water and wastewater systems are often planned and managed as separate entities. Only recently, Dobson et al. (2020) presented a framework to represent water and wastewater in a holistic simulation model, where they argued increasing adoption of such approaches could promote cross-sector sustainability and efficiency. Meanwhile, to the authors' knowledge, no simulation models have been developed to date that capture water-wastewater-energy system interactions to inform cross-sector planning and management. It is argued here that such an advance would be a significant step-forward in understanding the role of energy sustainability in the W&WW sector.

The purpose of this paper is to introduce a simulation model to capture water, wastewater, and energy interactions in a hard-linked mathematical setup. Specifically, this study adopts the generalised multi-commodity flow formulation (Section 3.2). The model is developed for the system in the River Thames basin (InfraSim.Thames), which is a region of widespread interest but currently lacks an open-source energy-water model (Section 4.3). This paper shares the preliminary model outputs and provides commentary on the model benchmarks and usage (Section 5.4). It's important to note that although InfraSim.Thames is tailored to the Thames

system, the software implementation has been designed to promote adaptability for other regions with relative ease.

3.2 Multi-commodity flow

The first objective of this paper is to introduce a generalised hard-linked modelling approach that can be used to simulate interconnected water, wastewater, and energy systems. Each of these systems is characterised by flow of resources i.e. water, wastewater and electricity. These networks are optimized to minimise the cost of flows, so we use the dynamic multi-commodity network flow optimisation formulation (Tomlin 1966). The problem can generally be explained as follows:

minimise: Cost of flows of all commodities across the network

subject to: (1) Conservation of mass
(2) Supply and demand constraints
(3) System operational rules

The optimisation model is formulated using linear programming, which is a technique commonly used in the literature on water-related simulation modelling (Wurbs 2005). The proceeding sub-sections outline the mathematical formulation of the multi-commodity flow model. Whilst this paper describes the model in the context of water-wastewater-energy networks, the formulation can feasibly be extended beyond this to incorporate other commodities.

3.2.1 General formulation

We consider a dynamic connected water, wastewater, and energy network as a directed graph $\mathcal{G} = (\mathcal{N}, \mathcal{A})$. Each arc in the network carries a unique commodity k from a start node i to end node j at time t such network edges are defined as $(i, j, k, t) \in \mathcal{A}$. Moreover, every arc has: (1) cost of flow $c^k_{ij,t}$, (2) flow $x^k_{ij,t} \geq 0$, (3) minimum flow $l^k_{ij,t} \geq 0$, and (4) maximum flow $u^k_{ij,t} \geq 0$. The set $\mathcal{N}$ is partitioned such that $\mathcal{N} = \{\mathcal{S}_1, \mathcal{S}_2, \mathcal{S}_3\}$, where $\mathcal{S}$ denotes a subset of nodes that belong to a specific sector, which in our case is either (1) water, (2) wastewater or (3) energy. We associate with each node $n \in \mathcal{N}_\mathcal{S}$ a real number $D^k_{n,t}$ representing its supply or demand. The node is: a source node if $D^k_{n,t} > 0$; a sink node if $D^k_{n,t} < 0$; and an intermediate junction or storage node if $D^k_{n,t} = 0$. Storage nodes are those that can store a commodity k up to a defined capacity Y^k (*e.g.* water storage reservoirs). The dynamic multi-commodity minimum cost flow problem can then be formulated as:

$$\min_{x^k_{ij,t}} \ \mathcal{Z} = \sum_{t=1}^{\mathcal{T}} \sum_{k \in \mathcal{K}} \sum_{ij \in \mathcal{A}} c^k_{ij,t} \cdot x^k_{ij,t} \tag{3.1}$$

Subject to:

$$\sum_{j:ij \in \mathcal{A}} x^k_{ij,t} - \sum_{j:ij \in \mathcal{A}} \psi^k_{ji} x^k_{ji,t} = D^k_i \ \ \forall \ i \in \mathcal{N}_S \text{ and } t \tag{3.2}$$

$$l^k_{ij,t} \leq x^k_{ij,t} \leq u^k_{ij,t} \ \ \forall \ (i,j), \ t, \text{ and } k \tag{3.3}$$

$$V^k_{i,t} = V^k_{i,t-1} + x^k_{ji,t} - x^k_{ij,t} \ \ \forall \ i \in \mathcal{N}_S \text{ and } t \tag{3.4}$$

$$G^k_{i,t} \leq V^k_{i,t} \leq Y^k_{i,t} \ \ \forall \ i \in \mathcal{N}_S \text{ and } t \tag{3.5}$$

The above Equation 3.1 represents the objective function of the linear programming (LP) optimisation routine, where $\mathcal{Z}$ is the cost function to be minimised across the simulation period. Equation 3.2 denotes that the total supply from a node minus the total flow leaving that node must equal the net supply or demand of that node. Here, the term ψ_{ji}^{k} represents a loss factor along a given arc. This equation represents the mass conservation throughout the network. Equation 3.3 shows that the decision variables $x_{ij,t}^{k}$ must satisfy the lower and upper bounds of the arc flows, where each of these variables is a non-negative real number. Meanwhile, Equations 4.5 represents the conservation constraint applied to storage nodes, which is a function of the inflow, outflow, and volume from the previous time step. The storage node volume must also satisfy the minimum G and maximum Y volumes at each time step (Equation 4.6).

In addition to the equation states defined above, additional constraints are implemented to define the linkages between commodities in the network. For instance, linkage constraints are used to define the outflow of wastewater from a node representing a water consumer. Such constraints are defined as follows:

$$x_{i:ij}^{k_1} = \phi x_{i:ji}^{k_2} \tag{3.6}$$

In Equation 3.6, the flow of commodity k_2 from node j is a function of the inflow of commodity k_1 into node j, where ϕ is a commodity conversion factor. Linkage constraints are used in InfraSim to define the relationships between: (i) water supply and wastewater, (ii) water supply and electricity, and (iii) wastewater and electricity. Future works that may seek to relate other sectors and/or commodities using a similar formulation will need to introduce such linkage constraints.

3.3 Model application

The second objective of this paper is to apply the multi-commodity flow formulation to the water, wastewater, and energy system in the Thames basin. In doing so, this study also aims to develop an open-source software that can facilitate future works within the region, as well as be adapted to similar systems in other parts of the world. This section provides a description of the Thames system, followed by a description of the methodological framework of the InfraSim.Thames model.

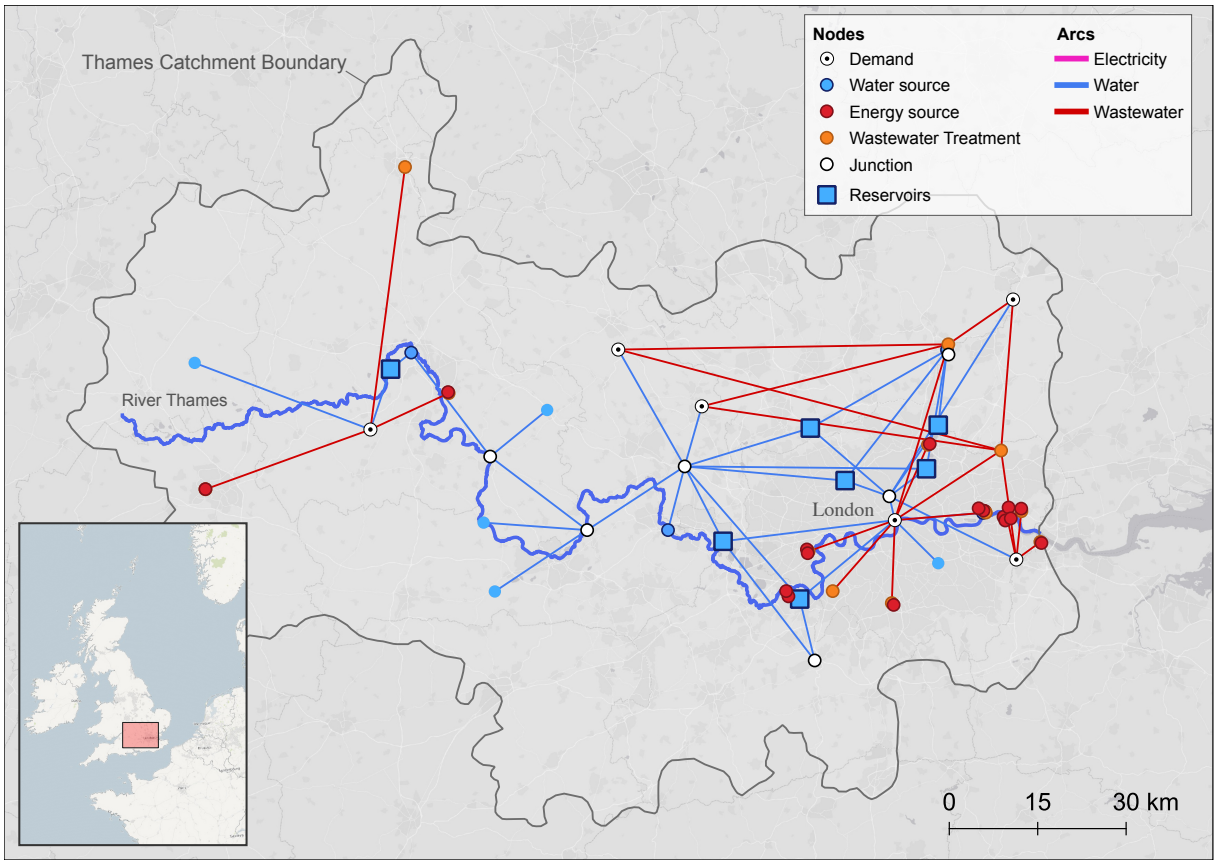


Figure 3.2: Map of the Thames basin in Southern England with a schematic representation of the regional water, wastewater, and energy system as modelled in InfraSim.Thames.

3.3.1 System description: Thames basin

This model developed here is for the water, wastewater, and energy system in the Thames basin, where the local W&WW utility—Thames Water Utilities Ltd. (TWUL)—is undergoing rapid energy-related changes. The Thames basin is located in South East England and encompasses the Greater London region (Figure 3.2). The basin area covers around 16,200 km^2 and local systems face chronic pressures from population growth, climate change, and ageing infrastructure, and as such the basin is regarded as a 'severely water-stressed region' (Environment Agency 2008). TWUL is the largest of four water utilities and the only wastewater utility in the region. Note, there are three other water supply utilities in the basin but these are not captured in InfraSim.Thames, nor are their interactions with TWUL's wastewater operations.

TWUL has a customer base of 10 million and 15 million persons in water supply and wastewater, respectively. The predominant water usage within the region is for public drinking supplies. Water is supplied by means of both groundwater and surface water, which must be treated, stored, and pumped to customers before consumption. Around 90–95% of post-consumption wastewater is captured by combined sewage and stormwater system, which is pumped through a sewer network prior to treatment. TWUL's water and wastewater system consumes a significant amount of energy at around 930 GWh per annum (Majid et al. 2020). This represents the largest process operational cost for TWUL at around £130 million per year. However, TWUL also have capacity to self-generate electricity by means of locally installed solar photovoltaics, wind turbines, and biogas. This self-generation capacity is currently estimated to produce around 293 GWh per annum with plans to augment capacity in the future (Thames Water 2014).

Planning of TWUL water systems in the context of future change have been studied in a number of previous studies. For example, previous works have focused on better incorporating climate uncertainties into long-term water resources management (Borgomeo et al. 2018; Borgomeo et al. 2016), robust multi-objective decision-making of infrastructure invest-

ments under uncertainty (Huskova et al. 2016; Matrosov et al. 2015), holistic management of water and wastewater (Dobson et al. 2020), and coupled water quality and quantity analyses (Mortazavi-Naeini et al. 2019). Meanwhile, the energy-influence of TWUL's system has also been studied in a few recent works (Cardenes et al. 2020; De Stercke et al. 2018; Majid et al. 2020).

For the moment, however, no studies have adopted a whole-systems approach to the water, wastewater, and energy system within the TWUL network. Moreover, most of the works to date have not published the models associated with their work. While Dobson et al. (2020) did release an open-source model of a section of the Thames system, this study used a mass-balance process model, which is advantageous for small-scale problems but can be unsuitable for planning problems with a large decision-space or high spatial heterogeneity. The approach used in this study can be more effective in such cases. Hence, the software published as part of this work could facilitate further studies in the region.

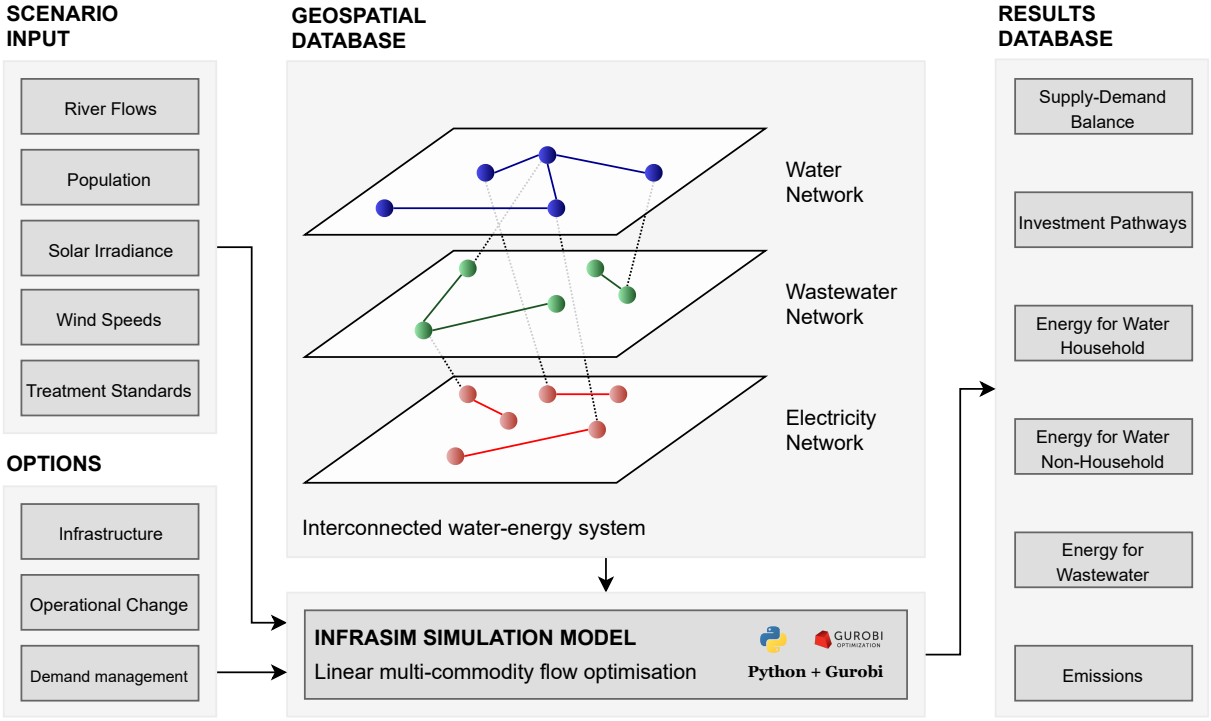


Figure 3.3: A schematic showing the methodological framework of InfraSim.

3.3.2 Model framework

Figure 3.3 shows the modelling framework developed here—referred to as the InfraSim framework—and applied to the TWUL system. As shown, the InfraSim framework has four components, which are: (i) a geospatial database, (ii) a simulation model, (iii) an input database containing information related to the climate, population, and technological scenarios, and (iv) an output database containing the model results. In this section, each of these components is described.

3.3.2.1 Geospatial database

Firstly, each sector is defined as a directed geospatial network, which also maps cross-sectoral linkages. For this purpose, the QGis geographical information systems software is used, which is a free and cross-platform software that is frequently used for infrastructure modelling and planner. Hence, the use of QGis as the primary modelling layer can allow InfraSim to be accommodated within existing workflows. Moreover, QGis provides access to an graphical user interface (GUI), which provides users an interactive means of defining the network and their inflows. QGis is also supported by an array of libraries and documentation that continue to be developed on all common operating systems (e.g. Windows, OSX, Linux). This would be an attractive means of interacting with a model for analysis.

Two shape files must be defined: one containing the nodal data and the other edge data. Each feature within the shape files should be assigned appropriate values within its attribute table. The data within the attribute table of the nodal file contains information such as name, network category (i.e. storage, sink, junction, demand), a subcategory (e.g. reservoir, treatment plant etc.), and sector (e.g. energy, water etc.), amongst other features. Meanwhile, the edge attributes include the commodity, cost of flow, lower bound, and upper bound. More information related to the attributes within the shape file can be found within the InfraSim

guides.

InfraSim contains automated scripts that process the spatial data defined within QGis so that they can be interpreted within the optimisation model. However, it is important that the user ensure consistent nomenclature and categorisation wherever applicable, as a failure to do so may yield infeasibilities or erroneous results.

InfraSim.Thames contains a total of 53 nodes, of which 19 are related to the water sector, 13 to the wastewater sector, and 17 are electricity-related nodes belonging to the water and wastewater operations, and the remaining are junctions without a sector classification. Meanwhile, there are a total of 64 edges in the network, from which 22 allow for flows of water, 20 of wastewater, and 22 of electricity. Each edge can only carry one commodity from water, wastewater, and electricity. The system is comprised of 216.5 GL of raw water storage capacity. Wastewater treatment plants can accommodate for approximately 9 GL of inflows per day. The energy system modelled within InfraSim.Thames has 40.1 MW, 16.5 MW, and 6.9 MW of bio-gas, solar PV, and wind generation capacity, respectively.

Figure 3.2 shows a schematic of the water, wastewater, and energy system as modelled within InfraSim.Thames. As shown, this is a simplified representation of the real system within the basin, which was created based on information from previous studies of the TWUL system (Hall et al. 2019; Huskova et al. 2016; Mortazavi-Naeini et al. 2019). For clarity, this study does not include the national electricity transmission and regional electricity distribution networks. Instead, the electricity network represents only those assets owned by TWUL, such as their wind turbines, solar farms, and biogas power plants. Edges connect TWUL owned generation sites with their energy consumptive process operations (*e.g.* desalination plant, water treatment facility etc.). It is assumed that the portion of electricity that cannot be met through self-generation is imported from the grid without constraints.

3.3.2.2 Simulation model

The simulation model adopts the multi-commodity network flow optimisation programme to simulate supply and demand balances across the network subject to operational rules and constraints. Network linear programming has been used to create simulation models of water systems for decades (Loucks et al. 2017). The method is computationally efficient and guarantees convergence to an optimal solution. It is particularly suited to planning problems with high spatial complexity and a large number of options to be evaluated, where network programming can facilitate exhaustive simulations over a large set of '*what-if*' scenarios (Hall et al. 2019). For example, Dogan et al. (2018) used a single-commodity (water) network flow optimisation algorithm to conduct hydroeconomic simulations of California's water network. Meanwhile, Ishimatsu (2013) used multi-commodity network flow to represent complex interconnected infrastructure systems.

The simulation model is written entirely in the Python programming language. Python is a widely used and open-source interpreted high-level programming language that emphasizes code-readability, and can support numerous important programming paradigms such as object-orientation, functionality, and procedural (van Rossum et al. 2011). The optimisation model is written using GurobiPy, which is a Python module that interfaces with the Gurobi optimisation solver (Gurobi Optimization LLC 2019). There are a number of state-of-the-art optimisation solvers available such as CPLEX, Gurobi, CBC, and GLPK. However, Gurobi has been shown to outperform most of these solvers in terms of computational speeds (e.g. Dogan et al. 2018), and it is available free-of-charge for academic use with extensive documentation and support, making it an attractive option for our purposes.

3.3.2.3 Nodal flow data

In addition to the geospatial data, the InfraSim model requires input data related to the local hydrology, climate, and operational parameters. For this purpose, the user must pass

a structured CSV file containing forcing data for each node. This file is known as the nodal file. Each row within the nodal file represents supply or demand data for a given time step and each column represents a unique node. There are additional columns that define date and time features (hour, day, month, year). A column can also be added to represent a unique replicate for multiple runs (e.g. for numerous stochastic simulations). Again, it is important that the user follows consistent nomenclature when defining column names in that they match the defined nodal names within the spatial database. The InfraSim.Thames project repository contains example nodal files that the user can view for guidance.

3.3.2.4 Outputs

The final component of InfraSim is the results database. A successful simulation will output a number of files to the outputs/ directory. The output data from the simulation show commodity flows across the network at each time step, which allows the user to compute statistics related to energy-for-water, energy-for-wastewater, and the overall emissions impact, amongst other factors. The output data is structured using the 'Tidy Data' convention (Wickham et al. 2017) and is supplied in CSV format, making it easy to read and process for further analysis.

3.3.2.5 Setup and requirements

The InfraSim optimisation model, as well as its associated data processing and analysis scripts, are all implemented entirely in the Python programming language. The software requires a number of standard scientific computing libraries for Python such as NumPy and pandas, as well as geospatial analysis libraries such as GeoPandas and Shapely. Additionally, plotting libraries for Python will also be required (e.g. matplotlib and seaborn). Each of the aforementioned libraries, as well as the Gurobi optimisation software, must be installed separately by the user. The entire InfraSim code base and its dependencies can be obtained and

used freely for academic purposes. The InfraSim software is distributed under an MIT license.

3.4 Examples and Benchmarks

3.4.1 Model run

The InfraSim.Thames model can be run with only a few lines of code. Figure 3.4 shows an example of how a user can run the model, output and process the results, and also debug the model, if necessary. Firstly, the user must define the file path to the node and edge shape file data, and also to the CSV files containing the supply and demand dataset. These are passed as arguments into the Model Python class (Figure 4, line 8). Next, the build function is executed to process the input data and formulate the optimisation model using GurobiPy sub-functions. Then, we attempt to run the simulation and postprocess the results using the try command in Python. The pprint flag will print the progress of the optimisation, as well as the mathematical setup to the user's console. If the model run is successful, the postprocess function outputs a number of figures and CSV files to the outputs/ directory, which contain graphics and data related to the arc flows at each time step, as well as data related to storage volumes. Should the model run result in an infeasible or unbounded model condition, the user can run the debug function (line 15), which will compute the Irreducible Inconsistent Subsystem (IIS) and output a text file containing the set of constraints or bounds that cause the model to become unbounded or infeasible (Gurobi Optimization LLC 2019).

3.4.2 Benchmarking

Figure 5 shows the reservoir volumes in the Greater London water resource zone as computed from a simulation in the Thames network between 2000 and 2010 (green line). Additionally, data from Mortazavi-Naeini et al. (2019) was also plotted as a reference to benchmark

```python
import sys
sys.path.append('../')
from infrasim.thames import *
from infrasim.plotting import *

# Define file paths
nodes       = '../data/demo/spatial/nodes-demo.shp'
edges       = '../data/demo/spatial/edges-demo.shp'
flows       = '../data/demo/csv/demo-flows.csv'

# initiate
thames = Model(nodes,edges,flows)

# build
thames.build()

# run
try:
    thames.run(pprint=False)    #pprint will print to console
except:
    thames.debug()
```

Figure 3.4: Sample Python code used to run the InfraSim.Thames model.

the results from the model developed in this study. Here, it is observed that the time series of reservoir volumes shows a good agreement with previous data. The computed coefficient of determination and Nash-Sutcliffe coefficient was calculated as $R^2 = 0.95$ and NSC $= 0.90$, respectively.

Electricity generated and consumed in the water and wastewater sector of the Thames basin is shown by the panel plots in Figures 3.6a and 3.6b, respectively. Firstly, it is noted that InfraSim.Thames simulated energy generation as being around 209 GWh. This is found to be an underestimate when compared statistics from TWUL (Figure 3.6a), which reported total utility production at near 300 GWh. Here, the discrepancy is between the biogas outputs, whereby InfraSim.Thames computes a lower output as compared with TWUL statistics. This arises as the spatial boundary of TWUL's wastewater operations is larger than their water supply service area. Hence, there are several wastewater treatment plants with biogas production facilities that are not incorporated into InfraSim.Thames, and hence are not captured by the model.

The amount of electricity consumed by TWUL operations was simulated at around 775 GWh per annum and this shows good agreement with values reported in previous studies

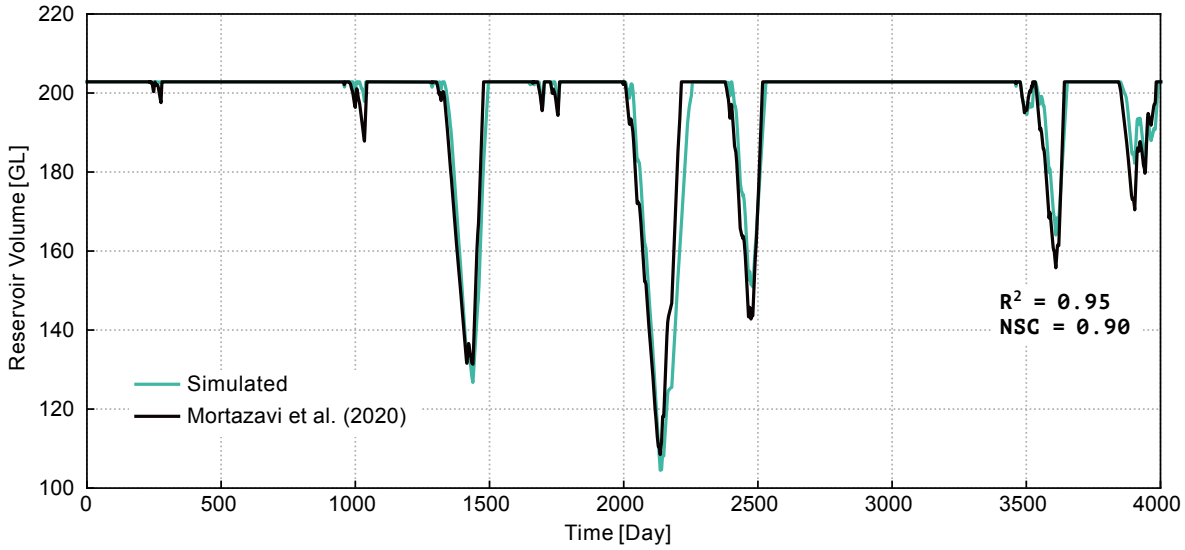


Figure 3.5: Simulated reservoir storage volumes from InfraSim.Thames compared with previously published data (Mortazavi-Naeini et al. 2019). Shown also are calculated values for the coefficient of determination ($R^2 = 0.95$) and the Nash-Sutcliffe coefficient (NSC $= 0.90$).

(Majid et al. 2020). Here, it was observed that pumping and treatment in the water supply sector consumed the largest amount of electricity in the water and wastewater supply chain. InfraSim.Thames underestimated the total electricity consumption at wastewater treatment facilities, which again is attributed to the incomplete representation of the TWUL spatial domain within the model.

Water-related services at the household level are known to consume substantially more energy when compared with water and wastewater operations. For example, Escriva-Bou et al. (2018a) and Escriva-Bou et al. (2018b) showed energy use in household water services accounted for 95% of the total consumption in the sector. This is primarily due to the amount of energy needed to heat water and to operate water-related appliances. Similarly, our simulations show that water-related energy at the consumer-level was around 8300 GWh per annum—over 10 times the energy used in the water and wastewater sector (Figure 3.6c). It is important, however, to differentiate between the modes of consumption. Whilst the majority of energy use at the utility-side is associated with electricity, household consumption of energy to heat water for domestic usage is from gas (e.g. Escriva-Bou et al. 2018a; Escriva-Bou

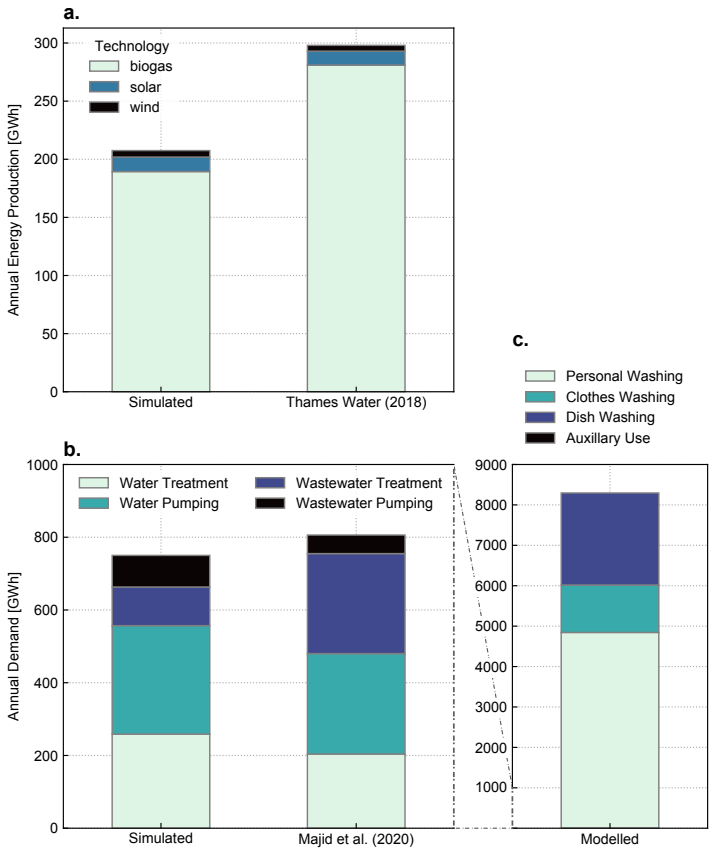


Figure 3.6: Panel plots showing annual (a) electricity production from the water and wastewater utilities in the Thames system, (b) energy demand for water and wastewater processes, and (c) energy demand for water-related services at the consumer level. All energy use statistics are given in GWh.

et al. 2018b). Nonetheless, when adopting a whole-system approach to water and wastewater, 91% of the energy is attributed to the consumer level. It is observed that personal washing, dish washing, and clothes washing are the most energy-intensive services, followed by auxiliary water usage (e.g. outdoor use), which accounts for a relatively negligible amount. Insights such as these demonstrate a potential advantage of the whole-systems modelling approach adapted here, in that water and wastewater managers can quantify energy-related benefits of demand-side measures, which are often neglected (Kenway et al. 2019).

3.4.3 Computational efficiency

There are a number of state-of-the-art optimisation solvers available such as CPLEX, Gurobi, CBC, and GLPK. Here, the model's computation efficiency is tested using Gurobi, which is the complementary solver to the GurobiPy package and has been shown to demonstrate the most efficient computation times (Dogan et al. 2018). However, users can export the model to a Mathematical Programming System (MPS) format for use with other solvers.

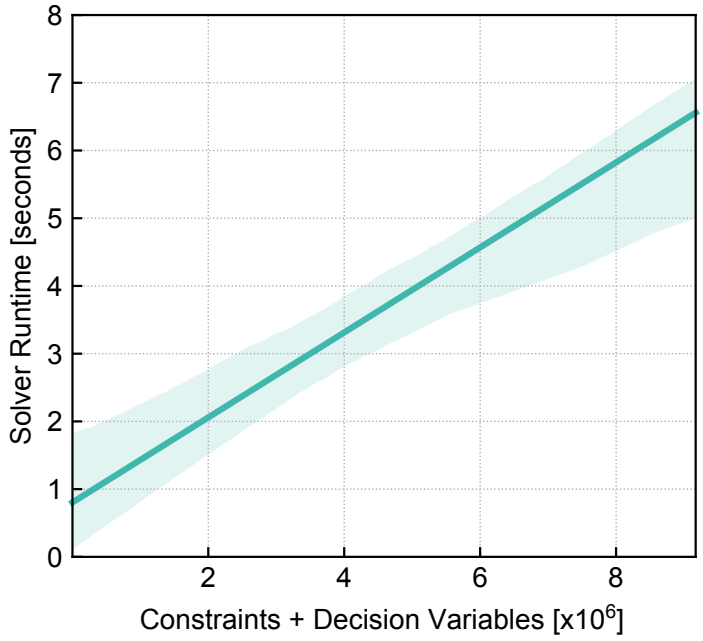


Figure 3.7: Linear regression between the total number of constraints and decision variables in the InfraSim.Thames model and the time (seconds) taken for the solver to converge to a solution. The results presented here were derived using a laptop PC with an Quad-Core i5 processor at 2 GHz and 16 GB of memory.

For the purpose of model benchmarking, the InfraSim.Thames model was run for a number of time steps $a \in A = \{1, 101, 201, ..., 14001\}$ and the solver convergence time was recorded. In each case, the model executed successfully without infeasibilities or errors. In total, 25 such trials were conducted, making a total of 3,500 model runs. The trials were conducted on a PC with a Quad-Core i5 processor running at 2 GHz and 16 GB of RAM. Figure 7 shows the

relationship derived between the total number of constraints and decision variables and the solver convergence time, as derived from the benchmarking run. The plot is a linear regression computed on the observations of the two variables in each run. Here, it is observed that the largest model consisting of around 6 million constraints and 3 million decision variables took around 7 seconds to converge.

In contrast to previous LP-based simulation models, InfraSim.Thames demonstrated much faster overall computation times. For instance, Dogan et al. (2018) also used the Gurobi solver to solve their California-based water model, CALVIN. A trial run in this study of a model with approximately 2 million decision variables took around 8 minutes to converge to a solution. Whilst the study did not provide sufficient information to deduce why the model performance might be slower, it may be because CALVIN is formulated using the Pyomo optimisation library, which is known to be computationally less efficient when compared with Gurobi's Python API (Gurobi Optimization LLC 2017).

3.4.4 Future extensions and limitations

This paper introduced the InfraSim framework, as well as the InfraSim.Thames model, both of which are precursors to future studies related to the energy-water nexus in the Thames region and beyond. For instance, a separate multinational model of the energy-water system across the Jordan Valley—the region encompassing Israel, Jordan, and the Occupied Palestinian Territories—applying the InfraSim framework is currently under development (InfraSim.JV). Such subsequent implementations of the InfraSim framework will be released in the future within the same code repository.

There are a number of limitations to the InfraSim implementation that should be recognised. Specifically, the following limitations are recognised:

- InfraSim uses linear programming in the simulation model to compute dynamic resource

allocation. This approach is commonly used for simulation modelling in both water and energy (Khan et al. 2017), yet it presents obvious limitations as it is seeking to represent systems that are inherently nonlinear. Certain nonlinear constraints can be reasonably approximated using linear programming (*e.g.* Darcy-Weisbach resistance equation (Swamee et al. 2013) and Hazen-Williams formula (Samani et al. 2006)), yet others may be more difficult to represent. However, as Loucks and Van Beek (Loucks et al. 2017) outlined, optimisation-based simulation models serve as a preliminary screening technique to narrow down a large set of options to a smaller subset that should be further investigated in more detail. The assumption of linearity can provide the analyst an advantage in terms of model tractability and computational efficiency. However, the modeller should recognise these limitations.

- Currently, constraints related to pumping delays are not imposed in the model. For example, travel time between nodes is not incorporated. However, these can be included with relative ease and is within the pipeline of features to be added.

- It is common in high-level models to lump multiple similar nodes into one node to reduce computational complexity. For instance, a number of storage reservoirs can be aggregated into one reservoir node, as we have done in this study. Though this has significant computational advantages, it is important to recognise the limitation of this approach. As only aggregate storage is used, it is not possible to model a situation when, for example, one service reservoir is full and another empty.

- Whilst the use of QGis provides an easy-to-use graphical interface for users to define and interact with an infrastructure network, modifications of specific model constraints cannot be made within QGis. For example, users may wish to implement specific water abstraction rules that cannot be adequately represented with the supply data. This would require the user to modify the GurobiPy code in the back end of the software, a step that requires an intermediate to advanced level of understanding in both optimisation and Python programming. However, both of these facets benefit from a wide-range of openly

available literature.

- Though not directly related to the InfraSim implementation, a general limitation of cross-sector modelling techniques that ought to be recognised relates to the issue of spatiality and temporality. Modelling techniques in the water, wastewater, and energy sectors vary significantly depending on the intended purpose of the analyst. For example, it is common for energy analysts to study a system at the hourly to minute temporal scale, which is an unfamiliar time horizon for water resources modellers. Hence, users are advised to take caution in choosing their spatial and temporal scales when constructing such models. This topic has been discussed at length in previous studies such as Khan et al. (2017) and Khan et al. (2018).

3.5 Conclusions

In this paper, a multi-sector modelling framework and applied this to model the water, wastewater, and energy system within the Thames basin was introduced. In doing so, an open-source software of the local system (InfraSim.Thames), which will be used to facilitate future works in the region, was developed. The software approach adopted here is open-source, cross-platform, and has been intentionally designed to be retrofitted into current workflows for modellers within the water and energy sectors. In demonstrating InfraSim.Thames, it was shown that the model displays good agreement with previously reported data and that it is computationally efficient. The InfraSim framework is to be used in subsequent studies on the energy-water nexus at a regional scale.

References

Borgomeo, E., Mortazavi-Naeini, M., Hall, J. W., & Guillod, B. P. (2018). Risk, Robustness and Water Resources Planning Under Uncertainty. *Earth's Future*, *6*(3), 468–487. https://doi.org/10.1002/2017EF000730

Borgomeo, E., Mortazavi-Naeini, M., Hall, J. W., O'Sullivan, M. J., & Watson, T. (2016). Trading-off tolerable risk with climate change adaptation costs in water supply systems. *Water Resources Research*. https://doi.org/10.1002/2015WR018164

Byers, E. A., Coxon, G., Freer, J., & Hall, J. W. (2020). Drought and climate change impacts on cooling water shortages and electricity prices in Great Britain. *Nature Communications*. https://doi.org/10.1038/s41467-020-16012-2

Byers, E. A., Hall, J. W., & Amezaga, J. M. (2014). Electricity generation and cooling water use: UK pathways to 2050. *Global Environmental Change*. https://doi.org/10.1016/j.gloenvcha.2014.01.005

Cardenes, I., Hall, J. W., Eyre, N., Majid, A., & Jarvis, S. (2020). Quantifying the energy consumption and greenhouse gas emissions of changing wastewater quality standards. *Water Science and Technology*, *2*, 1–10. https://doi.org/10.2166/wst.2020.228

De Stercke, S., Mijic, A., Buytaert, W., & Chaturvedi, V. (2018). Modelling the dynamic interactions between London's water and energy systems from an end-use perspective. *Applied Energy*. https://doi.org/10.1016/j.apenergy.2018.08.094

Dobson, B., & Mijic, A. (2020). Protecting rivers by integrating supply-wastewater infrastructure planning and coordinating operational decisions. *Environmental Research Letters*. https://doi.org/10.1088/1748-9326/abb050

Dogan, M. S., Fefer, M. A., Herman, J. D., Hart, Q. J., Merz, J. R., Medellín-Azuara, J., & Lund, J. R. (2018). An open-source Python implementation of California's hydroeconomic optimization model. *Environmental Modelling and Software*, *108*(June), 8–13. https://doi.org/10.1016/j.envsoft.2018.07.002

Environment Agency. (2008). *International comparisons of domestic per capita consumption* (tech. rep.).

Escriva-Bou, A., Lund, J. R., Pulido-Velazquez, M., Hui, R., & Medellín-Azuara, J. (2018a). Developing a water-energy-GHG emissions modeling framework: Insights from an application to California's water system. *Environmental Modelling and Software*, *109*(June 2017), 54–65. https://doi.org/10.1016/j.envsoft.2018.07.011

Escriva-Bou, A., Lund, J. R., & Pulido-Velazquez, M. (2018b). Saving Energy From Urban Water Demand Management. *Water Resources Research*, *54*(7), 4265–4276. https://doi.org/10.1029/2017WR021448

Giudici, F., Castelletti, A., Garofalo, E., Giuliani, M., & Maier, H. R. (2019). Dynamic, multi-objective optimal design and operation of water-energy systems for small, off-grid islands. *Applied Energy*, *250*(May), 605–616. https://doi.org/10.1016/j.apenergy.2019.05.084

Gonzalez, J. M., Tomlinson, J. E., Harou, J. J., Ceseña, E. A. M., Panteli, M., Bottacin-busolin, A., Hurford, A., Olivares, M. A., Siddiqui, A., Erfani, T., Strzepek, K. M., Mancarella, P., Mutale, J., Obuobie, E., Seid, A. H., & Ze, A. (2020). Spatial and sectoral benefit distribution in water-energy system design. *Applied Energy*, *267*(November 2019), 114794. https://doi.org/10.1016/j.apenergy.2020.114794

Gu, Y., Li, Y., Li, X., Luo, P., Wang, H., Robinson, Z. P., Wang, X., Wu, J., & Li, F. (2017). The feasibility and challenges of energy self-sufficient wastewater treatment plants. *Applied Energy*. https://doi.org/10.1016/j.apenergy.2017.02.069

Gurobi Optimization LLC. (2019). *Gurobi Optimizer reference manual* (tech. rep.).

Gurobi Optimization LLC. (2017). Switching from Another Solver to Gurobi. https://www.gurobi.com/pdfs/webinars/switching-to-gurobi-webinar-slides.pdf

Hall, J. W., Mortazavi-naeini, M., Borgomeo, E., Baker, B., Gavin, H., Gough, M., Harou, J. J., Hunt, D., Lambert, C., Piper, B., Richardson, N., & Watts, G. (2019). Risk-based water resources planning in practice : a blueprint for the water industry in England, *0*, 1–14. https://doi.org/10.1111/wej.12479

Hall, J. W., Tran, M., Hickford, A. J., & Nicholls, R. J. (2016). *The future of national infrastructure: A system-of-systems approach*. https://doi.org/10.1017/CBO9781107588745

Huskova, I., Matrosov, E. S., Harou, J. J., Kasprzyk, J. R., & Lambert, C. (2016). Screening robust water infrastructure investments and their trade-offs under global change: A London example. *Global Environmental Change*, *41*, 216–227. https://doi.org/10.1016/J.GLOENVCHA.2016.10.007

Ishimatsu, T. (2013). Generalized Multi-Commodity Network Flows: Case Studies in Space Logistics and Complex Infrastructure Systems. *Massachusetts Institute of Technology*, (2004).

Kenway, S. J., Lam, K. L., Stokes-draut, J., Twomey, K., Binks, A. N., Bors, J., Head, B., Olsson, G., & Mcmahon, J. E. (2019). Defining water-related energy for global comparison , clearer communication , and sharper policy. *Journal of Cleaner Production*, *236*, 117502. https://doi.org/10.1016/j.jclepro.2019.06.333

Kernan, R., Liu, X., McLoone, S., & Fox, B. (2017). Demand side management of an urban water supply using wholesale electricity price. *Applied Energy*, *189*, 395–402. https://doi.org/10.1016/j.apenergy.2016.12.082

Khan, Z., Linares, P., & García-gonzález, J. (2017). Integrating water and energy models for policy driven applications . A review of contemporary work and recommendations for future developments. *Renewable and Sustainable Energy Reviews*, *67*, 1123–1138. https://doi.org/10.1016/j.rser.2016.08.043

Khan, Z., Linares, P., Rutten, M., Parkinson, S., Johnson, N., & García-González, J. (2018). Spatial and temporal synchronization of water and energy systems : Towards a single integrated optimization model for long-term resource planning. *Applied Energy*, *210*, 499–517. https://doi.org/10.1016/j.apenergy.2017.05.003

Liu, J., Hull, V., Godfray, H. C. J., Tilman, D., Gleick, P., Hoff, H., Pahl-Wostl, C., Xu, Z., Chung, M. G., Sun, J., & Li, S. (2018). Nexus approaches to global sustainable development. Springer US. https://doi.org/10.1038/s41893-018-0135-8

Liu, L., Lopez, E., Dueñas-Osorio, L., Stadler, L., Xie, Y., Alvarez, P. J., & Li, Q. (2020). The importance of system configuration for distributed direct potable water reuse. *Nature Sustainability*. https://doi.org/10.1038/s41893-020-0518-5

Loucks, D. P., van Beek, E., Stedinger, J. R., Dijkman, J. P., & Villars, M. T. (2017). *Water Resources Systems Planning and Management and Applications: An Introduction to Methods, Models and Applications* (Vol. 51). https://doi.org/92-3-103998-9

Majid, A., Cardenes, I., Zorn, C., Russell, T., Colquhoun, K., Bañares-Alcantara, R., & Hall, J. W. (2020). An Analysis of Electricity Consumption Patterns in the Water and Wastewater Sectors in South East England, UK. *Water*, *12*(1), 225. https://doi.org/10.3390/w12010225

Matrosov, E. S., Huskova, I., Kasprzyk, J. R., Harou, J. J., Lambert, C., & Reed, P. M. (2015). Many-objective optimization and visual analytics reveal key trade-offs for London's water supply. *Journal of Hydrology*, *531*, 1040–1053. https://doi.org/10.1016/J.JHYDROL.2015.11.003

Menke, R., Abraham, E., Parpas, P., & Stoianov, I. (2016). Demonstrating demand response from water distribution system through pump scheduling. *Applied Energy*, *170*, 377–387. https://doi.org/10.1016/j.apenergy.2016.02.136

Mortazavi-Naeini, M., Bussi, G., Hall, J. W., & Whitehead, P. G. (2019). Assessment of risks to public water supply from low flows and harmful water quality in a changing climate. *Water Resources Research*. https://doi.org/10.1029/2018WR022865

Parkinson, S. C., Makowski, M., Krey, V., Sedraoui, K., Almasoud, A. H., & Djilali, N. (2018). A multi-criteria model analysis framework for assessing integrated water-energy system

transformation pathways. *Applied Energy*, *210*, 477–486. https://doi.org/10.1016/j.apenergy.2016.12.142

Plappally, A. K., & Lienhard, J. H. V. (2012). Energy requirements for water production, treatment, end use, reclamation ,and disposal. *Renewable and Sustainable Energy Reviews*, *16*(7), 4818–4848. https://doi.org/10.1016/j.rser.2012.05.022

Porse, E., Mika, K. B., Escriva-Bou, A., Fournier, E. D., Sanders, K. T., Spang, E., Stokes-Draut, J., Federico, F., Gold, M., & Pincetl, S. (2020). Energy use for urban water management by utilities and households in Los Angeles. *Environmental Research Communications*, *2*(1), 015003. https://doi.org/10.1088/2515-7620/ab5e20

Price, J., Zeyringer, M., Konadu, D., Sobral, Z., Moore, A., & Sharp, E. (2018). Low carbon electricity systems for Great Britain in 2050 : An energy-land- water perspective. *Applied Energy*, *228*(June), 928–941. https://doi.org/10.1016/j.apenergy.2018.06.127

Rothausen, S. G., & Conway, D. (2011). Greenhouse-gas emissions from energy use in the water sector. Nature Publishing Group. https://doi.org/10.1038/nclimate1147

Samani, H. M. V., & Mottaghi, A. (2006). Optimization of Water Distribution Networks Using Integer Linear Programming. *Journal of Hydraulic Engineering*. https://doi.org/10.1061/(asce)0733-9429(2006)132:5(501)

Scanlon, B. R., Ruddell, B. L., Reed, P. M., Hook, R. I., Zheng, C., Tidwell, V. C., & Siebert, S. (2017). The food-energy-water nexus: Transforming science for society. https://doi.org/10.1002/2017WR020889

Swamee, P. K., & Sharma, A. K. (2013). Optimal design of a sewer line using Linear Programming. *Applied Mathematical Modelling*. https://doi.org/10.1016/j.apm.2012.09.041

Thames Water. (2014). *Water Resources Management Plan 2014 (WRMP 14)* (tech. rep. June). Reading.

Tomlin, J. A. (1966). Minimum-Cost Multicommodity Network Flows. *Operations Research*. https://doi.org/10.1287/opre.14.1.45

Vakilifard, N., Anda, M., Bahri, P. A., & Ho, G. (2018). The role of water-energy nexus in optimising water supply systems – Review of techniques and approaches. *Renewable and*

Sustainable Energy Reviews, *82*(June 2016), 1424–1432. https://doi.org/10.1016/j.rser.2017.05.125

van Rossum, G., & Drake, F. (2011). *The Python Language Reference Manual*. https://doi.org/10.1159/0000113495

Watson, J., & Rai, N. (2013). Governance interdependencies between the water & electricity sectors, 50. https://itrc.ouce.ox.ac.uk/wp-content/PDFs/Water-Energy-Case-study-for-publication-final.pdf

Wickham, H., & Grolemund, G. (2017). *R for Data Science: Import, Tidy, Transform, Visualize, and Model Data*.

Wu, W., Maier, H. R., Dandy, G. C., Arora, M., & Castelletti, A. (2020). The changing nature of the water–energy nexus in urban water supply systems: a critical review of changes and responses. *Journal of Water and Climate Change*, 1–28. https://doi.org/10.2166/wcc.2020.276

Wurbs, R. A. (2005). Modeling river/reservoir system management, water allocation, and supply reliability. *Journal of Hydrology*, *300*(1-4), 100–113. https://doi.org/10.1016/j.jhydrol.2004.06.003

Chapter 4

Case-study: energy flexibility and water

Abstract

Urban water systems can be highly energy intensive. Yet, they are also excellent candidates for demand-side response since they possess readily controllable operations and large amounts of storage. However, real-worlds trials have delivered mixed results, which implies the need to understand the underlying mechanisms of flexibility in water operations. This paper studies the potential to shift energy demand in an urban water system located in the River Thames basin, a region encompassing the city of London, England. Results show that the system could theoretically shift up to 20.1% of its annual energy demand for pumping (2.1 GWh), saving the local water utility around £5.6 million in electricity costs. However, the water system's flexibility is shown to be highly variable due to the variability in water demands and electricity prices, in-turn affecting the financial returns from demand-side response. Sensitivity analysis reveals that factors such as the seasonal reservoir control strategies and total storage capacity are key determinants of system flexibility. A relationship between water storage capacity and flexibility is also derived, which could be used to estimate water sector flexibility in other regions.

4.1 Introduction

Energy systems are undergoing a period of rapid transition. Conventional modes of power generation, such as coal and gas fired power plants, are being replaced by relatively lower carbon electricity systems such as solar photovoltaics and wind turbines. Whilst this transition is essential for decarbonisation, the increased production from renewable energy is also introducing more complexity to the energy grid (Kroposki et al. 2017). Output from wind and solar are inherently variable, depending upon stochastic weather processes (wind speed and solar irradiance), and so their electrical output is only partially predictable and not necessarily matched to variation in demand. Therefore, increased penetrations of renewables into the energy system is highly disruptive to grid-balancing activities, the act of continuously matching consumer demand to energy supply. A number of approaches will be important in managing this volatility, one of which is demand-side response response (Behrangrad 2015).

4.1.1 Demand-side response

Electricity utilities across the world are actively deploying demand-side response (DSR) schemes. DSR is broadly defined as short-term changes in a user's normal electricity use in order to better match demand with available supplies (Albadi et al. 2007). The availability of supplies, relative to demand, may be signalled by the spot prices of electricity (units: monetary cost per unit electricity consumption). When considered alongside local generation, energy loads, and storage capacity, DSR will play a pivotal role in the widespread uptake of renewable energy supplies by allowing the energy system to shed energy demand during periods of insufficient supply and vice versa. There are three categories of DSR as noted by Albadi et al. (2007):

1. **Curtailment:** Customer responds to high electricity prices by reducing their usage.

This is an on-off operation and is usually associated with a short-term loss of service.

2. **Substitution:** Customer responds to high electricity prices by switching to a different energy source (*e.g.* onsite generation). This is an on-off operation and service is maintained.

3. **Shifting:** Customer shifts the 'flexible' portion of their energy demand from peak to off-peak periods. This is suitable for storage-type customers and service is maintained.

Ideas surrounding DSR mechanisms have existed for many years (Gellings 1985), but they are only now starting to be deployed as the energy sector modernises its information systems. It has long been understood that large industries—normally the biggest consumers of electricity within a country—are the best initial targets for DSR since these processes contain large controllable loads and a relatively low cost per control point (Roos 1998). Industries such as agriculture, manufacturing, waste management, and digital and telecommunications could bring substantial economic benefits whilst facilitating sustainable development (Heffron et al. 2020). For example, Papadaskalopoulos et al. (2018) estimate that flexible industrial demand could lower generation and transmission costs in Europe by up to €4.3 billion per annum. Meanwhile, the owner and operator of the high voltage transmission network in the United Kingdom (UK), National Grid, recently quoted that DSR will save the UK economy an additional £17–40 billion up to 2050 (National Grid 2018). The water sector is one such industry that is regularly touted as an excellent candidate for DSR.

4.1.2 Flexible operations in the water sector

The water industry is responsible for sourcing, cleaning, and delivering water to consumers on-demand. Figure 4.1 shows a simplified representation of a typical urban water supply system. Raw water is pumped into impounding storage reservoirs before being further pumped for treatment. Treated water is then conveyed through transmission mains to service

reservoirs or water towers at elevation near to population centres. Finally, water is delivered to the service area through distributional mains, where sufficient pressure is generated through gravitation.

Pumped water supply networks can provide DSR through a mechanism that is generally analogous to pumped hydro storage schemes. Pumps are activated during times of abundant renewable output or cheaper tariffs, and vice versa. The operations of large centrally owned pumps are interruptible and discrete. These pumps do not necessarily need to operate round the clock, but rather in relation to defined operational control curves set by network managers. There is a high degree of flexibility in the system since pumps can be dynamically controlled and both raw and treated water can be stored.

The benefits from DSR in the water industry could be substantial in terms of both the load shifted and costs saved. Pumps can account for around 70–80% of the total electricity consumption in the sector (Liu et al. 2012), while costs associated with electricity are the dominant operational expense for water companies (Majid et al. 2020).

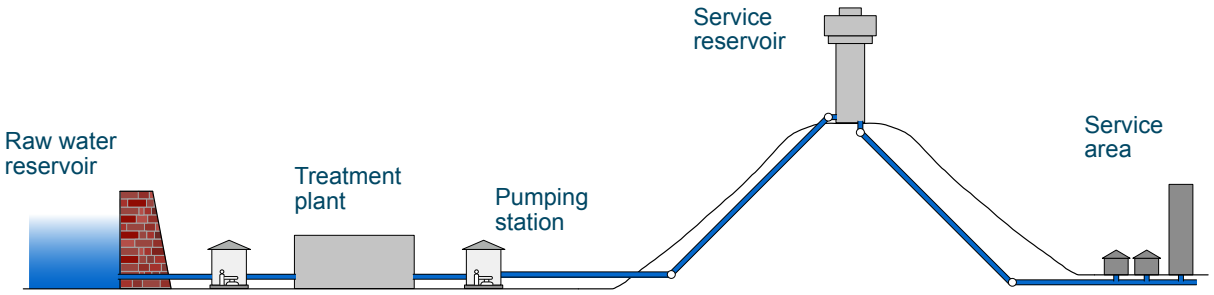


Figure 4.1: An illustration of a typical urban water supply system. The direction of flow is from left to right.

There is a growing but still scarce body of literature exploring the benefits of flexibility from pumped water supply systems. These studies have provided numerous insights. Firstly, a number of previous works have shown load shifting in water pumping schemes can yield substantial economic benefits for water operators. van Staden et al. (2011) demonstrated this in a water pumping scheme from a water purification plant in the Tshwane municipality, South

Africa. This study showed the plant could lower its electricity costs by 5.8% by dynamically altering its load relative to a price signal. Several studies have followed to demonstrate the benefits of optimal pump scheduling in water systems located in areas such as Ireland Kernan et al. (2017), France Mkireb et al. (2019), and the United States Oikonomou et al. (2018c). These works have reported varying monetary and environmental benefits from DSR in water systems, which is likely due to regional differences in climate, geography, market conditions and engineering practices Perrone et al. (2011).

Studies have also shown that DSR from pumped water networks provide benefits wider than merely economic savings for water utilities. In a series of studies from the UK, Menke et al. (2015), Menke et al. (2016), and Menke et al. (2017) studied the financial and environmental benefits of DSR from water pumps. Their analyses showed that the greenhouse gases (GHG) generated from water sector DSR (470–571 gCO2e/kWh) were much lower than alternative reserve technologies such as open-cycle gas turbines (480–575 gCO2e/kWh) and internal combustion diesel (520–700 gCO2e/kWh). Zohrabian et al. (2021a) also studied the GHG benefits from water system DSR. The paper presented an illustrative case-study that considered a 5% shift in the total daily average electricity load of 97 water-supply utilities in California. Their simulations demonstrated a substantial reduction in annual carbon dioxide emissions of 2–5%. Meanwhile, Meschede (2019) showed that pumped domestic water storage systems can increase the uptake of renewable energies in a small remote-island infrastructure system by providing DSR. Thus water system DSR does not only provide water operators financial rewards, but also delivers mutual benefits for energy managers by shaving peak-demand curves at a lower carbon-intensity than competing technologies.

Most of the studies to date have used electricity prices as a market signal for optimising pumping schedules. However, the tariff structure has differed between studies. Some works (Takahashi et al. 2017; Wei et al. 2020) adopted time-of-use (hereinafter TOU) style tariffs in which the price curve is usually split into no more than four discrete intervals. Such price regimes generally incentivise pumping overnight during off-peak hours for energy operations.

Other studies (Oikonomou et al. 2018a; Oikonomou et al. 2018b; Singh et al. 2020) have adopted wholesale real-time pricing (hereinafter RTP) tariffs and hence incorporate the real-time dynamics of energy markets. Kernan et al. (2017) used RTP tariffs to demonstrate DSR in a water network from Belfast, Northern Ireland, reporting 3–13% reductions in operational costs. The paper argued that RTP tariffs can be more profitable than TOU structures as they comprise a higher level of volatility that can be exploited. However, the study did not directly compare the benefits from RTP and TOU price profiles.

Though hardly acknowledged in the literature so far, water system DSR is not without its risks. Mkireb et al. (2019) optimised pumping schedules in an urban water system relative to RTP signals under a French DSR mechanism. The paper adopted scenario analysis to study the influence of water demand uncertainty on the economic benefits from DSR. Their findings demonstrated that water-related DSR is less profitable if demand uncertainties are not adequately incorporated.

There remain substantial gaps in the literature on water system DSR. The following gaps were identified for this paper, which to the best of the authors' knowledge have not previously been studied:

- **The influence of temporal variability in water demands on DSR:** Municipal water demands exhibit significant variability in both the short and long term. Contributing factors to seasonal and random variability include household sizes, income, social status, and climate (van Zyl et al. 2008). Studies to date have either assumed water demands to remain fixed (Meschede 2019) or adopt a short temporal horizon for the study (Mkireb et al. 2019). There is a need to understand how long-term variability in water demands can influence water system flexibility.
- **Comparison of TOU and RTP tariffs:** TOU and RTP style tariffs have not yet been directly compared despite some arguing that RTP is much more profitable (Kernan et al. 2017). This is an important factor to consider given that RTP pricing entails a greater

level of risk since the consumer is exposed to more market volatility.

- **Trade-off between operational risk and financial benefits from DSR:** Water storages (impounding and service reservoirs) follow strict operational curves, which vary seasonally based on the risk attitudes of operators. Running reservoirs to lower levels provides more flexible potential for DSR. Yet, running at a low level risks not being able to supply unexpected demand or vulnerability to droughts. This trade-off so far remains explored.
- **Identification of key parameters influencing water system flexibility:** Most studies to date have been devoid of sensitivity analyses. As such, the key parameters that have the most impact on water system flexibility have not been investigated. This study explores the influence of parameters such as water storage, pump capacity and tariff structure on DSR potential in water networks.

4.1.3 Paper scope and contribution

In light of the knowledge gaps discussed above, the aim of this paper is to address the following questions: (1) How does temporal variability in the water system influence its DSR potential? (2) Can water systems provide more flexibility under an RTP tariff when compared with a TOU tariff? If so, are the economic returns worth the greater operational risk? (3) What are the key parameters influencing water system flexibility?

To answer the questions above, this paper adopts a system-level approach to explore the potential for demand-side response in a real-world urban water supply network under temporal variability. An open-source simulation model is developed to conduct scenario analysis. The water supply system from the River Thames basin is studied, a region encompassing the mega-city of London, England. The energy flexibility in the local water system is quantified subject to the strict reservoir control strategies of the local water utility, as well as seasonal and random variability in water demands.

The main contributions of this paper can be summarised as follows:

1. Water system DSR is shown to be beneficial in terms of economic savings for water companies and increased energy grid flexibility, but these gains are highly variable, a fact that may deter decision-making investors.
2. Through scenario and sensitivity analyses, a trade-off between operational risk and DSR benefits is presented, providing water managers a framework for navigating these trade-offs.
3. A generalised relationship between water system storage and flexibility is derived for the first time, which can enable an estimation of water system flexibility beyond the case-study region.

The remainder of this paper is structured as follows: Section 5.3 introduces the mathematical formulation of the simulation model. Section 4.3 describes the Thames basin in detail, as well as the setup for the scenario and sensitivity analyses. Section 5.4 presents the results, discussion, limitations and area for future work. Section 4.5 concludes the paper.

4.2 Mathematical framework

This section outlines the mathematical and software setup of the simulation model developed to study DSR potential in water networks.

4.2.1 Simulation model overview

Simulation models are commonly used in water resources engineering. A simulation model is a representation of a system that is used to predict the behaviour of the system under

a given set of conditions. It allows for exhaustive explorations of '*what-if*' scenarios (Loucks et al. 2017). A common approach to model water systems is to use linear programming (LP) (Wurbs 1993). For example, Meschede (2019) developed a mixed-integer LP to simulate optimised dispatch from pumps in a water supply system on a remote island. Moreover, LP-based models have also been used in a number of previous works that have studied DSR in industrial water systems. As such, this study also uses LP, where the model can generally be described as:

minimise: Cost of pumped flow

subject to: (1) Conservation of mass flow
(2) Supply and demand constraints
(3) System operational rules

The proceeding subsections outline the mathematical setup of the simulation model. The objective function, decision variables, and constraints of the optimisation model are described.

4.2.2 General formulation

The water supply system is considered as a directed network $\mathcal{G} = (\mathcal{N}, \mathcal{A})$, where $\mathcal{N}$ and $\mathcal{A}$ denote a set of nodes ($n \in \mathcal{N}$) and arcs ($(i, j) \in \mathcal{A}$). Arcs in the network carry the flow of water q_{ij} from node i to j. Nodes represent supply nodes if the supply S is $S_{i,t} > 0$; a sink node if $S_{i,t} < 0$; and a junction node if $S_{i,t} = 0$. Junction nodes have neither supply nor demand and instead serve as either storage units or to join or split arcs. For example, reservoirs are classified as junction nodes, as are channels that merge flows of water.

4.2.2.1 Objective function

The objective of the LP optimisation routine is to minimise the total cost of electricity $\mathcal{C}$ across the simulation period such that:

$$\min\ \mathcal{C} = \sum_{t=1}^{T} c_t P_t \tag{4.1}$$

where c_t represents the cost of electricity (£/kWh) at time $t \in T$ and P represents the energy requirements of the pump (kWh). The energy consumption P at node i is calculated as:

$$P_i = \frac{q_{ij,t}\rho g h_{ij}}{\eta} \ \ \forall\ (i,j) \in \mathcal{A} \text{ and } t \in T \tag{4.2}$$

where q is the volumetric flowrate (m^3/s) from node i to j and is the decision variable within the optimisation programme. The terms ρ and g are constants representing the density of water (assumed as 1000 kg/m^3) and acceleration due to gravity (assumed as 9.81 m/s^2), respectively. Meanwhile, the term h_{ij} is the total head gain between i and j, where as η is the pumping efficiency (%) (Table 4.1).

4.2.2.2 Pumping constraints

A number of constraints are observed as with all optimisation models. Firstly, pumping stations in the network have capacity constraints in that their total outflow must be below a maximum value $\hat{q}$ and above a minimum value $\check{q}$. This is defined as equation 4.3:

$$\check{q}_{ij} \leq q_{ij} \leq \hat{q}_{ij} \ \ \forall\ (i,j) \in \mathcal{A} \tag{4.3}$$

The number of pump switches per day were not constrained as no data were available on these at a system-scale. Modern pumping stations can handle numerous switches each day without significantly altering the maintenance costs (Drinking Water Inspectorate 2017), and so these costs were ignored here. However, excessive pump switching can have an adverse effect on the system as dynamic loads could cause fatigue or transient related failures (Menke et al. 2016). Therefore, the number of pump switches are tracked and reported in the results.

4.2.2.3 Conservation constraints

Conservation of mass is observed throughout the network such that:

$$\sum_{j:ij\in\mathcal{A}} q_{ij,t} - \sum_{j:ij\in\mathcal{A}} q_{ji,t} = S_i \;\; \forall\, i \in \mathcal{N} \text{ and } t \in T \tag{4.4}$$

The constraint shown by equation 4.4 ensures that supply and demand is met throughout the network at each time step. The mass balance constraint at storage reservoir nodes $n_{res} \in \mathcal{N}$ is defined as:

$$v_{i,t} = v_{i,t-1} + \sum_{j:ij\in\mathcal{A}} q_{ij,t} - \sum_{j:ij\in\mathcal{A}} q_{ji,t} \;\; \forall\, i \in n_{res} \text{ and } t \in T \tag{4.5}$$

$$\check{v}_i \leq v_{i,t} \leq \hat{v}_i \;\; \forall\, i \in n_{res} \text{ and } t \in T \tag{4.6}$$

where v refers to the storage reservoir volume (m^3) at a given time step, $\check{v}$ is the minimum reservoir level to be maintained, and $\hat{v}$ is the storage capacity. Storage losses as a result of evaporation and leakage were neglected.

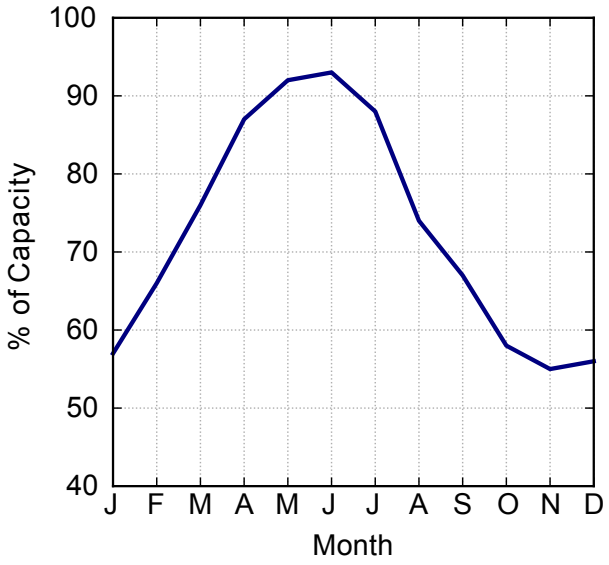


Figure 4.2: Thames basin storage reservoir control curve (Thames Water 2014).

4.2.2.4 Impounding reservoir control

Raw water storage reservoirs ($n_{rw} \in \mathcal{N}$) assume a seasonal control curve, such as that shown by Figure 4.2. The curve defines the minimum storage levels to maintain in each month ($m \in \mathcal{M}$) through the year. This operational feature is constrained as:

$$v_{i,t} \geq f_{id=AM]m}\hat{v}_i \;\; \forall \; i \in n_{rw} \text{ and } id = AM]m \in \mathcal{M} \tag{4.7}$$

where $f \in [0.0, 1.0]$ denotes a fractional component and $\hat{v}_i$ is the capacity of raw water storage node i. A unique f value is inferred for each month based on the seasonal control curve.

4.2.2.5 Service reservoir control

The control strategy of service reservoirs ($n_{sr} \in \mathcal{N}$) differs from that of raw water reservoirs. Service reservoirs are typically built to hold twice the average annual water demand

(van Zyl et al. 2008). A standard operational strategy is to recharge the reservoir to capacity once per day, normally overnight in preparation for the following day of service. This was the assumed operational strategy in the simulation model and constrained as:

$$v_{i,t} = k\hat{v}_i \;\; \forall \, i \in n_{sr} \text{ and } t \in id = AM]L \tag{4.8}$$

where $L \subset T$ and denotes the time steps in which service reservoir nodes are refilled. The variable $k \in [0.0, 1.0]$ is a fractional component representing the percentage of capacity to which the reservoir i is refilled to. The influence of parameter k on the system's flexibility potential is explored through scenario and sensitivity analysis (described in the proceeding sections).

4.2.3 Sensitivity analysis

A global sensitivity analysis was carried out to capture the uncertainty in the model output and characterise the key parameters in the optimisation. This technique was preferred over local methodologies for sensitivity analyses as it is more suited to complex systems such as water networks (Saltelli et al. 2008). Moreover, it can facilitate the understanding of interactions between model parameters and their influence on the objective function.

The following parameters were evaluated: (i) reservoir operational capacity $\hat{v}$, (ii) pumping station capacity q_{ij}, (iii) fractional recharge parameter k, and (iv) recharge times $t \in L$. For each of these parameters, a set of values were generated within respective parameter bounds using the Morris sampling approach (Morris 1991). This allows for optimal distribution of parameter values between the bounds. The model was then iteratively ran for each of the parameter sets generated and the objective function was evaluated. Further details regarding this methodology can be found in Morris (1991) and Herman et al. (2017).

4.2.4 Software carpentry

The model developed here is formulated entirely in Python, an interpreted high-level programming language that emphasizes code-readability and can support numerous important programming paradigms such as object-orientation, functionality, and procedural (van Rossum et al. 2011). The LP optimisation model is formulated using the GurobiPy package for Python, which is a popular library used to formulate optimisation problems (Gurobi Optimization Inc. 2019). The optimisation problem is solved using the Gurobi solver (Gurobi Optimization Inc. 2019). The open-source SALib library was used for the global sensitivity analysis. All of the software used in this work, as well as the sub-dependent libraries, are free to download and use for academic purposes. The model developed and applied in this work is openly available (Majid 2021; Majid et al. 2022).

4.3 Case-study: Thames basin, England

The model described in Section 5.3 was applied in a case-study from the River Thames basin, which is located in South East England and encompasses the region of Greater London. Figure 4.3 shows a map of the River Thames basin, as well as a schematic of the local water supply network as modelled in this study. This section describes the water supply system in the Thames region and the model setup.

4.3.1 System description

The River Thames basin area covers around 16,200 km^2. Water is supplied from a combination of groundwater and surface waters, as well as from one desalination plant (Thames Water 2014). There are approximately 15 million customers supplied with water every day and the mean water usage is around 160 L/person/day (Thames Water 2014). Regional water supply

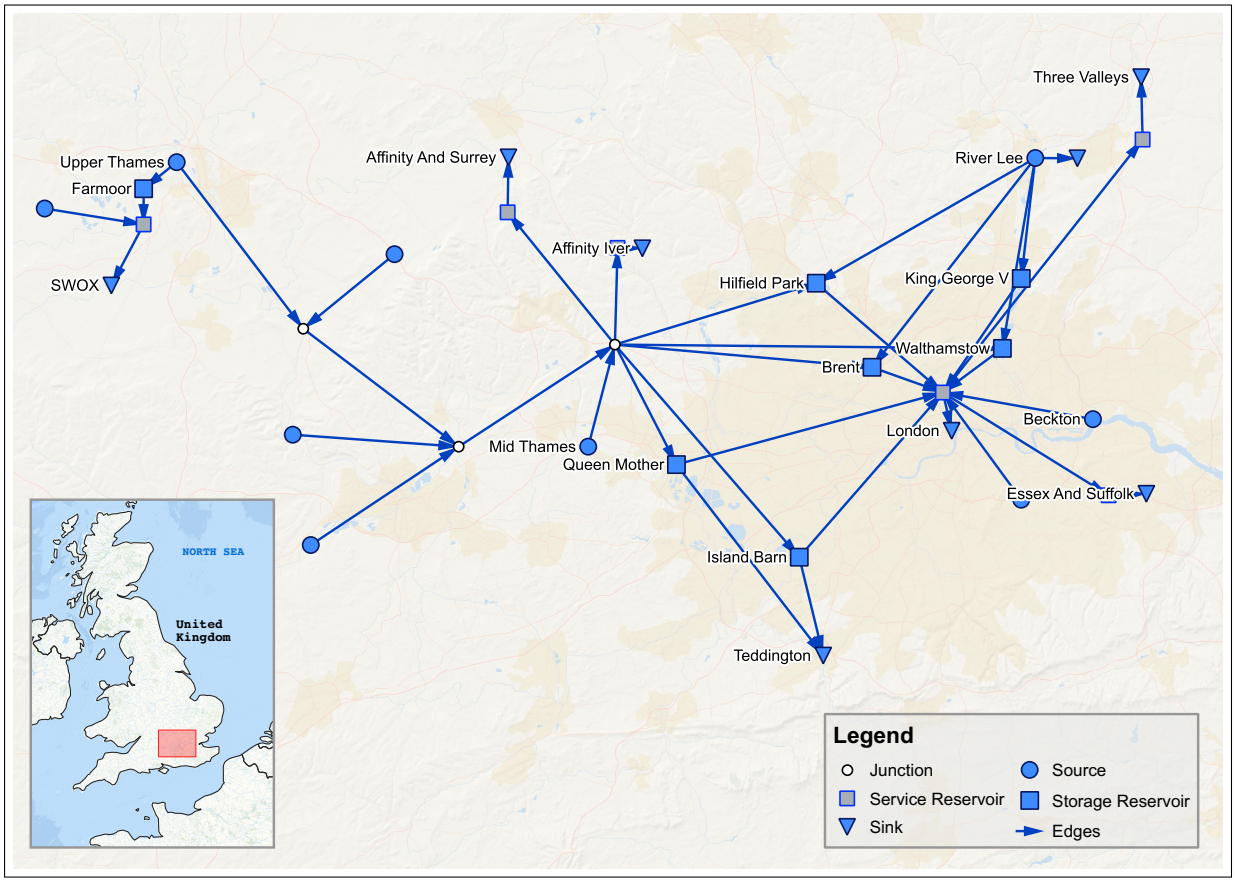


Figure 4.3: Schematic of a simplified network model of the water supply system in the River Thames basin in South East England.

infrastructure includes 32,000 km of water mains, 97 water treatment works, 26 raw water service reservoirs, 308 clean water pumping stations and 235 clean water service reservoirs, all of which can consume around 556 GWh per annum (Majid et al. 2020). Moreover, pumping for water supply accounts for approximately 56% of total electricity usage in the water system.

Table 4.1: Parameters and assumptions related to the case-study system.

Variable	Value	Units
Mean daily demand	3	GL
Raw water storage	216	GL
Service reservoir capacity	10	GL
Service reservoir recharge time	02:00	-
Pumping capacity	3800	ML/h
Assumed pumping efficiency	80	%

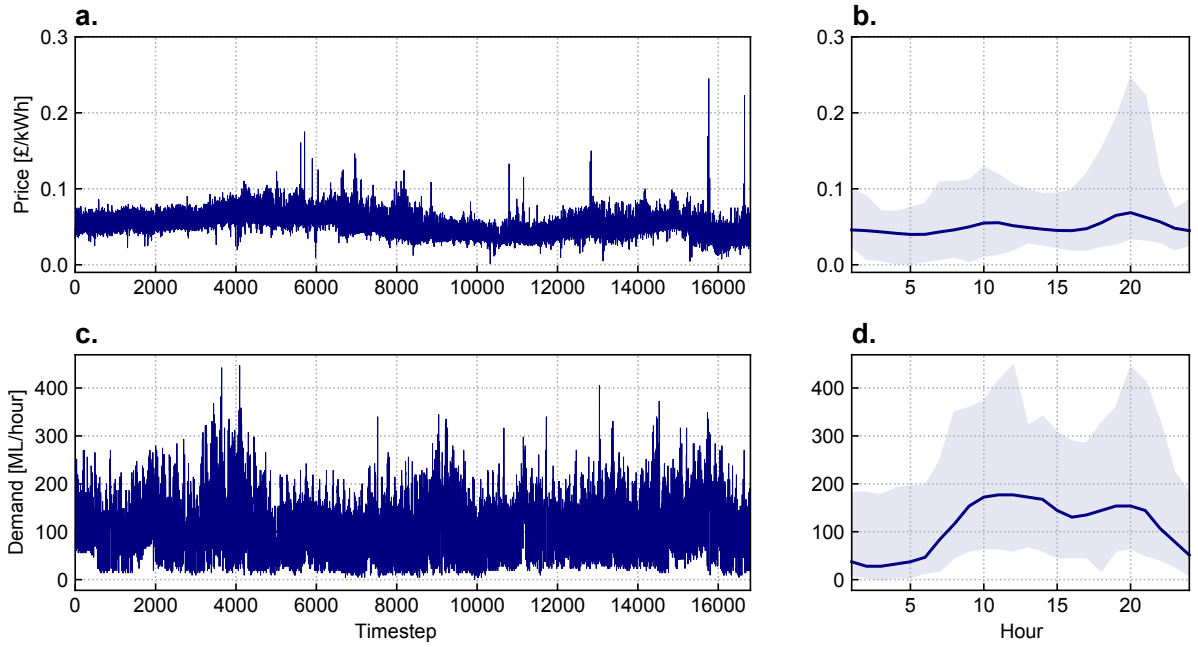


Figure 4.4: Electricity price and water demand data. Panel plots (a) and (c) show time series of prices and demands, respectively. Panel plots (b) and (d) show hourly medians of the price and water demands, where the shaded area shows the minimum and maximum observation for each hour.

The network model developed here is a highly simplified representation of the real system in the basin. The system is represented as a network comprised of 32 nodes and 40 arcs (Figure 4.3). There are seven impounding storage reservoirs and six service reservoirs with a combined capacity of 216,650 ML and 10,000 ML, respectively. Raw water storage reservoirs observe the control curve shown by Figure 4.2. The control curve was provided by the local water utility and is based on their internal analyses of water shortage risks (Thames Water 2014). At each time step in the simulation, the term f_m is inferred from the curve shown by the figure. For instance, an $f = 0.92$ is assumed for all time steps that fall within May. Meanwhile, a combination of service reservoir strategies are evaluated through scenario analysis, which reflect different operational risk appetites (discussed later in Section 4.3.4).

The operational rules and constraints within the system model were implemented with reference to the local water utility's water models and have previously been validated with

good agreement (Mortazavi-Naeini et al. 2019). The assumed parameters within the case-study system are shown by Table 4.1.

4.3.2 Electricity prices

A historical record of electricity spot prices was used following previous studies (Kernan et al. 2017). Price data was obtained from the N2EX market database, which comprises data related to the power exchange market in Great Britain and is managed by the Nord Pool group (Nord Pool 2019). The price data is a time series Y_t of wholesale electricity prices (£/kWh) at an hourly resolution (Figure 4.4a). Two peaks in the daily median prices were observed (Figure 4.4b): (i) 0.13 p/kWh at 10:00 and (ii) 0.24 p/kWh at 20:00. Electricity prices exhibit seasonal variations, though random effects are much more pronounced as compared with water demand profiles (Janczura et al. 2013).

Three price tariffs were tested in the case-study: (i) fixed-price, (ii) time-of-use, and (iii) real-time pricing. These tariffs are taken to be the market signal for demand-response. In other words, pump schedules are optimised on the basis of these price tariffs, where the price signal incentivises pump switching.

In the first case, a fixed-price electricity tariff was assumed, which is a common tariff structure for many water companies. The fixed-price tariff was calculated as the mean of the wholesale price record Y_t. Since this price signal does not exhibit any variation, this case represents a scenario without demand-response and is hence referred to as the baseline scenario (hereinafter BAS).

A time-of-use tariff splits the price curve into usually no more than four discrete intervals and is commonly used by water utilities (Finn et al. 2014). Yet, TOU tariffs vary between customers and regions, and data on these can be difficult to obtain due to their commercial sensitivity. Therefore, following previous works (Adika et al. 2014), in this study the TOU curve

was computed by averaging the wholesale price data Y_t based on four discrete time bins. The four bins z_b ($b \in \{1, ..., 4\}$) are as follows: (1) an early morning off-peak at 01:00–06:00, (2) morning to late afternoon mid-peak at 07:00–17:00, (3) evening peak at 18:00–21:00, and (4) late evening off-peak at 22:00–00:00. Each element in the series Y_t was binned into z_i based on the hour of the observation. For example, all elements in Y_t that were observed at 18:00 were placed into z_3. The tariff for each of the four TOU periods was then calculated by averaging all elements within that bin, which produced four discrete prices for the TOU curve (Figure 4.4b). This case is henceforth referred to as the TOU scenario.

The final price tariff assumed the real-time price of electricity as given by Y_t (Figure 4.4a). This represents the most volatile pricing scenario for a water utility. It is noted that this does not represent the actual cost a utility may pay in such a case but this data is not published. This case is henceforth referred to as the RTP scenario.

4.3.3 Water demands

An intra-annual demand curve was obtained from the regional water utility (Thames Water 2014) and combined with patterns of hourly water demands from (van Zyl et al. 2008). This process generated a two-year time series of hourly water demands (ML/hour) (Figure 4.4c). The figure shows significant temporal variation over the two-year period. Hourly water demands can be as low as 3 ML/hour and upper values are observed in excess of 100 ML/hour during the summer months. At the daily scale, median water demands show two clear peaks between: (1) 08:00–14:00 and (2) 16:00–21:00 (Figure 4.4d). It is noted that the water demand data shown here are only for municipal water demands as the majority of water use within the Thames basin is for public supply (Thames Water 2014).

4.3.4 Scenarios tested

As described previously in Section 4.3.2, three scenarios of electricity price tariffs were assumed: (i) BAS, (ii) TOU, and (iii) RTP. In addition to these, two service reservoir control strategies were also incorporated into the scenario analysis. The first is a risk-averse (RA) strategy, where service reservoirs are charged to capacity once per day. The second control strategy does not impose such a condition on the system and is known as the risk-neutral (RN) state. The RA and RN operations reflect the two extremes of an operator's risk attitudes and as such allows for the bounds of flexibility from service reservoirs to be explored.

Table 4.2: Experimental setup for the scenario analysis. The Boolean operator indicates whether service reservoirs are constrained to be recharged at least once per day for a given scenario.

Scenario	Price Tariff	Daily Refill
RA-BAS	Flat rate	True
RA-TOU	Time of use	True
RA-RTP	Real-time price	True
RN-BAS	Flat rate	False
RN-TOU	Time of use	False
RN-RTP	Real-time price	False

Therefore, a total of six scenarios were evaluated and these are outlined in Table 4.2. Scenarios in which a fixed-price electricity tariff was assumed (RA-BAS and RN-BAS) are non-optimised solutions and represent reference cases. Whereas under the TOU and RTP price schemes, pump schedules are optimised to minimise the total expenditure associated with pumping. The operational costs and load shifted under the TOU and RTP cases were then compared with the BAS scenarios. Further, the sensitivity of the derived results to key model parameters was also evaluated.

4.3.5 Computing flexibility

Flexibility is computed using the reference profile method following Meschede (2019). The flexible energy demand **F** (kWh) is calculated as the difference between the load curve of the non-optimised scenarios ($\mathbf{P}_{\text{BAS}}$) and scenarios with demand-response ($\mathbf{P}_{\text{DR}}$), where the area under the curve gives the flexible potential such that:

$$\mathbf{F} = \int_{a}^{b} (\mathbf{P}_{\text{BAS}} - \mathbf{P}_{\text{DR}})\, dt \tag{4.9}$$

In equation 4.9, $\mathbf{P}_{\text{BAS}}$ represent the load profiles of scenarios with fixed-price tariffs (i.e. RA-BAS and RN-BAS), whereas $\mathbf{P}_{\text{DR}}$ are the load curves of scenarios with dynamic prices. The integral is computed over the whole time series ($a = 1$ and $b = 17,520$) with respect to time.

4.3.6 Model computational requirements

The water system simulation was computed over two-year period at an hourly time resolution, making a total of 17,520 time steps. The GurobiPy optimisation routine converged to a solution in approximately 10–15 seconds on a PC with a 2.9 GHz Dual-Core Intel i5 processor and 16GB of installed RAM.

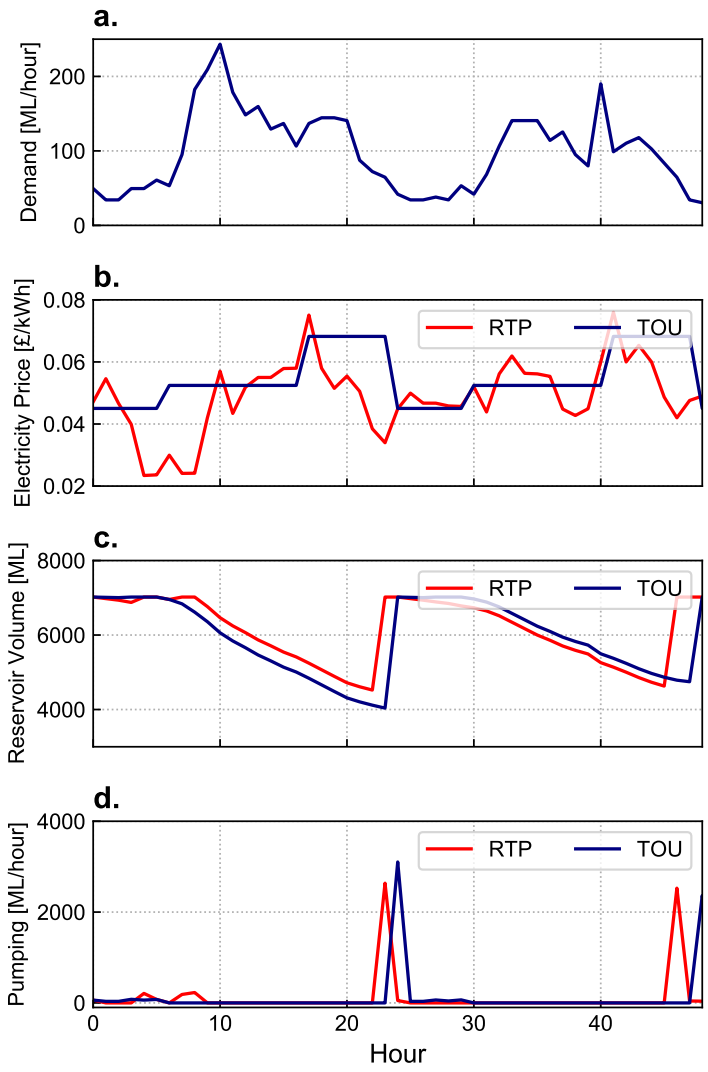


Figure 4.5: A two-day sample of hydraulic behaviour in a system operating under the risk-neutral (RN) reservoir control strategy. The panel plots show: (a) the water demand, (b) RTP and TOU prices, (c) operational storage volume under the RTP and TOU prices, and (d) pumping rates under RTP and TOU prices. In plots b–d, RTP and TOU prices are shown in red and blue, respectively.

4.4 Results and Discussion

4.4.1 Optimal pumping schedules

Figure 4.5 shows a two-day sample of the simulated hydraulic profiles from the RN-TOU and RN-RTP scenarios. The panel plots show the: (a) water demand curve, (b) RTP and TOU

price profiles, (c) service reservoir volumes, and (d) pumping rate into the service reservoir under the two price profiles. The hydraulic curves under both price regimes are similar. The majority of pumping occurred in the early morning hours with a midday top-up ahead of the second peak in water demand. In both cases, pumps were most active in the periods with the cheapest tariffs. However, under RTP pricing, the hydraulic curve shifted to the right, and a greater frequency in pumping was also observed.

Results from the six scenarios are outlined in Table 4.3. The total load for pumping under the RN and RA control strategies was measured as 10.5 GWh/year and 10.7 GWh/year. These model estimates were benchmarked against previously reported data (Majid et al. 2020) and showed good agreement. The difference in the pumping load between the two operations is due to the increased daily pumping required ($+2$ ML/hour) to recharge service reservoirs under the RA strategy. This is also highlighted by the average service reservoir volumes, which were observed to be higher under the RA strategy across all price structures.

Table 4.3: Summary of results from the six scenarios.

Mean values	Units	Baseline (BAS)	Time-of-use (TOU)	Real-time pricing (RTP)
RA				
Load for pumping	GWh/year	10.7	10.7	10.7
Pumped flow	ML/hour	120.9	120.9	120.9
Service reservoir volume	ML/hour	6,913	5,941	6,291
Total pump switch-offs	$\mathbb{N}$	11,288	14,271	15,683
Flexible load	GWh/year	–	0.3 (2.5%)‡	0.6 (5.9%)‡
Total operational cost	million	17.0	14.2 (-16.5%)†	13.9 (-18.2%)†
RN				
Annual load for pumping	GWh	10.5	10.5	10.5
Pumped flow	ML/hour	120.7	120.7	120.7
Service reservoir volume	ML/hour	2,249	5,769	3,422
Total pump switch-offs	$\mathbb{N}$	9,315	14,393	17,977
Flexible load	GWh/year	–	1.1 (10.5%)‡	2.1 (20.1%)‡
Total operational cost	million	16.9	14.1 (-16.6%)†	11.3 (-33.2%)†

†Percentage change computed relative to BAS value.
‡Percentage calculated relative to the annual load for pumping.

Across all scenarios, the mean flexible load was measured to be in the range of 0.3–2.1 GWh per annum. Further, the flexible load was substantially higher under RN operations when compared with the RA strategy. The model results showed between 10.5–20.1% of the annual load was shifted under RN, while only 2.5–5.6% could be shifted under RA. This is because RA operations require service reservoirs to be recharged at least once per day, which substantially hampers the system's flexible potential. The price structure was observed to impact the system's flexibility, where the network exhibited greater flexibility under RTP pricing in comparison to TOU. RTP tariffs show greater variations in prices, which increase the opportunity for pumps to capitalise on cheaper rates and hence increase the flexible load.

Overall, scenarios with demand-side response showed substantial reductions in electricity costs. When compared with the BAS case, the four scenarios with demand-side response exhibited operational cost reductions of 16.5–33.2%, equivalent to around £2.8–5.6 million assuming the price profiles used in this study. Thus demonstrating that water sector DSR is not only beneficial to regional energy systems, but could also be profitable for water utilities.

The benefits from DSR observed here are higher than those reported in previous studies. For example, one previous study found DSR based on TOU pricing from a small water pumping scheme in South Africa lowered operating costs by around 5.8% (van Staden et al. 2011). Meanwhile, a study from Ireland showed RTP pricing could lower costs by up to 13% (Kernan et al. 2017). There are explanations for the differences in reported data. Firstly, water systems differ significantly between regions in terms of their service demands, operational configurations, engineering design and climate, among other factors (Perrone et al. 2011). Such regional variability would clearly impact the flexible potential of water system. This highlights the need to conduct region-specific analyses when designing a energy management programme for a water system in order to maximise the efficiency of the scheme (Lam et al. 2018; Lam et al. 2017). A second reason for the differences between reported data in the literature relates to the modelling scale and assumption. Most previous studies have used short temporal horizons (*e.g.*, hours to days) and assumed water demands to remain fixed. Such model simplifications

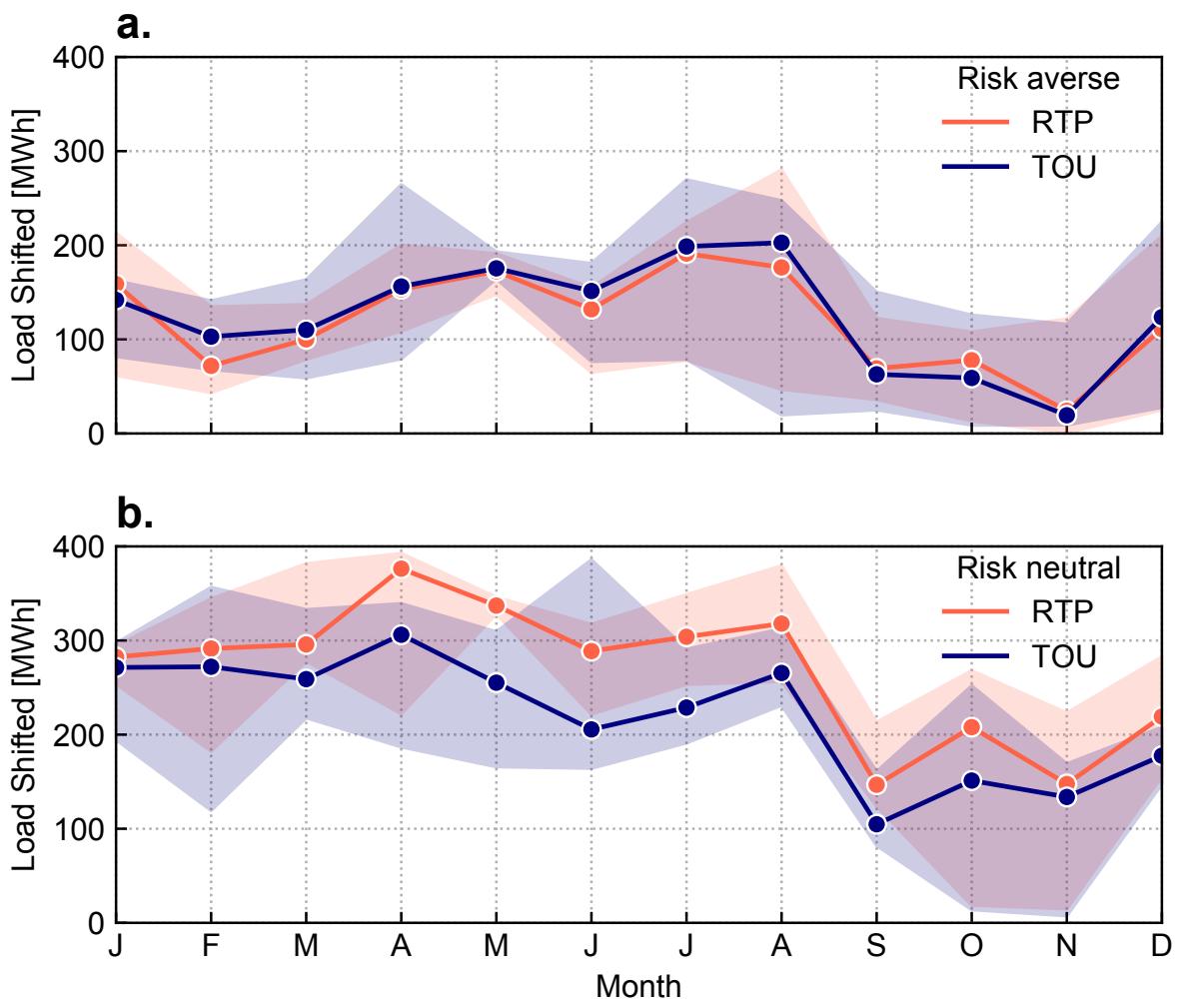


Figure 4.6: Median load shifted per month under each scenario. Shaded regions represent the 75% confidence interval.

neglect important features of a water system such as seasonal variability, which significantly impact model estimates of flexibility (discussed in the proceeding sections).

4.4.2 Temporal analysis of flexibility

The quantity of load shifted under the four scenarios with demand-side response was analysed temporally. Figure 4.6 shows the median load shifted by month under the (a) RA and (b)

RN control strategies. The shaded regions show the 75% confidence interval. The figure shows again that the energy shifted under RN exceeds that in the RA case, with median observations ranging between 4–21 MWh/month and 0.3–6.8 MWh/month, respectively. Further, a greater load was shifted under the RTP price regime when compared with TOU.

The temporal analysis reveals that the load shifted varied seasonally. Across all scenarios, the shifted load was at its lowest during the autumn months of September–November and peaked around spring. Whilst it had previously been hypothesised that water system DSR would peak during months with the lowest water demands (Mkireb et al. 2019), this current study found the opposite to be true. Water demands were found to correlate with: (1) total load shifted and (2) frequency of demand-side response events (not shown). This is because lower water demands reduces the pumping in the network and hence its energy load profile, which lowers the flexible potential.

All four scenarios with demand-side response showed significant variations in the energy load shifted. This finding has practical implications. Variability in the water system's load shifting capability will result in uncertainty in the financial returns from demand-side response. This uncertainty is further compounded by the fact that profits from DSR are inherently tied to local energy markets, which are continuously changing in the modern decarbonisation era. For example, recent changes in the UK frequency response scheme lowered the overall profits from DSR for clients in the water industry (National Grid 2019). These factors could be concerning for decision-making investors in the water sector, who may instead opt for investments that could guarantee a more stable payback. For instance, water managers may prefer to invest in upgrading older assets with more energy efficient technologies. Many water networks were constructed decades ago, so repairing and renewing equipment such as pumps and pipelines can substantially reduce energy bills (Majid et al. 2020; Wu et al. 2020). Other options include installing stand-alone wind or solar energy generation to power water pumping systems. This is advantageous as it can partially decouple a water utility from the energy grid and hence reduce their vulnerability to price shocks (Vakilifard et al. 2018). Overall,

for DSR to be an economically attractive proposition to water managers, it will be important to understand the variability in its financial returns.

4.4.3 Global sensitivity analysis

A global sensitivity analysis was carried out to capture the uncertainty in the model output and to characterise the key parameters in the optimisation model. The influence of the following parameters was tested: (i) reservoir operational capacity, (ii) pumping capacity, (iii) proportion of service reservoirs recharged daily, and (iv) the time at which reservoirs must be recharged. An overview of each of these parameters and their ranges are presented in Table 4.4. Note that the sensitivity analysis sought to understand the influence of variables on the load that could be *shifted* rather than the absolute load itself. Hence, operational assumptions such as pumping efficiency were not tested as these impact the total system load rather than flexibility.

Table 4.4: Parameters studied in the sensitivity analysis and their ranges.

Parameter	Ranges
Reservoir operational capacity	[−50%,+50%]
Pump capacity	[−50%,+50%]
Reservoir recharge quantity	[0%,100%]
Reservoir recharge time	[00:00,23:00]

The distribution of estimated load shifted (GWh/year) under the RTP and TOU price regimes is shown by Figure 4.7a. This distribution was generated by running the model assuming the sets of parameters generated by the Morris sampling. In the box plot, the bar shows the median value, while the box shows the interquartile range (25^{th} and 75^{th} percentiles). The whiskers extend to the minimum and maximum values in the id=AM]data sample. Extreme values (beyond the 95^{th} percentile) were removed and are hence not shown. The annual flexible load was observed between 0.1–2.4 GWh and 0.08–1.52 GWh in the RTP and TOU scenarios, respectively. Meanwhile, median values were observed at 1.0 GWh and 0.6 GWh for the two

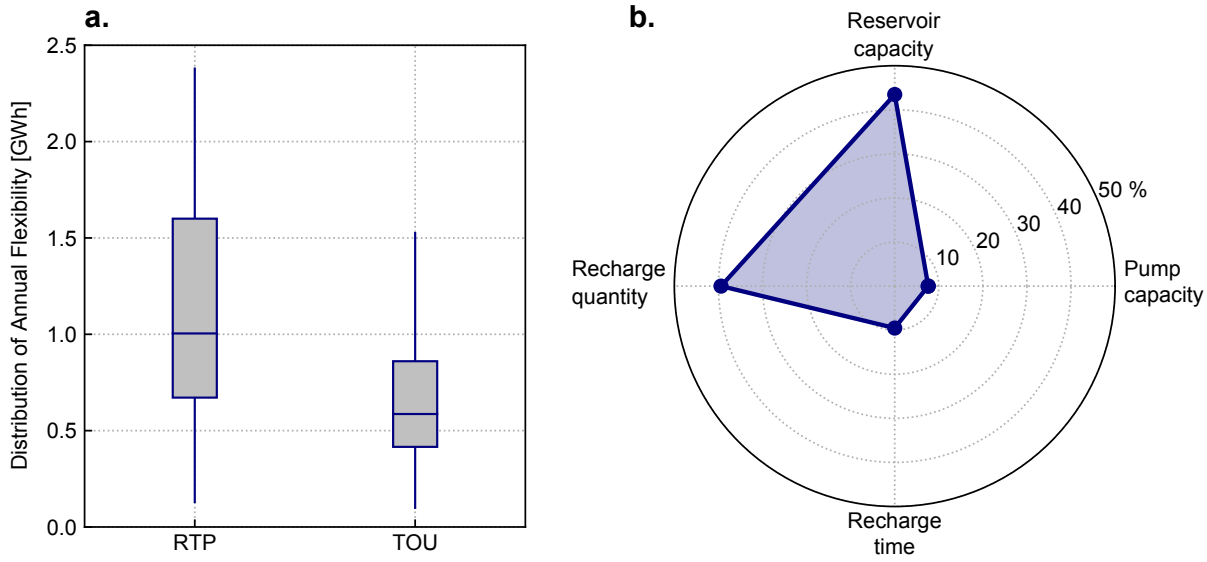


Figure 4.7: Results from the global sensitivity analysis showing (a) the distribution of annual flexibility under the time-of-use and real-time price tariffs relative to the baseline scenario and (b) the relative influence (%) on the flexibility from the four parameters listed.

price profiles, respectively.

The relative influence (%) on the load shifted from each of the four parameters is shown by Figure 4.7b. It shows that the reservoir capacity (42%) and the daily refill rate (40%) are the two most influential variables that affect system flexibility. There is also a strong interaction between these two parameters. In comparison, the influence of the service reservoir refill time (10%) and the pump capacity (8%) was relatively lower. These parameters influence the system flexibility as follows:

- **Reservoir capacity:** The reservoir capacity significantly affects the system flexibility as it relates to the network's capability to delay pumping, whilst observing reservoir control curves. Hence, increasing the storage yields a greater demand-side response potential, where the flexible potential would plateau at the point where total pumping capacity becomes a limiting factor.

- **Recharge quantity:** The daily refill rate of reservoirs strongly impacts the total system

flexibility. Increasing the recharge rate negatively influences the flexible portion of the energy demand.

- **Recharge time:** The time by which the daily recharge must be completed has a relatively minor affect on the total flexibility. This factor negatively influences the flexible potential if the recharge times are constrained to peak-price periods.

- **Pumping capacity:** Increasing the pump capacity facilitates the system in deferring a larger amount of pumping to a period with cheaper tariffs. However, the reservoir capacity, operational rules, and water demands constrain the overall flexibility pumps can provide. Hence, this factor had the lowest influence to the model output.

Overall the results from the sensitivity analysis demonstrate that the quantity of water storage in the system, as well as their control configurations, are the two most important factors in dictating the flexible potential of a pumped water network. The results also highlight a key trade-off between risk and reward. Allowing reservoirs to run at lower levels increases the flexible potential of the system. Yet, it raises the risk of being unable to meet unexpected demands.

In practice, reservoirs typically observe strict control protocols set by operators. Implementing DSR into water systems will require substantial changes to these protocols. Furthermore, assets and software will need to be upgraded in order to optimise DSR strategies. Such measures could ensure robust control strategies that can navigate the trade-offs between the profits from DSR and operational risk. Yet, it is also important to recognise that implementing these changes will challenge legacy operational practices and cultures. This could pose a significant practical barrier to wider adoption.

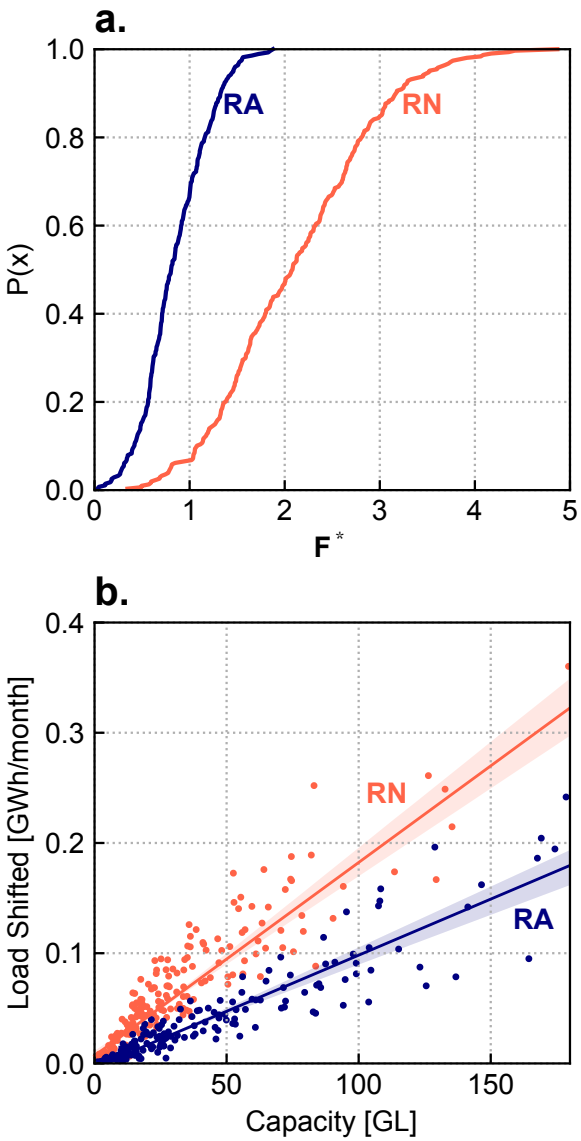


Figure 4.8: Relationship between reservoir capacity and load shifted, where (a) shows the cumulative distribution function (CDF) of $\mathbf{F}^* = \mathbf{F}/V$. and (b) a linear regression between the two parameters under the RN and RA scenarios.

4.4.4 Relating water storage and flexibility

As observed in the sensitivity analysis, water storage capacity and operational risk thresholds were found to be key determinants of the flexible potential in an urban water system. Hence, the relationship between water storage, operational risk, and energy flexibility could

serve as a meaningful indicator in gauging the flexible potential of other water systems. Figure 4.8 shows the following plots for this purpose: (a) a cumulative distribution function (CDF) of a flexibility index $\mathbf{F}^*$; and (b) a linear regression between median monthly capacity and load shifted. In Figure 4.8a, $\mathbf{F}^*$ was taken as the ratio between the shifted energy consumption $\mathbf{F}$ (kWh/month) and the total system water storage V (ML), such that:

$$\mathbf{F}^* \text{ (Flexibility Index)} = \frac{\mathbf{F}}{V} \tag{4.10}$$

In both plots, the functions are computed by averaging the results across all price structures for RA and RN operations. As such, the RA and RN series shown represent a lower and upper bound of the expected load shifting under two extreme operational strategies. For example, in Figure 4.8a, it can be observed that an $\mathbf{F}^*$ value of 0.9 and 2.3 was computed for 60% ($\mathrm{P}[x] = 0.6$) of the data points in the RA and RN case, respectively. Assuming a storage capacity of 100 GL, this would correspond to an average load shifting between 0.09–0.21 GWh/month. The regression models shown by Figure 4.8b show a similar estimate.

The derived relationship could be used to estimate the flexibility in the water sector at a system scale. Increasing the adoption of water sector DSR could have significant benefits for the energy and water sectors. In an energy system with an increasing share of renewables, the amount of flexibility and storage available to grid operators will be vital for ensuring reliable operations. Whilst significant innovations have been made in battery storage technologies, pumped water storage remains the most reliable and widespread form of energy storage and provides around 95% of the total global capacity (Hunt et al. 2020). However, the potential for pumped hydro storage is limited in many regions of the world, particularly large metropolitan regions such as that in the case-study. Yet, reservoirs in water supply may be an untapped source of flexibility and storage. In the context of the case-study area, the UK water sector currently has around 7390 GL of storage capacity (Durant et al. 2018), which is likely to be augmented in the future to cope with increasing water stresses. Based on the relationships derived here (Figure 4.8), this could theoretically provide a load shifting potential of 159–443

GWh per annum. Whilst this value is a nominal quantity of the national energy demand (0.04–0.12%), it could still nonetheless present an opportunity to realise mutual benefits for water utilities (lower operational costs) and electricity operators (system flexibility).

4.4.5 Future extensions

As with all studies that simulate complex systems, there were a number of assumptions and simplifications made in this work to constrain the scope of the study. There are several opportunities to extend this study for future research.

This current study explored priced-based demand-side response in a multi-reservoir water supply system, which is just one avenue for DSR in the water sector. As highlighted by Zohrabian et al. (2021b), there are several mechanisms by which the water sector can provide DSR. Considerable amount of pumping also occurs downstream in the water supply chain for post-use wastewater distribution, though relatively less storage is available to these systems. There is also potential for scheduling water and wastewater treatment processes at the plant level, which was also not considered here. Further, the amount of electricity used for water-related services at the consumer level are substantial (Kenway et al. 2011). For example, Escriva-Bou et al. (2018) showed that end-use of water accounted for 95% of water-related energy consumption in a Californian district. There are degrees of flexibility in how this electricity is consumed and future works could explore the potential benefits of shifting the time of water demands.

A number of assumptions were made in this work in order to keep the model setup tractable at a system scale. For example, it was assumed that all pumps in the system use variable speed drives as specific asset-level data were not available. This is not an accurate reflection of the entire water supply network in the River Thames basin. Future studies could zoom into specific areas of the Thames system and incorporate more refined asset information, as well as conduct a more detailed hydraulic analysis (Singh et al. 2020), in order to get

an improved estimate for DSR potential and risks.

A distinction made in this study was between RTP and TOU price profiles in that the latter have significantly less daily variation. It is generally the case that TOU price curves exhibit no more than four changes per day (Kernan et al. 2017). Yet, in principle, these tariffs could be made significantly more complex, and as such could better incentivise the consumer to shift their energy demand, though this remains uncommon for the moment. The fundamental difference between RTP and TOU tariffs relates to the risk. Since TOU tariffs are pre-agreed contracts, the risk stays with the energy supplier. On the other hand, under an RTP tariff, the risk shifts to the consumer as their tariff is subject to the day-to-day conditions in energy markets, which could leave them vulnerable to price shocks. Given that this study considered only two forms of price regimes, future works can explore the potential for water-related DSR under uncertainties in the energy markets.

The influence of climate variability was not incorporated into this work. It is widely understood that the global water sector is highly vulnerable to climate change with extreme weather events such as droughts becoming more frequent (Vörösmarty et al. 2000). Managing climatic risks requires careful planning of reservoir operations and management (Ahmad et al. 2014). Further work could explore the trade-offs between water system flexibility and reservoir resilience under varying climate scenarios. For example, Anghileri et al. (2018) developed a framework to devise robust hydropower operational strategies under uncertainties in future climate change and energy policies. Applying such a framework to design DSR strategies for water systems could facilitate water managers to balance climate and market risks with the rewards from DSR.

4.5 Conclusions

This study investigated the flexible potential of an urban water system located in a large metropolitan area through demand-side response based on price signals. It incorporated detailed dynamics in water demand and energy markets, as well as realistic operational parameters of a pumped water network. The main conclusions of this work are as follows:

- The regional water supply system can shift 2.5–20.1% of its annual energy demand (0.3–2.1 GWh). This could theoretically decrease electricity costs associated with pumping—often the largest operational expenditure for water companies—by around £2.8–5.6 million.
- Demand-side response (DSR) based on real-time pricing structures were found to be more profitable than time-of-use style tariffs, though the former entail substantially higher amount of risk.
- The benefits from DSR for a water utility can be significant but are highly variable across the year mainly due to intra-annual variability in water demands.
- Sensitivity analysis showed that the financial returns from DSR are highly dependant upon the storage capacity within the system, as well as the control configurations of reservoirs. It is essential to balance the trade-off between the profits from DSR and operational risk in order to devise robust DSR strategies in water systems.
- This study also derived for the first time a relationship between water system storage, operational risks, and flexible potential. This could faciliate the estimation of water sector DSR potential in other regions.

Overall, this study demonstrated that the water sector could play an important role in realising a more flexible electricity grid in the transition to a low-carbon energy sector. Yet, water

managers may be reluctant to invest into DSR schemes given that financial returns are volatile as they are inherently tied to variability within the energy and water system. Moreover, DSR at a system scale would require major cultural shifts in operations practices, an obstacle that may be difficult to surpass with network operators. Certainly, if the underlying mechanisms of demand-side response in the water sector are not properly understood, a significant potential to realise societal and economic benefit might go amiss.

References

Adika, C. O., & Wang, L. (2014). Autonomous appliance scheduling for household energy management. *IEEE Transactions on Smart Grid*, *5*(2), 673–682. https://doi.org/10.1109/TSG.2013.2271427

Ahmad, A., El-Shafie, A., Mohd Razali, S. F., & Mohamad, Z. S. (2014). Reservoir optimization in water resources: A review. https://doi.org/10.1007/s11269-014-0700-5

Albadi, M. H., & El-Saadany, E. F. (2007). Demand response in electricity markets: An overview. *2007 IEEE Power Engineering Society General Meeting, PES*, 1–5. https://doi.org/10.1109/PES.2007.385728

Anghileri, D., Botter, M., Castelletti, A., Weigt, H., & Burlando, P. (2018). A Comparative Assessment of the Impact of Climate Change and Energy Policies on Alpine Hydropower. *Water Resources Research*, *54*(11), 9144–9161. https://doi.org/10.1029/2017WR022289

Behrangrad, M. (2015). A review of demand side management business models in the electricity market. *Renewable and Sustainable Energy Reviews*, *47*, 270–283. https://doi.org/10.1016/j.rser.2015.03.033

Drinking Water Inspectorate. (2017). *What are the Drinking Water Standards?* (Tech. rep.). http://dwi.defra.gov.uk/consumers/advice-leaflets/standards.pdf

Durant, M., & Counsell, C. (2018). *Inventory of reservoirs amounting to 90% of total UK storage* (tech. rep.). NERC Environmental Information Data Centre. Wallingford. https://doi.org/https://doi.org/10.5285/f5a7d56c-cea0-4f00-b159-c3788a3b2b38

Escriva-Bou, A., Lund, J. R., & Pulido-Velazquez, M. (2018). Saving Energy From Urban Water Demand Management. *Water Resources Research*, *54*(7), 4265–4276. https://doi.org/10.1029/2017WR021448

Finn, P., & Fitzpatrick, C. (2014). Demand side management of industrial electricity consumption: Promoting the use of renewable energy through real-time pricing. *Applied Energy*, *113*(2014), 11–21. https://doi.org/10.1016/j.apenergy.2013.07.003

Gellings, C. W. (1985). The Concept of Demand-Side Management for Electric Utilities. *Proceedings of the IEEE*. https://doi.org/10.1109/PROC.1985.13318

Gurobi Optimization Inc. (2019). Gurobi Optimizer Reference Manual. *Www.Gurobi.Com*.

Heffron, R., Körner, M. F., Wagner, J., Weibelzahl, M., & Fridgen, G. (2020). Industrial demand-side flexibility: A key element of a just energy transition and industrial development. *Applied Energy*. https://doi.org/10.1016/j.apenergy.2020.115026

Herman, J. D., & Usher, W. (2017). SALib: An open-source Python library for Sensitivity Analysis. *The Journal of Open Source Software*. https://doi.org/10.21105/joss.00097

Hunt, J. D., Byers, E., Wada, Y., Parkinson, S., Gernaat, D. E., Langan, S., van Vuuren, D. P., & Riahi, K. (2020). Global resource potential of seasonal pumped hydropower storage for energy and water storage. *Nature Communications*. https://doi.org/10.1038/s41467-020-14555-y

Janczura, J., Trück, S., Weron, R., & Wolff, R. C. (2013). Identifying spikes and seasonal components in electricity spot price data: A guide to robust modeling. *Energy Economics*. https://doi.org/10.1016/j.eneco.2013.03.013

Kenway, S. J., Lant, P. A., Priestley, A., & Daniels, P. (2011). The connection between water and energy in cities: A review. https://doi.org/10.2166/wst.2011.070

Kernan, R., Liu, X., McLoone, S., & Fox, B. (2017). Demand side management of an urban water supply using wholesale electricity price. *Applied Energy*, *189*, 395–402. https://doi.org/10.1016/j.apenergy.2016.12.082

Kroposki, B., Johnson, B., Zhang, Y., Gevorgian, V., Denholm, P., Hodge, B. M., & Hannegan, B. (2017). Achieving a 100% Renewable Grid: Operating Electric Power Systems with Ex-

tremely High Levels of Variable Renewable Energy. *IEEE Power and Energy Magazine*. https://doi.org/10.1109/MPE.2016.2637122

Lam, K. L., Lant, P. A., & Kenway, S. J. (2018). Energy implications of the millennium drought on urban water cycles in Southeast Australian cities. *Water Science and Technology: Water Supply*, *18*(1), 214–221. https://doi.org/10.2166/ws.2017.110

Lam, K. L., Kenway, S. J., & Lant, P. A. (2017). Energy use for water provision in cities. *Journal of Cleaner Production*, *143*, 699–709. https://doi.org/10.1016/j.jclepro.2016.12.056

Liu, F., Ouedraogo, A., Manghee, S., & Danilenko, A. (2012). *A primer on energy efficiency for municipal water and wastewater utilities* (tech. rep.). Energy Sector Management Assistance Program, The World Bank Group. https://doi.org/ReportNo.:001/12

Loucks, D. P., van Beek, E., Stedinger, J. R., Dijkman, J. P., & Villars, M. T. (2017). *Water Resources Systems Planning and Management and Applications: An Introduction to Methods, Models and Applications* (Vol. 51). https://doi.org/92-3-103998-9

Majid, A. (2021). amanmajid/InfraSim: v0.1.0. Zenodo. https://doi.org/10.5281/zenodo.5207328

Majid, A., Cardenes, I., Zorn, C., Russell, T., Colquhoun, K., Bañares-Alcantara, R., & Hall, J. W. (2020). An Analysis of Electricity Consumption Patterns in the Water and Wastewater Sectors in South East England, UK. *Water*, *12*(1), 225. https://doi.org/10.3390/w12010225

Majid, A., van Zyl, J. E., & Hall, J. W. (2022). The influence of temporal variability and reservoir management on demand-response in the water sector. *Applied Energy*, *305*. https://doi.org/10.1016/j.apenergy.2021.117808

Menke, R., Abraham, E., Parpas, P., & Stoianov, I. (2015). Approximation of system components for pump scheduling optimisation. *Procedia Engineering*, *119*(1), 1059–1068. https://doi.org/10.1016/j.proeng.2015.08.935

Menke, R., Abraham, E., Parpas, P., & Stoianov, I. (2016). Demonstrating demand response from water distribution system through pump scheduling. *Applied Energy*, *170*, 377–387. https://doi.org/10.1016/j.apenergy.2016.02.136

Menke, R., Abraham, E., Parpas, P., & Stoianov, I. (2017). Extending the Envelope of Demand Response Provision though Variable Speed Pumps. *Procedia Engineering*, *186*, 584–591. https://doi.org/10.1016/j.proeng.2017.03.274

Meschede, H. (2019). Increased utilisation of renewable energies through demand response in the water supply sector – A case study. *Energy*, *175*, 810–817. https://doi.org/10.1016/j.energy.2019.03.137

Mkireb, C., Dembélé, A., Jouglet, A., & Denoeux, T. (2019). Robust Optimization of Demand Response Power Bids for Drinking Water Systems. *Applied Energy*, *238*(January), 1036–1047. https://doi.org/10.1016/j.apenergy.2019.01.124

Morris, M. D. (1991). Factorial sampling plans for preliminary computational experiments. *Technometrics*. https://doi.org/10.1080/00401706.1991.10484804

Mortazavi-Naeini, M., Bussi, G., Hall, J. W., & Whitehead, P. G. (2019). Assessment of risks to public water supply from low flows and harmful water quality in a changing climate. *Water Resources Research*. https://doi.org/10.1029/2018WR022865

National Grid. (2018). *Demand Side Flexibility Annual Report 2018* (tech. rep.). National Grid ESO. London. http://powerresponsive.com/wp-content/uploads/2019/04/Power-Responsive-Annual-Report-2018_19-FINAL.pdf

National Grid. (2019). Demand Side Flexibility Annual Report 2018. http://powerresponsive.com/wp-content/uploads/2020/04/Power-Responsive-Annual-Report-2019.pdf?utm_source=PR_Website&utm_medium=Website&utm_campaign=Annual%20Report%202019

Nord Pool. (2019). UK Day Ahead Auction Prices. https://www.nordpoolgroup.com/Market-data1/GB/Auction-prices/UK/Hourly/?view=table

Oikonomou, K., Parvania, M., & Burian, S. (2018a). Integrating water distribution energy flexibility in power systems operation, In *Ieee power and energy society general meeting*. https://doi.org/10.1109/PESGM.2017.8274374

Oikonomou, K., Parvania, M., & Burian, S. (2018b). Integrating water distribution energy flexibility in power systems operation. *IEEE Power and Energy Society General Meeting*, *2018-January*, 1–5. https://doi.org/10.1109/PESGM.2017.8274374

Oikonomou, K., Parvania, M., & Khatami, R. (2018c). Optimal Demand Response Scheduling for Water Distribution Systems. *IEEE Transactions on Industrial Informatics*. https://doi.org/10.1109/TII.2018.2801334

Papadaskalopoulos, D., Moreira, R., Strbac, G., Pudjianto, D., Djapic, P., Teng, F., & Papapetrou, M. (2018). Quantifying the potential economic benefits of flexible industrial demand in the european power system. *IEEE Transactions on Industrial Informatics*. https://doi.org/10.1109/TII.2018.2811734

Perrone, D., Murphy, J., & Hornberger, G. M. (2011). Gaining perspective on the water-energy nexus at the community scale. *Environmental Science and Technology*, *45*(10), 4228–4234. https://doi.org/10.1021/es103230n

Roos, J. G. (1998). Industrial power demand response analysis for one-part real-time pricing. *IEEE Transactions on Power Systems*, *13*(1), 159–164. https://doi.org/10.1109/59.651628

Saltelli, A., Ratto, M., Andres, T., Campolongo, F., Cariboni, J., Gatelli, D., Saisana, M., & Tarantola, S. (2008). *Global Sensitivity Analysis. The Primer*. https://doi.org/10.1002/9780470725184

Singh, M. K., & Kekatos, V. (2020). Optimal scheduling of water distribution systems. *IEEE Transactions on Control of Network Systems*. https://doi.org/10.1109/TCNS.2019.2939651

Takahashi, S., Koibuchi, H., & Adachi, S. (2017). Water Supply Operation and Scheduling System with Electric Power Demand Response Function. *Procedia Engineering*, *186*, 327–332. https://doi.org/10.1016/j.proeng.2017.03.257

Thames Water. (2014). *Water Resources Management Plan 2014 (WRMP 14)* (tech. rep. June). Reading.

Vakilifard, N., Anda, M., Bahri, P. A., & Ho, G. (2018). The role of water-energy nexus in optimising water supply systems – Review of techniques and approaches. *Renewable and*

Sustainable Energy Reviews, *82*(June 2016), 1424–1432. https://doi.org/10.1016/j.rser.2017.05.125

van Rossum, G., & Drake, F. (2011). *The Python Language Reference Manual*. https://doi.org/10.1159/0000113495

van Staden, A. J., Zhang, J., & Xia, X. (2011). A model predictive control strategy for load shifting in a water pumping scheme with maximum demand charges. *Applied Energy*, *88*(12), 4785–4794. https://doi.org/10.1016/j.apenergy.2011.06.054

van Zyl, J. E., Piller, O., & le Gat, Y. (2008). Sizing municipal storage tanks based on reliability criteria. *Journal of Water Resources Planning and Management*, *134*(6), 548–555. https://doi.org/10.1061/(ASCE)0733-9496(2008)134:6(548)

Vörösmarty, C. J., Green, P., Salisbury, J., & Lammers, R. B. (2000). Global water resources: Vulnerability from climate change and population growth. *Science*. https://doi.org/10.1126/science.289.5477.284

Wei, N., Zhang, R., Hua, T., & Ye, Y. (2020). Modeling and Optimization of Pumps Scheduling Considering the Time-of-use Electricity Tariff, In *Chinese control conference, ccc*. https://doi.org/10.23919/CCC50068.2020.9189152

Wu, W., Maier, H. R., Dandy, G. C., Arora, M., & Castelletti, A. (2020). The changing nature of the water–energy nexus in urban water supply systems: a critical review of changes and responses. *Journal of Water and Climate Change*, 1–28. https://doi.org/10.2166/wcc.2020.276

Wurbs, R. A. (1993). Reservoir-system simulation and optimization models. *Journal of Water Resources Planning and Management*, *119*(4), 455–472.

Zohrabian, A., & Sanders, K. T. (2021a). Emitting less without curbing usage? Exploring greenhouse gas mitigation strategies in the water industry through load shifting. *Applied Energy*. https://doi.org/10.1016/j.apenergy.2021.117194

Zohrabian, A., Plata, S. L., Kim, D. M., Childress, A. E., & Sanders, K. T. (2021b). Leveraging the water-energy nexus to derive benefits for the electric grid through demand-side man-

agement in the water supply and wastewater sectors. *Wiley Interdisciplinary Reviews: Water*, *8*(3), 1–23. https://doi.org/10.1002/wat2.1510

Chapter 5

Case-study: long-term planning

Abstract

Urban water utilities are increasing their use of energy-intensive technologies such as desalination and long-distanced pumped transfers. Under pressure to reduce their energy-related carbon emissions to zero, water utilities have devised a variety of energy management strategies, including the purchase of renewable energy and self-generation of electricity using locally installed renewables. These strategies will incur different costs for the utility, whilst some may have implications for the reliability of water supply systems. Yet the trade-offs between costs, water security and energy sustainability remain unexplored. Here, we present a regional scale analysis to test competing energy strategies, mapping pathways to zero carbon energy and water security. Results from a case-study of the London water system show a balanced approach that allows for some energy self-generation, using biogas, solar and wind, while also purchasing green energy credits from the electricity supply grid can best navigate this trade-off. Balanced investment plans can accommodate energy-intensive water supply techniques such as long-distance transfers, desalination and effluent reuse while meeting energy targets. By becoming energy generators and also adopting more flexible arrangements for energy use, water utilities could become significant players in energy markets.

5.1 Introduction

The water sector faces enormous challenges from climate change, population growth, and over-exploited freshwater resources (Vörösmarty et al. 2000). Water utilities operate a diverse portfolio of infrastructure that is responsible for conveying, treating, and delivering clean water to consumers through complex networks (Rothausen et al. 2011). These systems need to be continuously expanded or changed in order to adapt to ever-changing external conditions.

Water infrastructure are also closely linked with energy systems (Kenway et al. 2011). Substantial quantities of electricity are consumed by water utilities for processes such as pumping and treatment (Plappally et al. 2012), which are in a period of rapid change (Lam et al. 2017; Spang et al. 2015). Utilities are swiftly augmenting supplies to combat the challenges posed by climate change and demand growth. Technologies such as desalination, which can be highly energy-intensive, are becoming more prevalent (Elimelech et al. 2011). Such water sources are being explored to reduce the environmental impacts of over-exploitation of groundwater and surface water resources (Wada et al. 2014). Yet, this is causing electricity use by the water sector to grow sharply (Majid et al. 2020). This brings increased operational costs, and, unless electricity supplies are from zero-carbon sources, make a large contribution to the sector's carbon footprint.

There exist several opportunities to reduce energy use by water utilities. Ageing units within networks can be rehabilitated or replaced to enhance their energy efficiency and drive down their energy-intensiveness (Lam et al. 2018). Reducing water leakage from pipes and water use will also decrease the sector's energy use since this reduces the amount of water that needs to be conveyed and treated (Stokes et al. 2013). Sometimes incentivised by government renewable energy subsidies, water utilities have also begun to invest in local installations of renewable energy systems (RES) (*e.g.* solar, wind, and biogas). In combination, adoption of these technologies mean that water utilities are increasingly becoming energy *prosumers* (combined consumers and producers of energy). Some water companies may even become

entirely energy self-sufficient whilst exporting electricity back to the grid (Gu et al. 2017). This raises a number of questions: which RES options should utilities invest in? How much RES capacity might be needed? What are the trade-offs between water security and carbon emissions reduction? What are the costs to the utilities (and hence its customers) of these varying energy strategies? How could the uncertain future costs of RES, along with electricity price volatility, influence potential costs and benefits of such strategies? As of yet, these questions remain unanswered in the context of deeply uncertain future conditions, such as climate change, population growth, and changing electricity prices. We argue it is essential to address these questions to unravel the costs and benefits of water-related energy goals, as well as to identify the key trade-offs between water and energy.

Infrastructure planning methodologies that can capture the linkages between water and energy could help answer the questions posed above. Models that serve such purposes, often referred to as 'integrated energy-water nexus models', are being deployed widely for cross-sector planning (see reviews by Khan et al. 2017; J. Liu et al. 2018; Vakilifard et al. 2018; Wu et al. 2020). Multi-sector planning strategies have been shown to derive plans that are not only more economical, but also yield a greater level of sustainability (e.g. Khan et al. 2018; S. C. Parkinson et al. 2018; Payet-Burin et al. 2019; Vinca et al. 2020). Yet, most of the analyses to date have been at a national or global scale, which inevitably entails approximations, whilst water sector decisions are actually made at a more local scale, for which there is a dearth of methodologies and analysis (S. Parkinson et al. 2019; Scanlon et al. 2017). Whilst the trade-offs between water system resilience, cost, and energy-related carbon emissions have been illustrated previously (e.g. Huskova et al. 2016; Matrosov et al. 2015; Paton et al. 2014), water sector planning methods need to enhance integration of energy systems to better capture water-energy interactions, such as the role of an energy prosuming water industry. Such developments are needed to link hydrological variability in the water system (*e.g.* reservoir dynamics) with volatility in the local energy system from stochastic weather processes (*e.g.* variable solar output), thus facilitating water managers to plan a water sector that is reliable, energy sustainable, and *robust* to uncertainties. This study provides such a methodological

advance.

Here we introduce a highly resolved coupled system modelling approach to inform cross-sectoral decision-making at a regional scale (Majid et al. 2021). We harmonise water-energy systems in stochastic simulations, which allows us to examine in detail the effects of variability, on a day-to-day basis, in energy use by the water utility and renewable energy supplies and prices. We explicitly model the risk of insufficient energy supplies and the impact that this has on security of water supplies. Use of multi-objective optimisation enables us to elucidate the trade-offs between cost (combining operation and capital costs) and security of water supply, subject to a constraint of transitioning to carbon-free electricity supplies.

To illustrate our methods, we turn our attention to the Thames basin, England, where local water systems face chronic pressures from climate change and population growth, while the energy footprint of water infrastructure is increasing rapidly (Majid et al. 2020). The local water utility, Thames Water Utilities Ltd (TWUL), has invested in a desalination plant and plans to invest in large-scale indirect wastewater reuse, which may further add to energy costs. At the same time, TWUL has ambitious plans to achieve net-zero energy consumption by 2030. We apply our methodological framework to derive infrastructure investment strategies that can balance the trade-offs between water and energy, while also ensuring plans *robust* to uncertainties in the climate, water demands and electricity price fluctuation.

5.2 Case-study

5.2.1 Study Area

The Thames basin is located in south east England and is considered to be 'seriously water stressed' (Environment Agency 2013) (Figure 5.1). It is among the driest areas across England, receiving around 690 mm of annual rainfall compared to the national average of 897 mm.

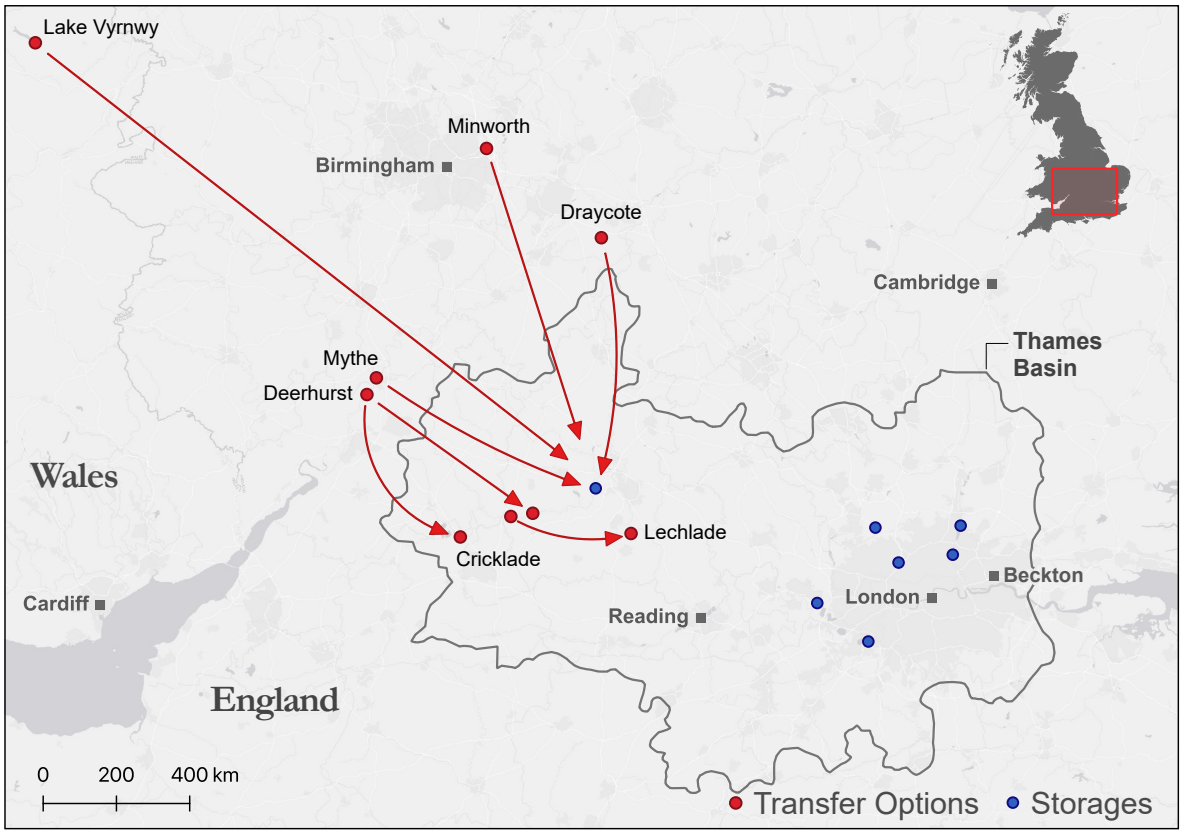


Figure 5.1: Map of the Thames basin in south England. The nodes show major water storage reservoirs and options in blue and red, respectively. Red arrows indicate proposed water transfer schemes by means of new pipelines and inter-basin transfers.

The region is the most densely populated in the country and it comprises one of the largest mega-cities in the world, London.

TWUL faces a number of challenges. Average urban water demand of 15 million persons is currently estimated at 160 L/person/day and total water demands are projected to increase by 0.25–0.75% per year with regional population growth (Thames Water 2014). Climate projections predict warming across the Thames basin (Jenkins et al. 2009), which is expected to result in more uncertain and stressed water resources (Bell et al. 2012; Christierson et al. 2012). In order to meet increasing water demands and adapt to predicted climatic changes, TWUL needs to expand its water supply capacities in the future. However, because the aquatic environment is already stressed, there is practically no scope for extracting more water from

natural surface and groundwater bodies within the Thames basin, so attention is shifting to energy-intensive non-conventional water sources or to long-distance water transfers.

Table 5.1: Infrastructure alternatives considered in the case-study with their meta-variables. The sets show the capacities possible for each option.

No.	Name	Capacity [ML or MW]	Capital Cost [£k year^{-1}]	Start
Water				
1	48 km pipeline from Deerhurst to Cricklade	{0,100,300,600}	0–47,000	2027
2	58 km pipeline from Deerhurst to Radcot	{0,100,300,600}	0–40,000	2027
3	87 km pipeline from Lechlade to Culham	{0,300}	0–17,000	2027
4	Indirect effluent reuse scheme	{0,100,150,200,300}†	0–40,000	2021
5	Brackish desalination at Beckton	{0,150}	0–22,275	2024
6	Seawater desalination at Beckton	{0,150,300}	0–32,000	2024
7	21 km transfer from Draycote	{0,25}	0	2027
8	40 km transfer from Minworth	{0,88}	0	2027
9	5 km transfer from Mythe	{0,15}	0	2027
10	170 km transfer from Lake Vyrnwy	{0,180}	0	2023
Energy				
11	Solar PV	{0,20,40,60,80,100}	0–5,847	2024
12	Wind turbines	{0,10,20,30,40,50,55}	0–8,430	2024
13	Biogas	{0,20,40,60,80,100}	0–45,000	2025

†The maximum possible capacity for this option (300 MLD) represents approximately 12% of average daily drinking water demand in the basin.

The utility's rising electricity use is also a significant concern. Between 2009 and 2014, electricity consumption by TWUL grew by 10% per year due to changing treatment standards and growth in service demands (Cardenes et al. 2020). Current system consumption stands at around 941 GWh per annum and makes up the largest carbon source and operational cost for TWUL (Thames Water 2019a). The utility self-generates around 23% of its total energy demand using local installations of solar, wind, and bio-gas generation. TWUL plans on growing this self-generation capacity to eventually obtain all of its energy from renewable sources. This is with the aim of realising net-zero carbon emissions by 2030, as set by water utilities across England and Wales (Water UK 2020).

We conduct a water and energy infrastructure planning study for the TWUL system to 2035, mapping efficient pathways to water system resilience whilst achieving net-zero energy use by 2030. We consider 13 supply-side water and energy expansion options (Table 5.1). The

upper bounds for feasible capacities are based on TWUL's management plans (Thames Water 2014) and the options are discretised to reduce the complexity of the decision space. Based on these options, water supplies could be augmented through desalination and inter-basin water transfers using existing or new pipelines, as well as indirect effluent reuse schemes in which treated wastewater could be pumped into storage reservoirs during periods of drought (Thames Water 2014). Figure 5.1 illustrates the proposed transfer schemes, some of which involve transporting water over hundreds of kilometres.

Three energy supply expansion options are considered: solar PV, wind, and biogas. It is assumed that for the portion of electricity not generated by TWUL (i.e. difference between consumption and self-generation), green energy credits will be purchased from the grid operator to meet TWUL's net-zero ambitions. As TWUL is a combined water and wastewater utility, biogas was considered in the planning problem given that it is touted as a significant opportunity for self-generation. However, our study does not incorporate the wastewater cycle of TWUL's business and the limitations of this are discussed later in this paper.

5.3 Methods

We adopt a multi-objective robust decision (MORDM) framework to map pathways towards a resilient and energy-sustainable water sector (Figure 5.2). The conceptual framework, first introduced by Kasprzyk et al. (2013), has been applied for planning the TWUL system in a number of previous studies (e.g. Huskova et al. 2016; Matrosov et al. 2015), and is embedded within the contemporary literature on water resources planning under uncertainty. Whilst there exist several methodological variants, robust decision frameworks generally emphasize: (1) recognition of critical uncertainties in the planning problem and extensive stress-testing of infrastructure alternatives to reveal key vulnerabilities (Fletcher et al. 2017; Groves et al. 2007; Hall et al. 2012; Lempert et al. 2003); (2) identification of solutions that are robust to uncertainties in that they perform acceptably well under a wide range of future conditions (Giuliani

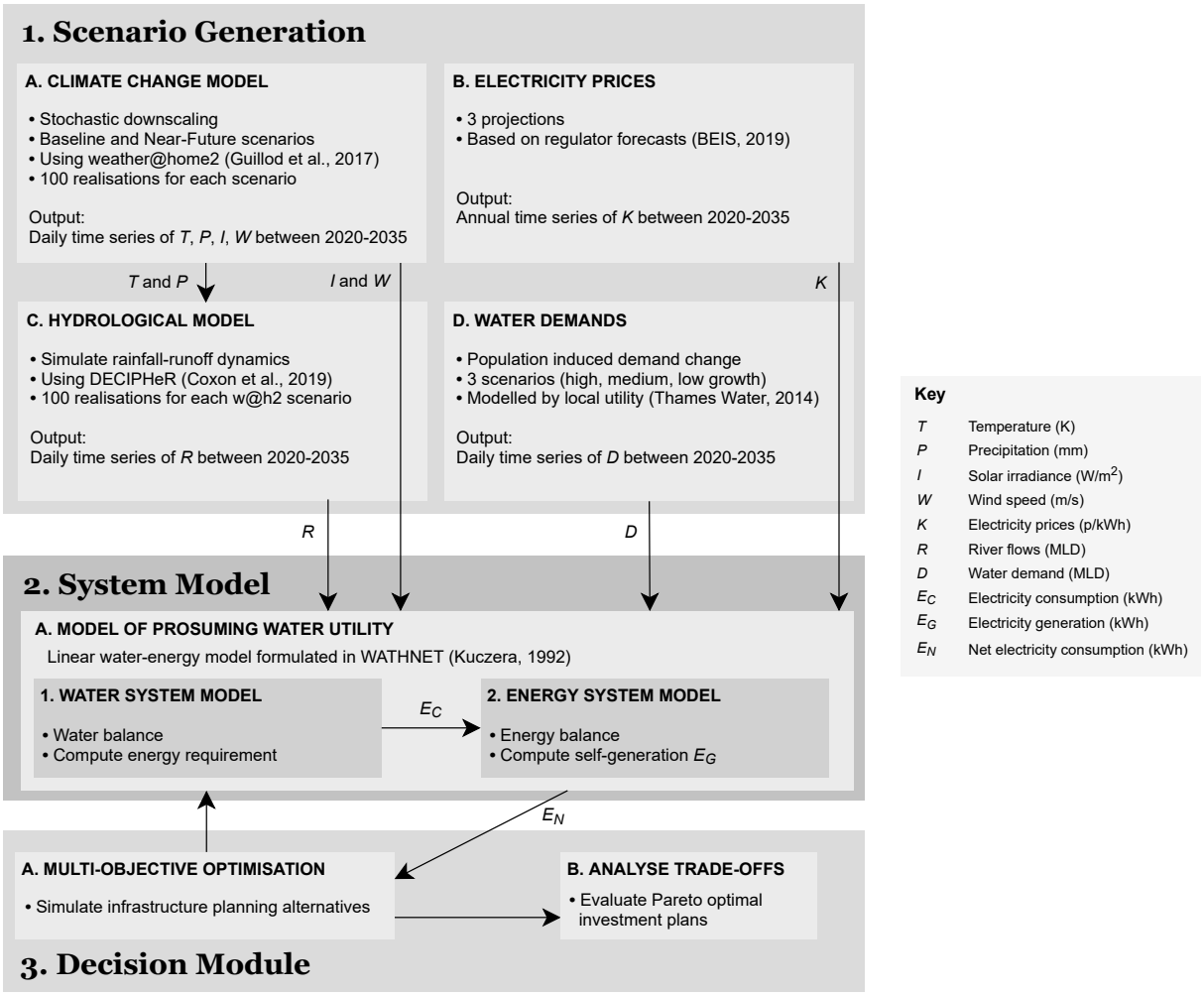


Figure 5.2: Illustration of the three-part integrated water-energy modelling framework. In the first part, stakeholders define future scenarios in the climate and local water system, as well as infrastructure alternative options. Next, a water-energy model exhaustively simulates various option combinations under the scenario set, where spatio-temporal dynamics of energy are tracked. Finally, a risk profile is derived for stakeholders to assess potential pathways to achieve their targets.

et al. 2016; Herman et al. 2015; Roach et al. 2018); and (3) multi-objective framing of the planning problem to allow decision-makers to trade-off competing objectives under uncertainty (Mortazavi-Naeini et al. 2014a; Mortazavi-Naeini et al. 2015b; Roach et al. 2016). Similarly, we develop and apply an MORDM framework to conduct integrated water-energy planning under a wide range of uncertainties to derive robust plans. This section describes that three-part framework with references to supplementary materials provided in Sections B.1–B.4.

5.3.1 Scenario generation

Our analysis incorporates aleatory uncertainties via stochastic simulation, whilst also exploring sensitivity and robustness to epistemic uncertainties about future changes in population and technology.

First, the weather@home2 (w@h) climate model was used to generate large sets of weather sequences (Guillod et al. 2018; Guillod et al. 2017). The w@h platform is based on the HadAM3P Global Circulation Model (GCM), which has been downscaled with the HadRM3P Regional Climate Model (RCM) by the UK Met Office Hadley Centre model (Gordon et al. 2000). It can be used to generate high-resolution (25 km) RCM weather sequences across Europe, which have been demonstrated to well represent extreme events (Guillod et al. 2017). Synthetic weather sequences of rainfall P (mm), temperature T (K), wind speed W (m/s), and solar irradiance I (W/m^2) were simulated at a daily time-resolution over the Thames region assuming two climate scenarios. The first uses historic climatic conditions and is referred to as the Baseline (BL) scenario, whereas the second assumes the Representative Concentration Pathway 8.5 (RCP 8.5)—a pathway with high greenhouse gas emissions and greater overall warming (Riahi et al. 2011)—and is referred to as the Near-Future (NF) scenario. These two scenarios represent the lower and upper bounds of the projected global emissions scenarios and hence capture the climatic variability under uncertain decarbonisation pathways. In total, 100 synthetic realisations were derived for each emissions scenario (200 in total), each of a length of 15 years.

Time series of rainfall P and temperature T generated by w@h were used to simulate river flows using the DECIPHeR hydrological model (Coxon et al. 2019). DECIPHeR explicitly characterises connectivity and fluxes across landscapes using a flexible modelling framework and has demonstrated good performance in replicating hydrological behaviour across Great Britain. A more detailed account of the DECIPHeR methodology can be found in previous works (Coxon et al. 2019), as well as the process of simulating rainfall-runoff dynamics histor-

ical and future naturalised flows across England and Wales (Dobson et al. 2020b). Figure B.1 shows the flow-duration curves of the total simulated river flows under the BL and NF scenarios. Perturbations in groundwater availability induced by the climate sequences were not considered in this work and are instead held constant at the dry year annual average following the methodology developed by previous work (Borgomeo et al. 2018).

Three water demand scenarios were used, referred to as the low, medium, and high growth scenarios. Each case assumes a growth of 0.25%, 0.50%, and 0.75% per annum, using the TWUL supplied intra-annual demand curve shown by Figure B.2. These scenarios are based on regional modelling of future population and socioeconomic status by TWUL (Thames Water 2014). We used water demands at monthly temporal resolution as more granular data were not available. Hence, the results presented here may underestimate the water shortage risks given that the influence of daily variability is not incorporated.

Finally, we used three scenarios of average annual electricity prices, which are based on forecasts from the UK Department for Business, Energy, and Industrial Strategy (BEIS) (BEIS 2019). These scenarios assume an annual rate of change of 0.69%, 1.06%, and 1.4% respectively, where the growth rate is applied to a baseline price of 13.1 p/kWh for renewable electricity from the grid. We incorporated only the grid price for renewable energy since TWUL intends to source all of its electricity from zero-carbon sources. For instances within the modelling where TWUL can produce more energy than it consumes, we assumed the energy is sold back to the grid for a feed-in-tariff (FiT) of 5.24 p/kWh, which was adjusted annually by an RPI of 1.2%. The baseline electricity price and FiT were both derived from TWUL's current power purchase agreement for renewable energy (Thames Water 2019b). We did not model the influence of weather or climate change on electricity prices as others have done previously (e.g. Byers et al. 2020; Su et al. 2020). This is because water utilities typically operate off fixed-price contracts agreed to by energy utilities and hence are not as vulnerable to climate-driven risks within dynamic day-ahead electricity markets.

5.3.2 Simulation model

The system simulation model, known as TWmod, formulates the TWUL system as a set of nodes and edges and runs between 2020 to 2035. TWmod incorporates sociological, hydrological, and environmental parameters to represent the TWUL system. The model aggregates processes based on six water resource zones (WRZs) as shown by Figure B.3. For example, a single node captures all groundwater abstractions in the SWOX WRZ (Figure B.3, top-left). Similarly, all water storages within this WRZ are also aggregated into one reservoir node. This methodology to 'lump' operation is common in water resources modelling but represents a highly simplistic model of the real-world system. Yet, it ensures fast computation times and model tractability, as well as the ability to publish materials without compromising privacy or national security (Dobson et al. 2020a). However, due to the simplicity of this approach, the results here should be treated as a preliminary screening that ought to be evaluated with further analysis. Nonetheless, TWmod was developed in extensive partnership with the local water utility and was calibrated and validated against the company's own models as described previously (Mortazavi-Naeini et al. 2019). Further, TWmod has been deployed in a number of studies of the Thames basin (e.g. Borgomeo et al. 2018; Mortazavi-Naeini et al. 2019)

TWmod incorporates the processes shown by Figure 5.3. Based on the inflows produced by rainfall-runoff modelling, TWmod uses network linear programming (NLP) (B.3.1) to simulate and optimise supply allocation to demand nodes at a daily timestep. The NLP is subject to several constraints as outlined by the equations in Sections B.3.1 and B.3.2. Numerous operational and environmental constraints are implemented including but not limited to: (i) reservoir releases are constrained subject to the control curve shown in Figure B.4, (ii) maximum daily to weekly abstractions from surface water resources as set by the water regulator, and (iii) essential environmental releases to preserve downstream water quality. Due to a lack of information related to the wastewater system, TWUL's wastewater operations were not included in the modelling process, which represents a significant limitation that is discussed later in the paper.

Following Porse et al. (2020), each edge carrying water is assigned a unique energy-intensity value (e_i, kWh/ML) depending on the process or technologies associated with the given edge. The assumed e_i values are outlined by Table B.1. For example, an edge carrying groundwater to a water treatment plant over a distance of 10 km would be assigned an $e_i = 300\,\text{kWh/ML} + (5\,\text{kWh/ML/km} \times 10\,\text{km})$. The modelled energy consumption was benchmarked against previously reported empirical data and showed reasonable agreement Majid et al. 2020. However, it is acknowledged that this is a significantly simplified method to compute energy use in the water system given that it neglects the actual topology and hydraulics of the system. The total electricity consumption by the water system (E_C) was computed as the sum of usage by each of these edges.

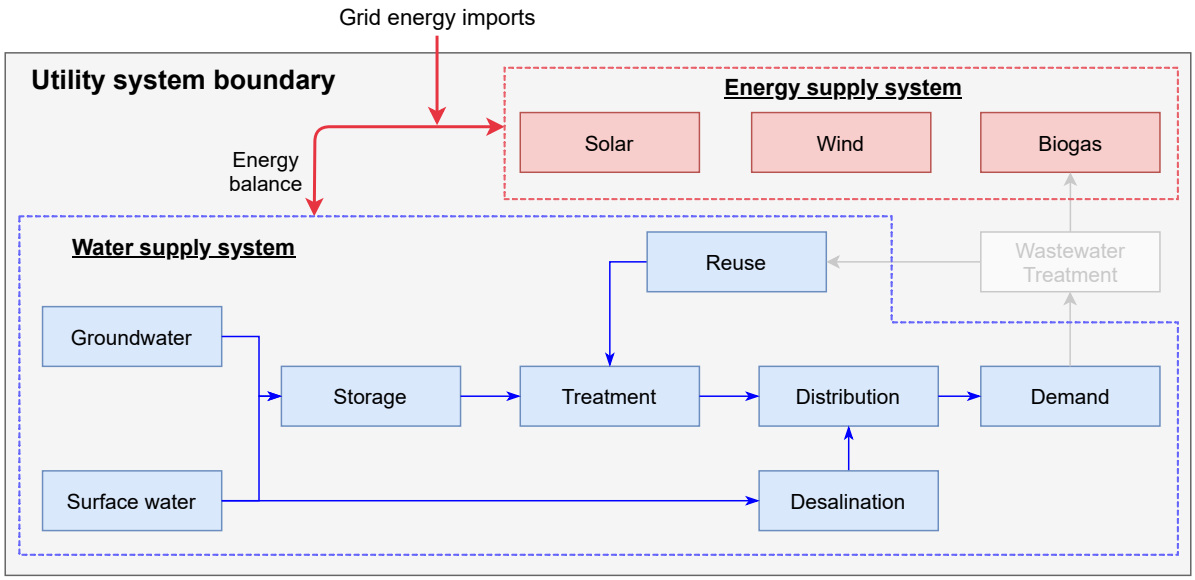


Figure 5.3: Schematic representation of the simulation model representing the energy prosuming water utility. The box and arrows shown in grey represent the processes not captured by our model.

TWUL's own energy supply (E_G) was modelled as the sum of generation from their solar (E_{PV}), wind (E_W), and biogas (E_{BG}) assets. Biogas was included within the energy system representation despite the omission of TWUL's wastewater treatment cycle since it constitutes a significant portion of TWUL's energy supply portfolio. The procedure for solar, wind, and biogas modelling are described in Section B.3.3 with equations. The difference between

TWUL's electricity consumption and self-generation is assumed to be imported from the grid (E_{IMP}) without constraints, such that:

$$E_{IMP} = E_C - (E_{PV} + E_W + E_{BG}) = E_C - E_G \tag{5.1}$$

As described previously (Section 5.3.1), all imports from the grids are assumed to be purchased in the form of green energy credits, while any excess electricity produced by TWUL is sold back to the grid at the FiT rate. Though studied by previous works (e.g. Kernan et al. 2017; Oikonomou et al. 2019), the dynamics of intra-day market trading are not incorporated here since it is still uncommon for utilities to participate in these schemes.

5.3.3 Decision module

The third part of the framework used ϵ-dominance multi-objective evolutionary optimisation (ϵ–MOEA), a meta-heuristic search and optimisation algorithm (Deb 2011), to search the decision space to identify infrastructure combinations that best minimise overall costs, while performing adequately across the defined scenario states. This approach facilitates the evaluation of trade-offs between competing objectives and has been used widely in water resources planning and management (Reed et al. 2013). A dual objective problem was formulated in which we seek to minimise: (1) total cost of operational and capital expenditure (f_1) and (2) total economic costs due to restrictions on water use associated with water shortages (f_2) such that:

$$\min_{x \in \Omega} \; F(x) = [f_1, f_2] \tag{5.2}$$

where $x = (x_i, \text{Cap}_i)$ and x_i is a binary decision variable to activate decision i at capacity Cap_i. f_1 is a function of the options implemented and total electricity costs of the system,

whereas f_2 is computed as a function of the total reservoir volumes, where a restriction cost penalty is imposed should the volume fall below those defined by TWUL's operational curve (Figure B.4 and Table B.2). These two objectives are further described in Section B.4.1.

The ϵ–MOEA yields a set of solutions, where each solution is a unique intervention of infrastructure investments and considered to be *Pareto optimal*, in that it is non-dominated or not exceeded with respect to all objectives by any other solution. The visualisation of each Pareto optimal set with respect to their objective values generates the *Pareto frontier*. The ϵ–MOEA was configured using the parameters defined in Table B.3 following previous studies Borgomeo et al. 2016; Mortazavi et al. 2012; Mortazavi-Naeini et al. 2014b; Mortazavi-Naeini et al. 2015a. The termination conditions for the optimisation, as well as the procedure for ensuring a complete Pareto frontier, are discussed in Section B.4.2.

5.3.4 Experiments conducted

A total of six experiments were conducted (Table 5.2), which incorporated the Baseline (BL) and Near-Future (NF) climate scenarios, in addition to three energy strategies. Each of these strategies sees TWUL obtain all of its energy from renewable sources by 2030, using a combination of self-generation and the purchase of green energy credits from the grid. The first is the Importer (IMP) strategy, in which no further expansions in RES are considered, instead the utility's energy target is met entirely by purchasing green energy credits from the grid. The second strategy, Prosumer (PRO), represents a case in which the utility energy goal is met entirely by self-generating its energy demand using RES. Hence, the IMP and PRO scenarios represent two opposing and extreme energy strategies. Meanwhile, the Balanced (BAL) strategy is a course of action in which TWUL achieve their energy targets by combining self-generation with grid energy purchases at a 50:50 ratio.

Table 5.2: Experimental setup for the optimisation. Six experiments were considered based on two climate scenarios and three energy strategies. RES and GC refer to renewable energy systems and green energy credit purchases, respectively.

			Energy options explored		
Experiment	Climate scenario	Energy strategy	RES	GC	Experimental meaning
BL-IMP	Baseline (BL)	Importer	✗	✓	Meet energy goal with only green credits purchases under baseline (historic) climate conditions
BL-PRO	Baseline (BL)	Prosumer	✓	✗	Meet energy goal with only self-generation under baseline (historic) climate conditions
BL-BAL	Baseline (BL)	Balanced	✓	✓	Meet energy goal through a balanced (50:50) approach to energy imports and self-generation under baseline (historic) climate conditions
NF-IMP	Near-Future (NF)	Importer	✗	✓	Meet energy goal with only green credits purchases under near-future (RCP8.5) climate conditions
NF-PRO	Near-Future (NF)	Prosumer	✓	✗	Meet energy goal with only self-generation under near-future (RCP8.5) climate conditions
NF-BAL	Near-Future (NF)	Balanced	✓	✓	Meet energy goal through a balanced (50:50) approach to energy imports and self-generation under near-future (RCP8.5) climate conditions

5.3.5 Post-optimisation analysis

A post-optimisation analysis was conducted on a small sample of solutions derived from the optimisation. Specifically, three solutions were selected from both the BL-BAL and NF-BAL strategies, making a total of six solutions (Table 5.3). The selected solutions represent (1) cheapest solution, (2) best from the perspective of water security, and (3) optimal solution (in principle) where the gradient of the Pareto frontier is equivalent to 45° (Borgomeo et al. 2018). We compare the cost, investment composition, *robustness*, and *reliability* of each of the six solutions. We define *robustness* following Paton et al. (2014):

$$\mathbf{R} = \frac{\mathbf{T}}{\Omega} \tag{5.3}$$

where **R** is robustness, **T** is the number of scenarios in which the solution exhibits "acceptable performance" and Ω is the total number of scenarios. We define "acceptable performance" in terms of reliability (**W**): $\geq$95% of days without restrictions and a maximum failure duration of 100 days.

5.4 Results

5.4.1 Trade-off between water security, cost, and energy sustainability

Figure 5.4 shows the results from the multi-objective optimisation under the NF climate scenarios for the three energy strategies evaluated. The curves depict the Pareto frontier (PF) fitted onto the non-dominated solution set for each energy strategy (see B.5.1). The non-dominated solutions derived for each of the six experiments are shown by Figure B.5 and further described in Section B.5.2. The IMP curve on Figure 5.4 represents the cheapest way for TWUL to transition to zero-carbon electricity. Solutions to the right of the PRO curve are uneconomical since cheaper solutions exist that can achieve the same security of supply. Plans within the IMP and PRO range (green shaded region) are those that can balance objectives in cost and water security whilst achieving the zero-carbon electricity goal.

A distinct trade-off between total cost and water use restriction cost is observed, whereby increasing the investment lowers the risk of water use restrictions. Though the gradients of the PFs are nearly identical the PFs under the BAL and PRO strategies shift upwards relative to the IMP case, demonstrating that these two strategies are more costly. The PFs shown quantify the marginal cost of incremental increases in RES. For example, the distance between the IMP and BAL curves represents the marginal cost of shifting from 0% to 50% RES self-generation in the TWUL system. The dashed curves show linearly interpolated estimations of PFs representing

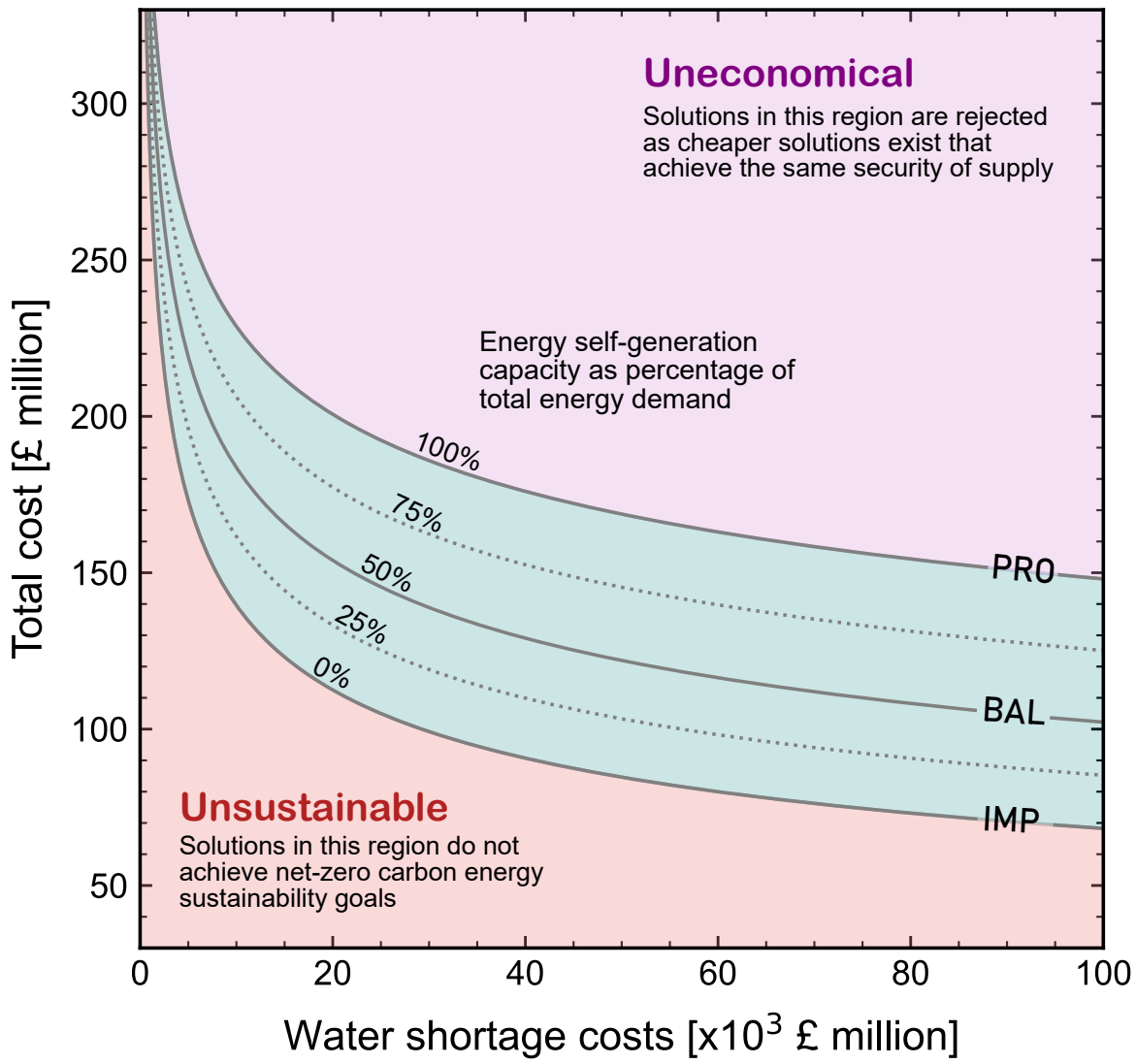


Figure 5.4: Pareto frontiers (PFs) fitted onto the non-dominated solutions derived under the NF climate scenario for the IMP, BAL, and PRO energy strategies. Dashed lines are linearly interpolated curves representing the marginal cost of increasing self-generation capacity between 0–100%.

plans with 25% and 75% RES self-generation, therefore allowing decision-makers to estimate the marginal cost of increasing RES capacity.

The trade-off frontiers also capture the climate sensitivity in the space of choices. For example, Figure 5.5 shows the non-dominated Pareto optimal solution sets derived under BL

and NF climate conditions (see also Figure B.5). A right-shift is observed in the PF from the NF case when compared to that from the BL case. This shows that achieving a given level of water security requires substantially greater investment in water supply infrastructure to mitigate against the climate impacts of a high-emissions future.

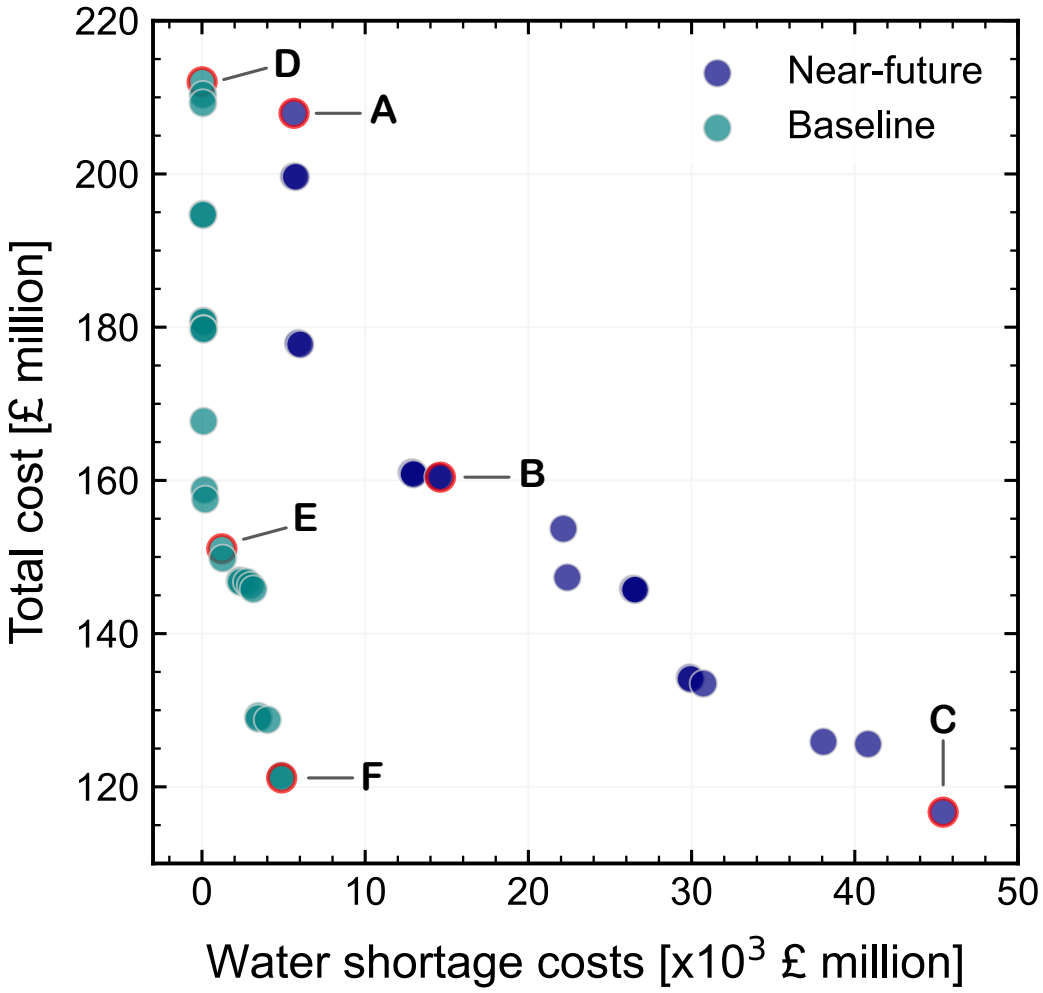


Figure 5.5: Non-dominated Pareto optimal solutions derived from the BL-BAL and NF-BAL experiments. The highlighted points (A–F) show the six investment plans chosen for post-optimisation analysis.

5.4.2 Post-optimisation analysis

Three plans from the BL-BAL and NF-BAL experiments were selected for post-optimisation analysis. These are denoted plans A–F and are shown by Figure 5.5. These plans represent the following: (i) the best solutions from the perspective of water security (A and D); (ii) the best solutions from the perspective of cost (C and F); and (iii) the optimal points in principle (B and E).

The composition of each strategic investment plan A–F is shown by Figure 5.6. The plot shows that inter-basin transfer schemes (*e.g.*, options 8–10) are selected with the highest frequency. On the other hand, transfer schemes that involve the construction of new pipelines (*e.g.* options 1–3) are chosen with relatively lesser frequency. Similarly, options such as desalination and effluent reuse were selected within fewer plans. Inter-basin transfer schemes can entail significant energy costs due to the requirement of long-distance pumping, yet they can circumvent large capital costs by utilising existing pipelines, hence they were selected more often by the optimiser.

Analysis of the investment plans also shows that plans included a combination of biogas, solar, and wind supply. However, total biogas capacity is the highest out of all energy supply options across all plans. This is likely due to biogas plants not being subject to strong seasonal variability as wind and solar. However, as discussed in B.3.3, our modelling process does not capture the TWUL's wastewater system and as a result omits key feedback loops and linkages in this portion of the system boundary.

Figure 5.7 shows the results from the simulation across all scenarios Ω as a parallel coordinates visualisation for (a) plans A–C under the near-future climate conditions and (b) plans D–F under the baseline climate conditions. Grey lines show the output from each scenario, whereas the lines in colour represent the mean values for each plan computed across all scenarios. The plot demonstrates that there is a significant amount of variation under each scenario.

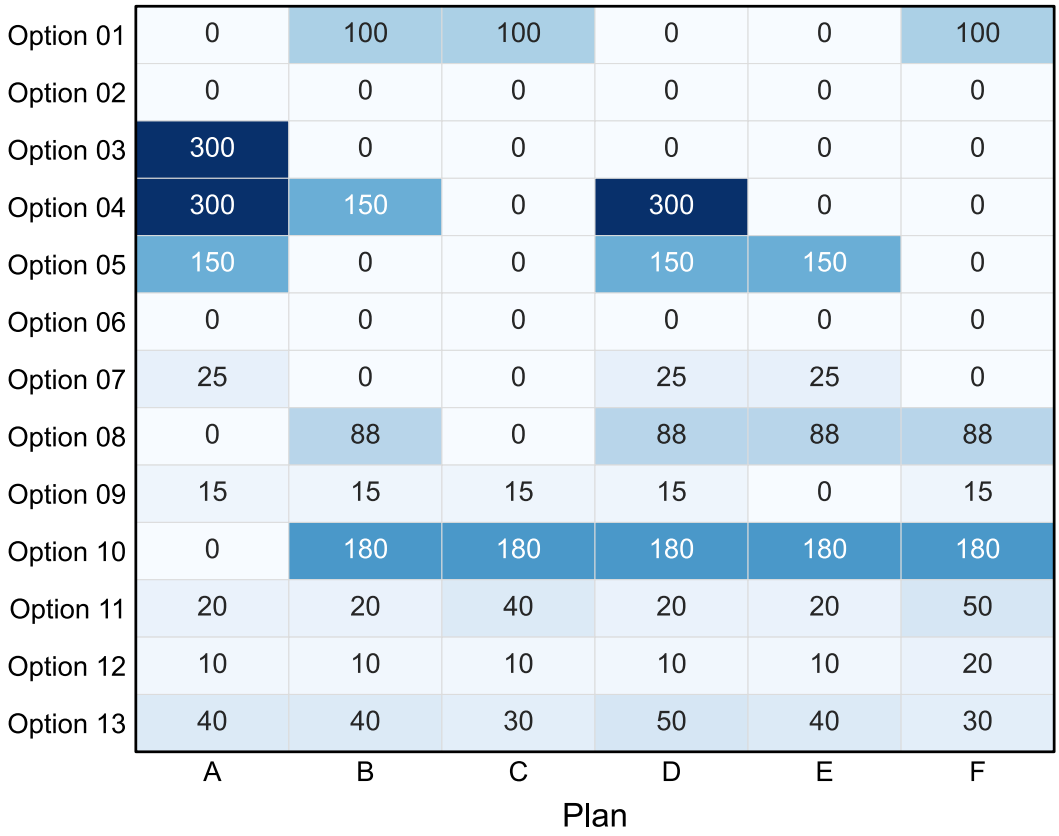


Figure 5.6: Composition of investment plans A–F showing the capacities of water (options 1–10 in ML) and energy (options 11–13 in MW) infrastructure implemented.

Mean reliability for all plans is over 90%, yet it can be below 80% under certain scenarios, particularly under plans C and F, which undermines the overall robustness of the plans. The robustness metrics computed for each of the plans A–F are given by Table 5.3. The results demonstrate that maximising robustness requires greater investment in supply infrastructure.

The parallel coordinates curve illustrates a number of water-energy trade-offs. Firstly, it shows that plans that deliver a higher reliability, and hence that exhibit fewer number of water use restrictions on average, are more energy consumptive on average. In other words, increasing the level of water supply reliability results in a commensurate increase in the system's energy consumption. Secondly, whilst all plans exhibit a minimum energy self-sufficiency of $>$50% as constrained by the BAL strategy, the average self-sufficiency is in fact higher across

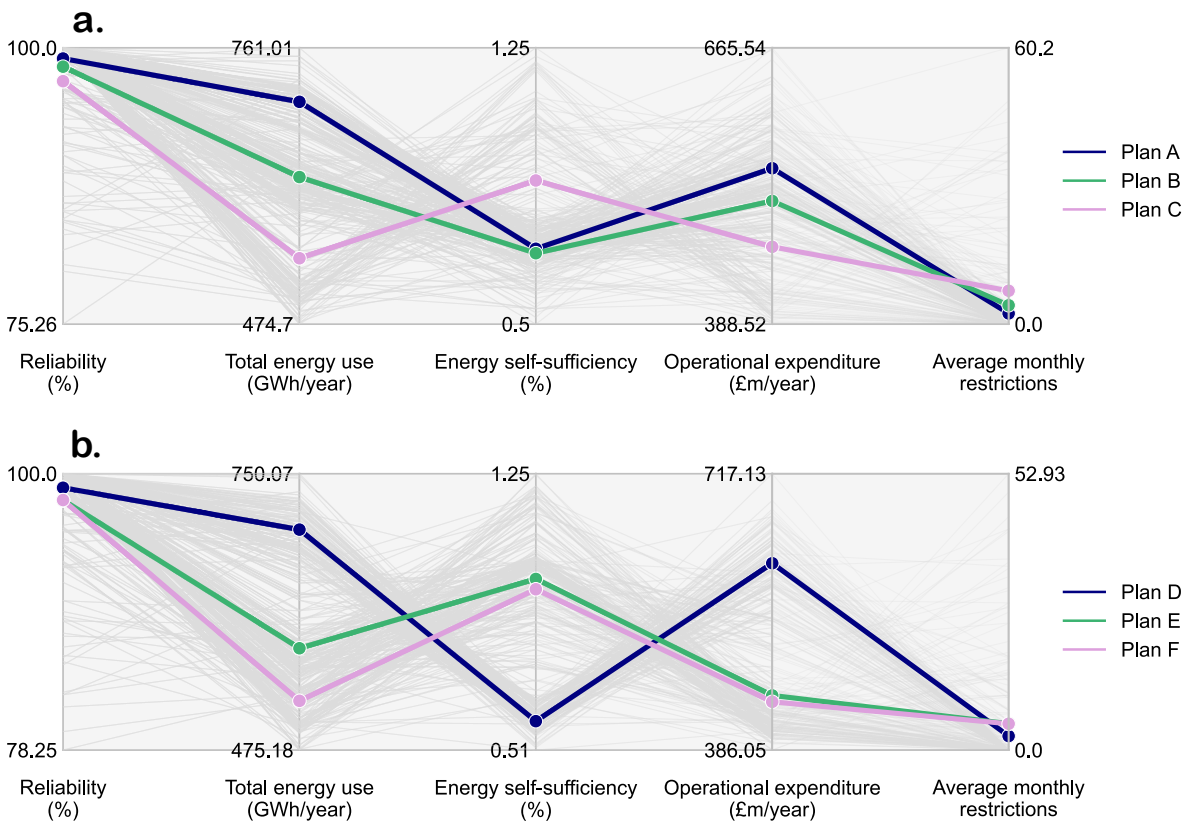


Figure 5.7: Parallel coordinates plot showing results from the simulation of plans (a) A–C under the NF climate scenarios and (b) D–F under the BL climate scenarios. Light grey lines show results simulation results for each plan under each scenarios Ω, whereas the coloured lines show mean values computed over all scenarios.

all plans, reaching up to 125% of overall demand (*i.e.* generating excess electricity that is sold back to the grid). For example, the average self-sufficiency under Plan A is around 70%. This demonstrates that guaranteeing a minimum level of self-sufficiency involves over-production on average to cope with the inherent variability within the water system.

5.5 Discussion

The utility of multi-objective optimisation to plan water supplies whilst balancing costs and water supply reliability in the face of uncertainty has been demonstrated previously (e.g.

Table 5.3: Results from the post-optimisation analysis of the six selected plans. The objective values for total cost f_1 and water use restriction costs f_2 are given in million Great British Pounds (GBPs). The $\bar{\mathbf{W}}$ and $\mathbf{R}$ denote the mean reliability and robustness, respectively.

Plan	Climate scenario	Sense	f_1 (£)	f_2 (£)	$\bar{\mathbf{W}}$ (%)	$\mathbf{R}$ (%)
A	Near-future	Best water restrictions	207.7	5.74	99.0	91.0
B	Near-future	Optimal†	160.2	14.65	95.2	81.9
C	Near-future	Best cost	116.7	45.45	91.9	74.3
D	Baseline	Best water restrictions	211.8	0.15	99.2	96.3
E	Baseline	Optimal†	150.9	1.31	98.1	92.4
F	Baseline	Best cost	121.2	4.96	97.6	88.7

†Optimal point in principle based on TWUL's tolerable level of risk (Borgomeo et al. 2018).

Huskova et al. 2016; Matrosov et al. 2015) and this process is now recognised as an integral part of the decision-making process (Hall et al. 2019). Yet, as demonstrated here, extending the decision framework to incorporate increasingly important energy sustainability targets has substantial effects on the decision space. Doing so allows decision-makers to balance critical water-energy trade-offs to maximise the reliability of water supply in a manner that is sustainable. This could provide practical benefits for water managers. Even within the same water organisations, decisions related to securing future water supplies and energy targets are often made within separate departments or entities (Farid et al. 2016; Porse et al. 2020), which could lead to sub-optimal management plans. Cross-cutting decision methodologies could facilitate the integration of such entities (Khan et al. 2017; Khan et al. 2018).

Achieving energy targets by partially or fully self-generating energy demands was shown to be a costly proposition. It also entails the implementation of significant amounts of RES, which may be technically infeasible due to constraints on land use and storage availability. However, there are a number of strategic advantages to maximising energy self-generation. Firstly, it can partially decouple the water system from the energy grid and decrease water utilities' vulnerability to price increases. Secondly, utilities that both possess storage and are

able to dynamically alter their energy demands (*e.g.,* a water treatment facility) have been shown to increase the utilisation of RES within local energy systems (Kernan et al. 2017). This could provide mutual benefits for the water and energy sectors in the form of lower operational expenditures and greater RES uptake respectively. Thirdly, recent studies behavioural studies have demonstrated a shift in consumer behaviour towards *green energy* products (e.g. Diaz-Rainey et al. 2011; Ebeling et al. 2015). In regions such as England and Wales, where water utilities operate in a privatised market, demonstrating energy sustainability may have benefits in terms of consumer confidence.

Given that the timescales to meet energy targets are short, additional synergies between water and energy systems will need to be explored to gain project financing and achieve objectives in a cost-effective manner. One of the most promising energy-water synergies is for water utilities to participate in demand-side response (DSR) programmes, schemes proposed by the energy sector to incentivise the shift of consumers' demands to off-peak periods to alleviate grid pressures. Kernan et al. (2017) showed dynamically altering water-related energy demands to signals from energy systems could lower operational costs by up to 13% whilst ensuring the same level of service. This could materialise large cost savings given that energy consumption is typically the dominant portion of operational costs for water companies. The advent of high-resolution smart metering data in the water sector could facilitate such schemes without compromising supply (Cominola et al. 2019). Increasing biogas production from the water sector, which still remains under-utilised, could also enhance participation in DSR programmes as it can provide additional flexibility through the ability to store gas, whilst also exhibiting negligible variability and high ramping rates. Biogas capacity also provides the benefit of being able to export gas supplies to the grid and also utilising its heat energy output through combined heat and power (CHP) technologies (Kang et al. 2014). However, it is important to recognise that the adoption of schemes such as DSR will require major cultural changes as operational practices will need to be overhauled.

As with any study that attempts to model multiple complex sectors for future planning,

there are a number of important limitations in the methodology presented here. Firstly, this study did not incorporate the wastewater cycle of 's system. Though is a combined water and wastewater utility, these two operations are managed independently in practice with limited integration of models and data systems. Multi-sector approaches that can capture water and wastewater interactions have only just begun to be developed (Dobson et al. 2020a). As this field advances, our efforts could be improved upon in future through a more holistic representation of water-wastewater-energy links and feedback loops. For example, the influence of variability in the wastewater system on biogas production could be incorporated, as well as the downstream impacts of effluent reuse schemes due to the removal of a stream of water. Our study also used simplistic forecasts of grid energy prices. While this is a common method for dealing with deep uncertainties (Fletcher et al. 2017), others have linked climate model data to create energy price forecasts (e.g. Anghileri et al. 2018; Su et al. 2020). Using such approaches could provide a more reliable means of studying the affects of future emissions pathways and their implications for water and energy systems. Also, whilst the models used here were validated against historical data to show good agreement, it is important to recognise that there remain uncertainties in methods to validate integrated models (L. Liu et al. 2020). Finally, our case-study considered only supply-side options, whilst considerable opportunities exist to secure future water and energy supplies using demand-side management options such as leakage reduction and upgrading older assets to more energy-efficient units.

Despite these limitations, this study provides a first analysis of the achieving energy sustainability in the water sector by means of utilities transitioning into prosumers using a multi-objective robust decision-making framework. Such multi-sector approaches at a regional scale will be critical in ensuring utilities are developing in line with the sustainable development goals (Khan et al. 2017). By unravelling the key trade-offs, we have provided a blueprint toward realising a water sector that is reliable, robust and sustainable.

References

Anghileri, D., Botter, M., Castelletti, A., Weigt, H., & Burlando, P. (2018). A Comparative Assessment of the Impact of Climate Change and Energy Policies on Alpine Hydropower. *Water Resources Research*, *54*(11), 9144–9161. https://doi.org/10.1029/2017WR022289

BEIS. (2019). *Updated energy and emissions projections: 2019* (tech. rep.). UK Department for Business, Energy, and Industrial Strategy. London. https://www.gov.uk/government/publications/updated-energy-and-emissions-projections-2018

Bell, V. A., Kay, A. L., Cole, S. J., Jones, R. G., Moore, R. J., & Reynard, N. S. (2012). How might climate change affect river flows across the Thames Basin? An area-wide analysis using the UKCP09 Regional Climate Model ensemble. *Journal of Hydrology*, *442-443*, 89–104. https://doi.org/10.1016/j.jhydrol.2012.04.001

Borgomeo, E., Mortazavi-Naeini, M., Hall, J. W., & Guillod, B. P. (2018). Risk, Robustness and Water Resources Planning Under Uncertainty. *Earth's Future*, *6*(3), 468–487. https://doi.org/10.1002/2017EF000730

Borgomeo, E., Mortazavi-Naeini, M., Hall, J. W., O'Sullivan, M. J., & Watson, T. (2016). Trading-off tolerable risk with climate change adaptation costs in water supply systems. *Water Resources Research*, *52*(2), 622–643. https://doi.org/10.1002/2015WR018164

Byers, E. A., Coxon, G., Freer, J., & Hall, J. W. (2020). Drought and climate change impacts on cooling water shortages and electricity prices in Great Britain. *Nature Communications*. https://doi.org/10.1038/s41467-020-16012-2

Cardenes, I., Hall, J. W., Eyre, N., Majid, A., & Jarvis, S. (2020). Quantifying the energy consumption and greenhouse gas emissions of changing wastewater quality standards. *Water Science and Technology*, *2*, 1–10. https://doi.org/10.2166/wst.2020.228

Christierson, B. v., Vidal, J. P., & Wade, S. D. (2012). Using UKCP09 probabilistic climate information for UK water resource planning. *Journal of Hydrology*, *424-425*, 48–67. https://doi.org/10.1016/j.jhydrol.2011.12.020

Cominola, A., Nguyen, K., Giuliani, M., Stewart, R. A., Maier, H. R., & Castelletti, A. (2019). Data Mining to Uncover Heterogeneous Water Use Behaviors From Smart Meter Data. *Water Resources Research*. https://doi.org/10.1029/2019WR024897

Coxon, G., Freer, J., Lane, R., Dunne, T., Knoben, W. J., Howden, N. J., Quinn, N., Wagener, T., & Woods, R. (2019). DECIPHeR v1: Dynamic fluxEs and ConnectIvity for Predictions of HydRology. *Geoscientific Model Development*, *12*(6), 2285–2306. https://doi.org/10.5194/gmd-12-2285-2019

Deb, K. (2011). Multi-objective Optimisation Using Evolutionary Algorithms: An Introduction, In *Multi-objective evolutionary optimisation for product design and manufacturing*. https://doi.org/10.1007/978-0-85729-652-8{_}1

Diaz-Rainey, I., & Ashton, J. K. (2011). Profiling potential green electricity tariff adopters: Green consumerism as an environmental policy tool? *Business Strategy and the Environment*. https://doi.org/10.1002/bse.699

Dobson, B., & Mijic, A. (2020a). Protecting rivers by integrating supply-wastewater infrastructure planning and coordinating operational decisions. *Environmental Research Letters*. https://doi.org/10.1088/1748-9326/abb050

Dobson, B., Coxon, G., Freer, J., Gavin, H., Mortazavi-Naeini, M., & Hall, J. W. (2020b). The Spatial Dynamics of Droughts and Water Scarcity in England and Wales. *Water Resources Research*, *56*(9). https://doi.org/10.1029/2020WR027187

Ebeling, F., & Lotz, S. (2015). Domestic uptake of green energy promoted by opt-out tariffs. *Nature Climate Change*. https://doi.org/10.1038/nclimate2681

Elimelech, M., & Phillip, W. A. (2011). The future of seawater desalination: Energy, technology, and the environment. *Science*, *333*(6043), 712–717. https://doi.org/10.1126/science.1200488

Environment Agency. (2013). *Water stressed areas – final classification* (tech. rep. July). https://assets.publishing.service.gov.uk/government/uploads/system/uploads/attachment_data/file/244333/water-stressed-classification-2013.pdf

Farid, A. M., Lubega, W. N., & Hickman, W. W. (2016). Opportunities for energy-water nexus management in the Middle East & North Africa. *Elementa*, *4*, 1–17. https://doi.org/10.12952/journal.elementa.000134

Fletcher, S. M., Miotti, M., Swaminathan, J., Klemun, M. M., Strzepek, K., & Siddiqi, A. (2017). Water Supply Infrastructure Planning: Decision-Making Framework to Classify Multiple Uncertainties and Evaluate Flexible Design. *Journal of Water Resources Planning and Management*, *143*(10), 04017061. https://doi.org/10.1061/(asce)wr.1943-5452.0000823

Giuliani, M., & Castelletti, A. (2016). Is robustness really robust? How different definitions of robustness impact decision-making under climate change. *Climatic Change*. https://doi.org/10.1007/s10584-015-1586-9

Gordon, C., Cooper, C., Senior, C. A., Banks, H., Gregory, J. M., Johns, T. C., Mitchell, J. F. B., & Wood, R. A. (2000). The simulation of SST, sea ice extents and ocean heat transports in a version of the Hadley Centre coupled model without flux adjustments. *Climate Dynamics*, *16*(2-3), 147–168. https://doi.org/10.1007/s003820050010

Groves, D. G., & Lempert, R. J. (2007). A new analytic method for finding policy-relevant scenarios. *Global Environmental Change*. https://doi.org/10.1016/j.gloenvcha.2006.11.006

Gu, Y., Li, Y., Li, X., Luo, P., Wang, H., Robinson, Z. P., Wang, X., Wu, J., & Li, F. (2017). The feasibility and challenges of energy self-sufficient wastewater treatment plants. *Applied Energy*. https://doi.org/10.1016/j.apenergy.2017.02.069

Guillod, B. P., Jones, R. G., Dadson, S. J., Coxon, G., Bussi, G., & Freer, J. (2018). A large set of potential past , present and future hydro-meteorological time series for the UK, 611–634.

Guillod, B. P., Jones, R. G., Bowery, A., Haustein, K., Massey, N. R., Mitchell, D. M., Otto, F. E. L., Sparrow, S. N., Uhe, P., Wallom, D. C. H., Wilson, S., & Allen, M. R. (2017). weather@home 2: validation of an improved global–regional climate modelling system. *Geoscientific Model Development*, *10*(5), 1849–1872. https://doi.org/10.5194/gmd-10-1849-2017

Hall, J. W., Mortazavi-naeini, M., Borgomeo, E., Baker, B., Gavin, H., Gough, M., Harou, J. J., Hunt, D., Lambert, C., Piper, B., Richardson, N., & Watts, G. (2019). Risk-based water resources planning in practice : a blueprint for the water industry in England, *0*, 1–14. https://doi.org/10.1111/wej.12479

Hall, J. W., Lempert, R. J., Keller, K., Hackbarth, A., Mijere, C., & McInerney, D. J. (2012). Robust Climate Policies Under Uncertainty: A Comparison of Robust Decision Making and Info-Gap Methods. *Risk Analysis*, *32*(10), 1657–1672. https://doi.org/10.1111/j.1539-6924.2012.01802.x

Herman, J. D., Reed, P. M., Zeff, H. B., & Characklis, G. W. (2015). How should robustness be defined for water systems planning under change? *Journal of Water Resources Planning and Management*. https://doi.org/10.1061/(ASCE)WR.1943-5452.0000509

Huskova, I., Matrosov, E. S., Harou, J. J., Kasprzyk, J. R., & Lambert, C. (2016). Screening robust water infrastructure investments and their trade-offs under global change: A London example. *Global Environmental Change*, *41*, 216–227. https://doi.org/10.1016/J.GLOENVCHA.2016.10.007

Jenkins, G. J., Murphy, J. M., Sexton, D. M. H., Lowe, J. A., Jones, P., & Kilsby, C. G. (2009). UK Climate Projections: Briefing report. *Met Office Hadley Center*, (June), 59. https://doi.org/ISBN978-1-906360-04-7

Kang, J. Y., Kang, D. W., Kim, T. S., & Hur, K. B. (2014). Comparative economic analysis of gas turbine-based power generation and combined heat and power systems using biogas fuel. *Energy*. https://doi.org/10.1016/j.energy.2014.01.009

Kasprzyk, J. R., Nataraj, S., Reed, P. M., & Lempert, R. J. (2013). Many objective robust decision making for complex environmental systems undergoing change. *Environmental Modelling and Software*, *42*, 55–71. https://doi.org/10.1016/j.envsoft.2012.12.007

Kenway, S. J., Lant, P. A., Priestley, A., & Daniels, P. (2011). The connection between water and energy in cities: A review. https://doi.org/10.2166/wst.2011.070

Kernan, R., Liu, X., McLoone, S., & Fox, B. (2017). Demand side management of an urban water supply using wholesale electricity price. *Applied Energy*, *189*, 395–402. https://doi.org/10.1016/j.apenergy.2016.12.082

Khan, Z., Linares, P., & García-gonzález, J. (2017). Integrating water and energy models for policy driven applications . A review of contemporary work and recommendations for future developments. *Renewable and Sustainable Energy Reviews*, *67*, 1123–1138. https://doi.org/10.1016/j.rser.2016.08.043

Khan, Z., Linares, P., Rutten, M., Parkinson, S., Johnson, N., & García-gonzález, J. (2018). Spatial and temporal synchronization of water and energy systems : Towards a single integrated optimization model for long-term resource planning. *Applied Energy*, *210*, 499–517. https://doi.org/10.1016/j.apenergy.2017.05.003

Lam, K. L., Lant, P. A., & Kenway, S. J. (2018). Energy implications of the millennium drought on urban water cycles in Southeast Australian cities. *Water Science and Technology: Water Supply*, *18*(1), 214–221. https://doi.org/10.2166/ws.2017.110

Lam, K. L., Kenway, S. J., & Lant, P. A. (2017). Energy use for water provision in cities. *Journal of Cleaner Production*, *143*, 699–709. https://doi.org/10.1016/j.jclepro.2016.12.056

Lempert, R. J., Popper, S. W., & Bankes, S. C. (2003). *Shaping the next one hundred years : new methods for quantitative, long-term policy analysis and bibliography*. RAND. https://books.google.co.uk/books?hl=en&lr=&id=F2SzOwE0_bIC&oi=fnd&pg=PP1&dq=Shaping+the+next+one+hundred+years:+new+methods+for+quantitative,+long-term+policy+analysis&ots=WUBSWBZjEb&sig=g1jBbNj0Agg7H2K46agPPnIulos&redir_esc=y#v=onepage&q=Shaping%20the%20next

Liu, J., Hull, V., Godfray, H. C. J., Tilman, D., Gleick, P., Hoff, H., Pahl-Wostl, C., Xu, Z., Chung, M. G., Sun, J., & Li, S. (2018). Nexus approaches to global sustainable development. Springer US. https://doi.org/10.1038/s41893-018-0135-8

Liu, L., Lopez, E., Dueñas-Osorio, L., Stadler, L., Xie, Y., Alvarez, P. J., & Li, Q. (2020). The importance of system configuration for distributed direct potable water reuse. *Nature Sustainability*. https://doi.org/10.1038/s41893-020-0518-5

Majid, A., Cardenes, I., Zorn, C., Russell, T., Colquhoun, K., Bañares-Alcantara, R., & Hall, J. W. (2020). An Analysis of Electricity Consumption Patterns in the Water and Wastewater Sectors in South East England, UK. *Water*, *12*(1), 225. https://doi.org/10.3390/w12010225

Majid, A., Mortazavi-Naeini, M., & Hall, J. W. (2021). Efficient pathways to zero-carbon energy use by water supply utilities: an example from London, UK. *Environmental Research Letters*, *16*(10), 105010. https://doi.org/10.1088/1748-9326/ac2931

Matrosov, E. S., Huskova, I., Kasprzyk, J. R., Harou, J. J., Lambert, C., & Reed, P. M. (2015). Many-objective optimization and visual analytics reveal key trade-offs for London's water supply. *Journal of Hydrology*, *531*, 1040–1053. https://doi.org/10.1016/J.JHYDROL.2015.11.003

Mortazavi, M., Kuczera, G., & Cui, L. (2012). Multiobjective optimization of urban water resources: Moving toward more practical solutions. *Water Resources Research*, *48*(3). https://doi.org/10.1029/2011WR010866

Mortazavi-Naeini, M., Kuczera, G., & Cui, L. (2014a). Application of multiobjective optimization to scheduling capacity expansion of urban water resource systems. *Water Resources Research*. https://doi.org/10.1002/2013WR014569

Mortazavi-Naeini, M., Kuczera, G., & Cui, L. (2014b). Application of multiobjective optimization to scheduling capacity expansion of urban water resource systems. *Water Resources Research*, *50*(6), 4624–4642. https://doi.org/10.1002/2013WR014569

Mortazavi-Naeini, M., Bussi, G., Hall, J. W., & Whitehead, P. G. (2019). Assessment of risks to public water supply from low flows and harmful water quality in a changing climate. *Water Resources Research*. https://doi.org/10.1029/2018WR022865

Mortazavi-Naeini, M., Kuczera, G., & Cui, L. (2015a). Efficient multi-objective optimization methods for computationally intensive urban water resources models. *Journal of Hydroinformatics*, *17*(1), 36–55. https://doi.org/10.2166/hydro.2014.204

Mortazavi-Naeini, M., Kuczera, G., Kiem, A. S., Cui, L., Henley, B., Berghout, B., & Turner, E. (2015b). Robust optimization to secure urban bulk water supply against extreme drought and uncertain climate change. *Environmental Modelling and Software*. https://doi.org/10.1016/j.envsoft.2015.02.021

Oikonomou, K., & Parvania, M. (2019). Optimal Coordination of Water Distribution Energy Flexibility with Power Systems Operation. *IEEE Transactions on Smart Grid*. https://doi.org/10.1109/TSG.2018.2824308

Parkinson, S. C., Makowski, M., Krey, V., Sedraoui, K., Almasoud, A. H., & Djilali, N. (2018). A multi-criteria model analysis framework for assessing integrated water-energy system transformation pathways. *Applied Energy*, *210*, 477–486. https://doi.org/10.1016/j.apenergy.2016.12.142

Parkinson, S., Krey, V., Huppmann, D., Kahil, T., McCollum, D., Fricko, O., Byers, E., Gidden, M. J., Mayor, B., Khan, Z., Raptis, C., Rao, N. D., Johnson, N., Wada, Y., Djilali, N., & Riahi, K. (2019). Balancing clean water-climate change mitigation trade-offs. *Environmental Research Letters*, *14*(1). https://doi.org/10.1088/1748-9326/aaf2a3

Paton, F. L., Maier, H. R., & Dandy, G. C. (2014). Including adaptation and mitigation responses to climate change in a multiobjective evolutionary algorithm framework for urban water supply systems incorporating GHG emissions. *Water Resources Research*, *50*(8), 6285–6304. https://doi.org/10.1002/2013WR015195

Payet-Burin, R., Kromann, M., Pereira-Cardenal, S., Marc Strzepek, K., & Bauer-Gottwein, P. (2019). WHAT-IF: An open-source decision support tool for water infrastructure investment planning within the water-energy-food-climate nexus. *Hydrology and Earth System Sciences*. https://doi.org/10.5194/hess-23-4129-2019

Plappally, A. K., & Lienhard, J. H. V. (2012). Energy requirements for water production, treatment, end use, reclamation ,and disposal. *Renewable and Sustainable Energy Reviews*, *16*(7), 4818–4848. https://doi.org/10.1016/j.rser.2012.05.022

Porse, E., Mika, K. B., Escriva-Bou, A., Fournier, E. D., Sanders, K. T., Spang, E., Stokes-Draut, J., Federico, F., Gold, M., & Pincetl, S. (2020). Energy use for urban water management by utilities and households in Los Angeles. *Environmental Research Communications*, *2*(1), 015003. https://doi.org/10.1088/2515-7620/ab5e20

Reed, P. M., Hadka, D., Herman, J. D., Kasprzyk, J. R., & Kollat, J. B. (2013). Evolutionary multiobjective optimization in water resources: The past, present, and future. *Advances in Water Resources*, *51*, 438–456. https://doi.org/10.1016/j.advwatres.2012.01.005

Riahi, K., Rao, S., Krey, V., Cho, C., Chirkov, V., Fischer, G., Kindermann, G., Nakicenovic, N., & Rafaj, P. (2011). RCP 8.5—A scenario of comparatively high greenhouse gas emissions. *Climatic Change*, *109*(1-2), 33–57. https://doi.org/10.1007/s10584-011-0149-y

Roach, T., Kapelan, Z., Ledbetter, R., & Ledbetter, M. (2016). Comparison of Robust Optimization and Info-Gap Methods for Water Resource Management under Deep Uncertainty. *Journal of Water Resources Planning and Management*, *142*(9), 04016028. https://doi.org/10.1061/(asce)wr.1943-5452.0000660

Roach, T., Kapelan, Z., & Ledbetter, R. (2018). Resilience-based performance metrics for water resources management under uncertainty. *Advances in Water Resources*, *116*(October 2017), 18–28. https://doi.org/10.1016/j.advwatres.2018.03.016

Rothausen, S. G., & Conway, D. (2011). Greenhouse-gas emissions from energy use in the water sector. Nature Publishing Group. https://doi.org/10.1038/nclimate1147

Scanlon, B. R., Ruddell, B. L., Reed, P. M., Hook, R. I., Zheng, C., Tidwell, V. C., & Siebert, S. (2017). The food-energy-water nexus: Transforming science for society. https://doi.org/10.1002/2017WR020889

Spang, E. S., & Loge, F. J. (2015). A High-Resolution Approach to Mapping Energy Flows through Water Infrastructure Systems, *19*(4). https://doi.org/10.1111/jiec.12240

Stokes, J. R., Horvath, A., & Sturm, R. (2013). Water Loss Control Using Pressure Management: Life-cycle Energy and Air Emission E ff ects. https://doi.org/10.1021/es4006256

Su, Y., Kern, J. D., Denaro, S., Hill, J., Reed, P., Sun, Y., Cohen, J., & Characklis, G. W. (2020). An open source model for quantifying risks in bulk electric power systems from spatially and temporally correlated hydrometeorological processes. *Environmental Modelling and Software*, *126*(February), 104667. https://doi.org/10.1016/j.envsoft.2020.104667

Thames Water. (2019a). Facts and figures. https://corporate.thameswater.co.uk/media/Facts-and-figures

Thames Water. (2014). *Water Resources Management Plan 2014 (WRMP 14)* (tech. rep. June). Reading.

Thames Water. (2019b). *Water Resources Management Plan 2019 (WRMP 19)* (tech. rep.).

Vakilifard, N., Anda, M., Bahri, P. A., & Ho, G. (2018). The role of water-energy nexus in optimising water supply systems – Review of techniques and approaches. *Renewable and Sustainable Energy Reviews*, *82*(June 2016), 1424–1432. https://doi.org/10.1016/j.rser.2017.05.125

Vinca, A., Parkinson, S., Riahi, K., Byers, E., Siddiqi, A., Muhammad, A., Ilyas, A., Yogeswaran, N., Willaarts, B., Magnuszewski, P., Awais, M., Rowe, A., & Djilali, N. (2020). Transboundary cooperation a potential route to sustainable development in the Indus basin. *Nature Sustainability*. https://doi.org/10.1038/s41893-020-00654-7

Vörösmarty, C. J., Green, P., Salisbury, J., & Lammers, R. B. (2000). Global water resources: Vulnerability from climate change and population growth. *Science*. https://doi.org/10.1126/science.289.5477.284

Wada, Y., Gleeson, T., & Esnault, L. (2014). Wedge approach to water stress. https://doi.org/10.1038/ngeo2241

Water UK. (2020). *Net Zero 2030 Routemap* (tech. rep.). https://www.water.org.uk/routemap2030/wp-content/uploads/2020/11/Water-UK-Net-Zero-2030-Routemap.pdf

Wu, W., Maier, H. R., Dandy, G. C., Arora, M., & Castelletti, A. (2020). The changing nature of the water–energy nexus in urban water supply systems: a critical review of changes and responses. *Journal of Water and Climate Change*, 1–28. https://doi.org/10.2166/wcc.2020.276

Chapter 6

Conclusions

6.1 Thesis summary

Energy use in the water and wastewater sectors is a growing issue. Efforts to mitigate against the effects of climate change, as well as deal with greater demands induced by population growth, the energy-intensiveness of W&WW systems is rising sharply across the world (Lam et al. 2018; Lam et al. 2017). Yet, there are also a number of opportunities to enhance energy efficiency in the sector. Further, W&WW utilities can also become prosumers of electricity. However, there is a distinct lack of cross-sectoral decision-models and frameworks that can currently be used to explore the scale of these benefits (Wu et al. 2020). This thesis attempted to address this knowledge gap. Here, the W&WW system within the Thames basin was studied. The local utility within the region faces a number of energy-related challenges and opportunities. Specifically, this thesis presented the following analyses (Chapters 2–5):

This thesis started off by presenting an analysis of high-resolution electricity use data in the TWUL system. Here, it was demonstrated that water-related energy use in the network has been growing sharply at a rate of around 10.8% per year. This empirical study also quantified the energy-intensiveness of the TWUL system relative to cities across the world from

similarly developed OECD nations. This chapter provided novel data and statistics that was used throughout the thesis.

Chapter 3 introduced a novel software, InfraSim, which is implemented in an open-source framework and can capture water, wastewater, and energy interactions. InfraSim was used to model the W&WW network in the TWUL system, where we demonstrated the model reasonably captured the system characteristics. The software developed was the main contribution in this paper. It was argued that InfraSim is a significant step forward in the modelling literature since it can circumvent licensing and source-code issues that are all too common in alternative options.

In Chapter 4, InfraSim was used to investigate the potential for demand-side response in the TWUL system. We observed that up to 20.1% of TWUL's annual energy demand could be shifted to periods with relatively lower electricity prices, which could theoretically lower electricity costs by £5.6 million per annum. However, the demand flexibility was also observed to be highly variable and hence financial returns from DSR could be volatile.

Finally, Chapter 5 adopted a long-term planning perspective to study pathways to realising TWUL's energy sustainability targets to 2030. A multi-objective robust decision-making (MORDM) framework was presented to unravel the trade-offs between cost, water security, and energy sustainability, in the context of deeply uncertain futures in climate change, population growth, and electricity prices. This chapter demonstrated that achieving energy sustainability entails significant costs. However, balancing trade-offs can yield investment pathways that can minimise future water risks whilst managing overall electricity use using a combination of efficiency, self-generating via locally installed renewable energy, and purchasing green credits from the grid.

6.2 Conclusions

The work developed in this thesis can be surmised into a number of overarching conclusions:

(i) **Water-related energy is a significant cost that needs to be managed.** Chapters 2 and 5 both showed that water-related energy use is already rising sharply and this trend is on-track to continue. Left unchecked, this has the potential to significantly compromise the long-term affordability and sustainability of the sector. Yet, empirical regional-scale studies (e.g. Chapters 2) can help identify the most energy-intensive assets within a network, as well as the key trade-offs between maintaining future levels of services and energy sustainability. Such analyses can lead water managers to design effective and targeted energy management strategies. For example, it can lead to the identification of the most inefficient assets, which can be optimised, rehabilitated, or replaces with more modern processes (Wu et al. 2020).

(ii) **Tracking water-related energy use.** Temporal analysis revealed that water-related energy evolves dynamically in the system (Chapter 2). Therefore, it is recommended to track a water-related energy over time to understand the energy impacts of major infrastructure implementations (*e.g.* the Thames Tideway Tunnel), as well as the effectiveness of energy management schemes.

(iii) **Utilising energy data to develop optimisation programmes and models.** In this work, we utilised a high-quality energy dataset from TWUL to firstly understand their energy use, and to also develop water-energy nexus models. It is common for utilities to collect large amounts of energy-related data from process control systems software (*e.g.* SCADA systems), but these data often remain unanalysed. Yet, this data could have immense benefits for water utilities. As we demonstrated, not only can it be used to understand water-related energy patterns, but also facilitate system-level planners to better

capture cross-sector risks and opportunities. Moreover, with the advent of digitisation in the water sector, such data can be used for system-level energy optimisation programmes using data mining and machine learning (e.g. Cominola et al. 2019).

(iv) **The use of open-source modelling software in W&WW sector planning.** One of the main contributions of this paper was the presentation of an open-source infrastructure planning software, InfraSim (Chapter 3). In water resources planning and management, in both academic and practical contexts, a number of software are commonly used such as WATHNET (Kuczera 1992), WEAP (Yates et al. 2005), and IRAS Matrosov et al. 2013. Software licensing, fees, and a lack of source-code are a barrier to using such software, particularly now that open-sourcing data and models is becoming a common requirement. Open-source frameworks have numerous advantages such as: (1) increased research productivity, (2) more effective collaboration across science-policy boundary, and (3) rapid software improvements (Pfenninger et al. 2017). Despite a number of recent innovations within water (e.g. Dogan et al. 2018; Tomlinson et al. 2020), the W&WW field is lagging behind in the open-source movement. In that regard, the software framework presented in this thesis are a significant step forward.

(v) **The changing role of W&WW companies as energy prosumer.** This thesis demonstrated that W&WW utilities can: (1) map pathways to energy sustainability by means of self-generating electricity (Chapter 5) and (2) participate in energy market programmes such as demand side response (Chapter 3). At the scale of the W&WW sector, if these two schemes become widely adopted, a new paradigm for the W&WW could be established, in which the sector becomes a significant player in the energy market. These could yield energy-water co-benefits in that the energy sector could gain substantial flexibility in the system, as well as greater RES penetration at the grid level, whereas the W&WW utilities could substantially lower operational costs. Decision-makers and managers within the W&WW sector should encourage greater adoption of these schemes.

6.3 Practical recommendations

The methods and insights from this work have the potential to impact practical decision-making. Recently, water companies in England and Wales unveiled a plan to deliver a net zero water sector for customers by 2030 (Water UK 2020). The route map to net zero outlines that companies will need to balance renewable self-generation with demand-side solutions. Despite the clear-cut interest in ensuring reliable water provisions whilst managing water-related energy use, there is a significant lack of methodologies that allow decision-makers to evaluate energy-water trade-offs under uncertainty. The methodological insights in this thesis could be valuable for such purposes.

Meanwhile, in the energy policy landscape, the UK Climate Change Committee's sixth carbon budget and the UK energy white paper both outlined the key steps to achieving net zero with specific details related to the energy sector (BEIS 2020; Climate Change Committee 2020). Yet, despite the rapid changes in the water sector's energy dimension, both of these policy documents made rare mention to the water and wastewater industries, and their role in the net zero transition. Such omissions may lead to both missed opportunities and undue propagation of burdens through inefficient policies (Kenway et al. 2019). Continuing to understand the energy-influence of the water sector and identify water-energy synergies could aid in circumventing this.

6.4 Directions for future work

The research presented within this thesis forms a subset of a growing global literature set seeking to understand the energy-influence of W&WW systems, as well as the interactions between energy-water systems. Due to the myriad interactions between energy and water systems in natural and social systems, there will be many subfields emerging within this topic.

Yet, from the perspective of topics addressed in this thesis, there are a number of potential future avenues for research such as:

(i) **Further exploration of DSR and RES using operational models.** It is important to recognise that much of the modelling work conducted in this thesis was based on simplified representations of W&WW systems in the Thames basin. In order to fully understand the scale of the opportunities presented above, further research is required at greater spatial and temporal scale. For instance, the potential for DSR needs to be tested in water distribution models (such as EPANET (Environmental Protection Agency 2014)), where the hydraulics of the water system can be fully incorporated.

(ii) **Understanding water-related energy use at the demand-side.** Throughout this thesis, we only considered W&WW related energy use from the supply-side. Yet, emerging research from regions such as California and Australia is showing demand-side energy use for water-related provisions are substantially higher (e.g. Escriva-Bou et al. 2018a; Escriva-Bou et al. 2018b; Renouf et al. 2018; Spang et al. 2018). Hence, future research can explore the energy-related benefits of planned demand-side management techniques. For example, TWUL are set to expand smart metering, low-flow shower heads, modernisation of toilet cisterns, among other demand-side solutions with the overall objective to reduce water demands (Thames Water 2019). The energy savings from such measures remain unknown. The model of the TWUL system developed in Chapter 3 is capable of exploring this.

(iii) **Improved integration of water and wastewater systems.** This thesis considered the interactions between water and wastewater networks in a highly simplified manner. These systems are usually managed and planned seperately despite being operationally connected. Integrated water and wastewater systems modelling are now under development. For example, Dobson et al. (2020) introduced a combined water-wastewater modelling framework for the TWUL system, where they demonstrated that holistic planning approaches may improve our understanding of the effects of wastewater effluents on wa-

ter quality, which could theoretically save up to £1 billion in mitigation costs. Yet, this study neglected the energy-influence of the water and wastewater cycle. It is critical to close the energy gap in such works since even small changes in wastewater treatment standards can lead to exponential increases in energy requirements (e.g. Baleta et al. 2012; Cardenes et al. 2020).

(iv) **Incorporation of battery storage into pumped water storage systems with RES capacity.** As demonstrated in this research, the role of the W&WW sector in the energy sector could change as utilities begin to self-generate their energy demands and participate in demand response programmes. We demonstrated that pumped water storage systems within W&WW networks can be utilised to store potential energy—a mechanism that resembles pumped hydro storage. Yet, we did not study the potential to integrate battery storage in this system. A technoeconomic analysis of a pumped water storage system with RES capacity and battery storage remains to be seen, particularly in the context of energy self-generation targets.

In summary, our understanding of water and energy interactions are still in their infancy. Even at this early-stage, however, the need to develop improved cross-sector decision-tools at a regional scale has emerged has an essential requirement. Zooming into local areas to understand the relationships between water and energy will be critical to form effective management strategies. Such analyses will be fundamental in ensuring the resilience and sustainability of our water services.

References

Baleta, H., & Mcdonnell, R. (2012). Water quality standards or carbon reduction: Is there a balance? *Area*. https://doi.org/10.1111/j.1475-4762.2011.01066.x

BEIS. (2020). *Energy White Paper - Powering our Net Zero Future* (tech. rep. December). http://www.ret.gov.au/energy/facts/white_paper/Pages/energy_white_paper.aspx

Cardenes, I., Hall, J. W., Eyre, N., Majid, A., & Jarvis, S. (2020). Quantifying the energy consumption and greenhouse gas emissions of changing wastewater quality standards. *Water Science and Technology*, *2*, 1–10. https://doi.org/10.2166/wst.2020.228

Climate Change Committee. (2020). *The Sixth Carbon Budget: The UK's path to Net Zero* (tech. rep. December). https://www.theccc.org.uk/publication/sixth-carbon-budget/

Cominola, A., Nguyen, K., Giuliani, M., Stewart, R. A., Maier, H. R., & Castelletti, A. (2019). Data Mining to Uncover Heterogeneous Water Use Behaviors From Smart Meter Data. *Water Resources Research*. https://doi.org/10.1029/2019WR024897

Dobson, B., & Mijic, A. (2020). Protecting rivers by integrating supply-wastewater infrastructure planning and coordinating operational decisions. *Environmental Research Letters*. https://doi.org/10.1088/1748-9326/abb050

Dogan, M. S., Fefer, M. A., Herman, J. D., Hart, Q. J., Merz, J. R., Medellín-Azuara, J., & Lund, J. R. (2018). An open-source Python implementation of California's hydroeconomic optimization model. *Environmental Modelling and Software*, *108*(June), 8–13. https://doi.org/10.1016/j.envsoft.2018.07.002

Environmental Protection Agency. (2014). EPANET.

Escriva-Bou, A., Lund, J. R., Pulido-Velazquez, M., Hui, R., & Medellín-Azuara, J. (2018a). Developing a water-energy-GHG emissions modeling framework: Insights from an application to California's water system. *Environmental Modelling and Software*, *109*(June 2017), 54–65. https://doi.org/10.1016/j.envsoft.2018.07.011

Escriva-Bou, A., Lund, J. R., & Pulido-Velazquez, M. (2018b). Saving Energy From Urban Water Demand Management. *Water Resources Research*, *54*(7), 4265–4276. https://doi.org/10.1029/2017WR021448

Kenway, S. J., Lam, K. L., Stokes-draut, J., Twomey, K., Binks, A. N., Bors, J., Head, B., Olsson, G., & Mcmahon, J. E. (2019). Defining water-related energy for global comparison , clearer communication , and sharper policy. *Journal of Cleaner Production*, *236*, 117502. https://doi.org/10.1016/j.jclepro.2019.06.333

Kuczera, G. (1992). Water supply headworks simulation using network linear programming. *Advances in Engineering Software*. https://doi.org/10.1016/0965-9978(92)90084-S

Lam, K. L., Lant, P. A., & Kenway, S. J. (2018). Energy implications of the millennium drought on urban water cycles in Southeast Australian cities. *Water Science and Technology: Water Supply*, *18*(1), 214–221. https://doi.org/10.2166/ws.2017.110

Lam, K. L., Kenway, S. J., & Lant, P. A. (2017). Energy use for water provision in cities. *Journal of Cleaner Production*, *143*, 699–709. https://doi.org/10.1016/j.jclepro.2016.12.056

Matrosov, E. S., Padula, S., & Harou, J. J. (2013). Selecting Portfolios of Water Supply and Demand Management Strategies Under Uncertainty-Contrasting Economic Optimisation and 'Robust Decision Making' Approaches. *Water Resources Management*, *27*(4), 1123–1148. https://doi.org/10.1007/s11269-012-0118-x

Pfenninger, S., DeCarolis, J., Hirth, L., Quoilin, S., & Staffell, I. (2017). The importance of open data and software: Is energy research lagging behind? *Energy Policy*, *101*(October 2016), 211–215. https://doi.org/10.1016/j.enpol.2016.11.046

Renouf, M. A., Kenway, S. J., Lam, K. L., Weber, T., Roux, E., Serrao-Neumann, S., Choy, D. L., & Morgan, E. A. (2018). Understanding urban water performance at the city-region

scale using an urban water metabolism evaluation framework. *Water Research*. https://doi.org/10.1016/j.watres.2018.01.070

Spang, E. S., Holguin, A. J., & Loge, F. J. (2018). The estimated impact of California's urban water conservation mandate on electricity consumption and greenhouse gas emissions. *Environmental Research Letters*, *13*(1). https://doi.org/10.1088/1748-9326/aa9b89

Thames Water. (2019). Facts and figures. https://corporate.thameswater.co.uk/media/Facts-and-figures

Tomlinson, J. E., Arnott, J. H., & Harou, J. J. (2020). A water resource simulator in Python. *Environmental Modelling and Software*. https://doi.org/10.1016/j.envsoft.2020.104635

Water UK. (2020). *Net Zero 2030 Routemap* (tech. rep.). https://www.water.org.uk/routemap2030/wp-content/uploads/2020/11/Water-UK-Net-Zero-2030-Routemap.pdf

Wu, W., Maier, H. R., Dandy, G. C., Arora, M., & Castelletti, A. (2020). The changing nature of the water–energy nexus in urban water supply systems: a critical review of changes and responses. *Journal of Water and Climate Change*, 1–28. https://doi.org/10.2166/wcc.2020.276

Yates, D., Sieber, J., Purkey, D., & Huber-Lee, A. (2005). WEAP21 - A demand-, priority-, and preference-driven water planning model. Part 1: Model characteristics. *Water International*. https://doi.org/10.1080/02508060508691893

Appendix A

Additional materials for Chapter 2

A.1 Cost-benefit analysis of leakage reduction

In this section, the methodology used in the calculations for Figure 2.7 is discussed. Data on the capital cost (£) required per megalitre reduction in leakages were produced by TWUL (Hall et al. 2019). The benefit in operational expenditure b per unit reduction in leakage was calculated as:

$$b = \mathcal{L} \cdot \bar{\epsilon} \cdot c \tag{A.1}$$

where $\mathcal{L}$ is the leakage reduction (ML d^{-1}), $\bar{\epsilon}$ is the mean energy-intensity across the Thames network (kWh m^{-3}), and c is the cost of electricity (£ kWh^{-1}) for TWUL. The $\bar{\epsilon}$ value was calculated in our analysis as 0.65 kWh m^{-3}. The value of c could be calculated based on reports from TWUL, which state that 160.6 GWh of electricity consumption is equivalent to £30 million in operational expenditures to the utility (Thames Water 2019).

Appendix B

Additional materials for Chapter 5

B.1 weather@home scenarios

Figure B.1 shows the flow-duration curves generated from the baseline and near-future scenarios from the weather@home2 platform for the Thames basin. These curves demonstrate that near-future climate conditions yield lower flows in comparison to the baseline climate sequences. This is expected as future scenarios with greater warming (high-emissions) are expected to yield more severe drought sequences across the Thames basin.

B.2 Water demands

Three scenarios for water demands were assumed in the modelling process. These assume a growth of 0.25%, 0.50%, and 0.75% per annum. The growth rates were computed based on TWUL's internal future socioeconomic and population modelling. The growth rates were applied to the intra-annual demand curve shown by Figure B.2.

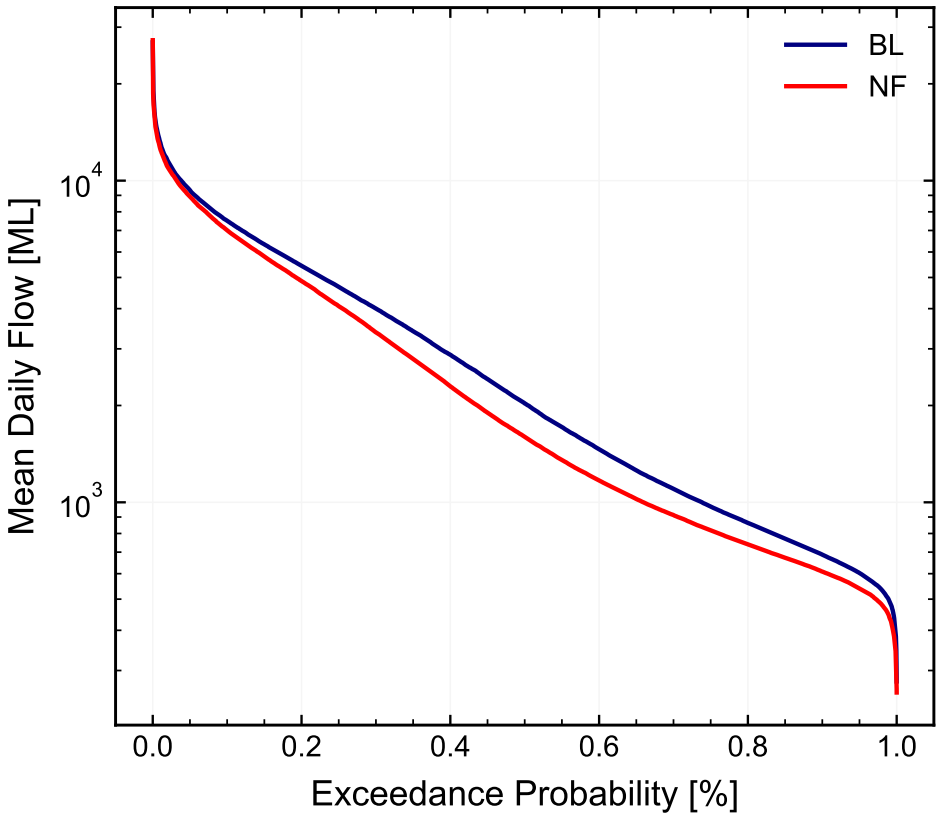


Figure B.1: Flow duration curves from the baseline and near-future scenarios.

B.3 Simulation model setup

B.3.1 Network linear programme

The system simulation model uses network linear programming (NLP), which is a commonly used technique in water resources planning studies (Wurbs 1993). A directed graph G defines the system as a set of nodes $n \in \mathcal{N}$ and arcs $a \in \mathcal{A}$. Nodes represent supply, demand, or transfer points in the network, whereas arcs define pipes or channels that transfer a commodity between points. The NLP finds the minimum cost solution for conveying a commodity through a network of unidirectional arcs connecting supply, demand and junction nodes.

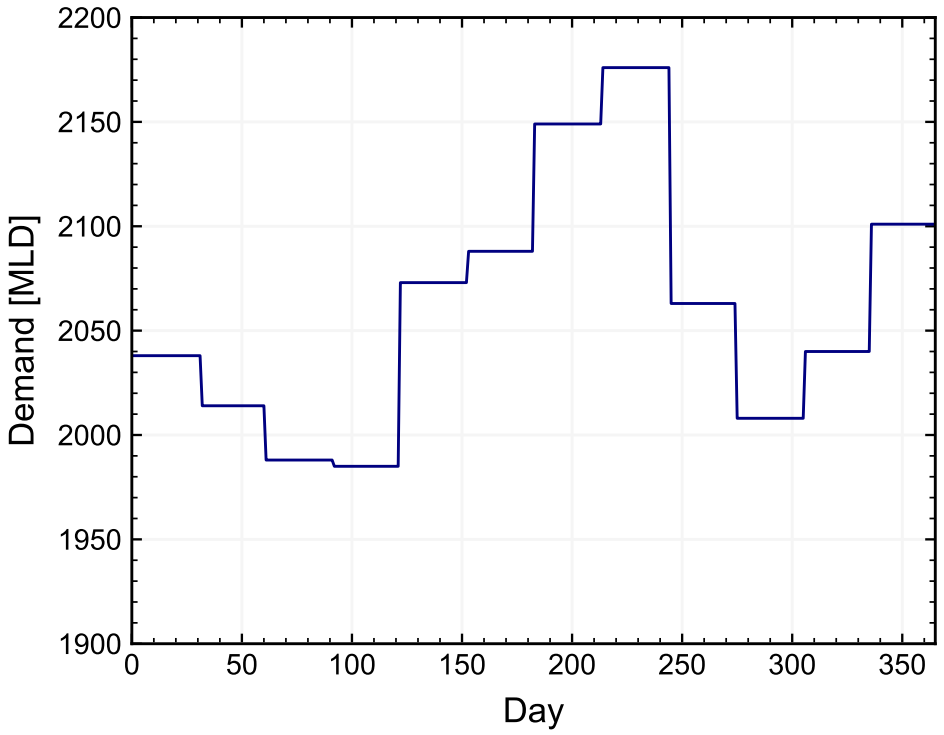


Figure B.2: Intra-annual demand curve (Thames Water 2014).

$$\min c^T q \tag{B.1}$$

subject to:

$$Aq = b \tag{B.2}$$

$$0 \leq q \leq u \tag{B.3}$$

where c is an vector of costs or penalties, q is an vector of flow volumes in the arcs, b is an m-vector of known nodal inflow or outflow volumes (or requirements), u is a known upper bound on q, and A is an (m,n) node-incidence matrix that ensures that a mass balance

is achieved at every node in the network. The NLP is implemented within the WATHNET software (Kuczera 1992).

B.3.2 WATHNET Model

The model of the Thames water supply system is implemented in the WATHNET software using a generalised arc-node setup (Section B.3.1). The formulation adopts a 'lumped graph' methodology to represent the water supply network. Through this process, operations across the process chain are aggregated by water resource zones as shown by Figure B.3. For example, all groundwater abstractions in a particular water resource service zone are aggregated into one node. Similarly, one reservoir node represents all of the water storages within a given service area.

The model of the TWUL system (TWmod) is constructed within the WATHNET software, a generalised arc-node simulation model that is used widely for water resources planning and management under uncertainty (Kuczera 1992). The model deploys linear programming, which finds the minimum cost solution for conveying commodities through a network of uni-directional arcs. The WATHNET model of the Thames system was developed in conjunction with the local water utility. It comprises TWUL's operational configurations the model has been calibrated and validated against the company's own models.

The model incorporates numerous operational and environmental constraints in line with guidance from the local water utility, regulator, and environmental agency. These include limits on water abstraction licenses and reservoir control strategies. TWmod was developed to function at daily temporal resolution as this best captured critical operational rules within the TWUL system.

In order to estimate water-related energy consumption, each edge carrying water be-

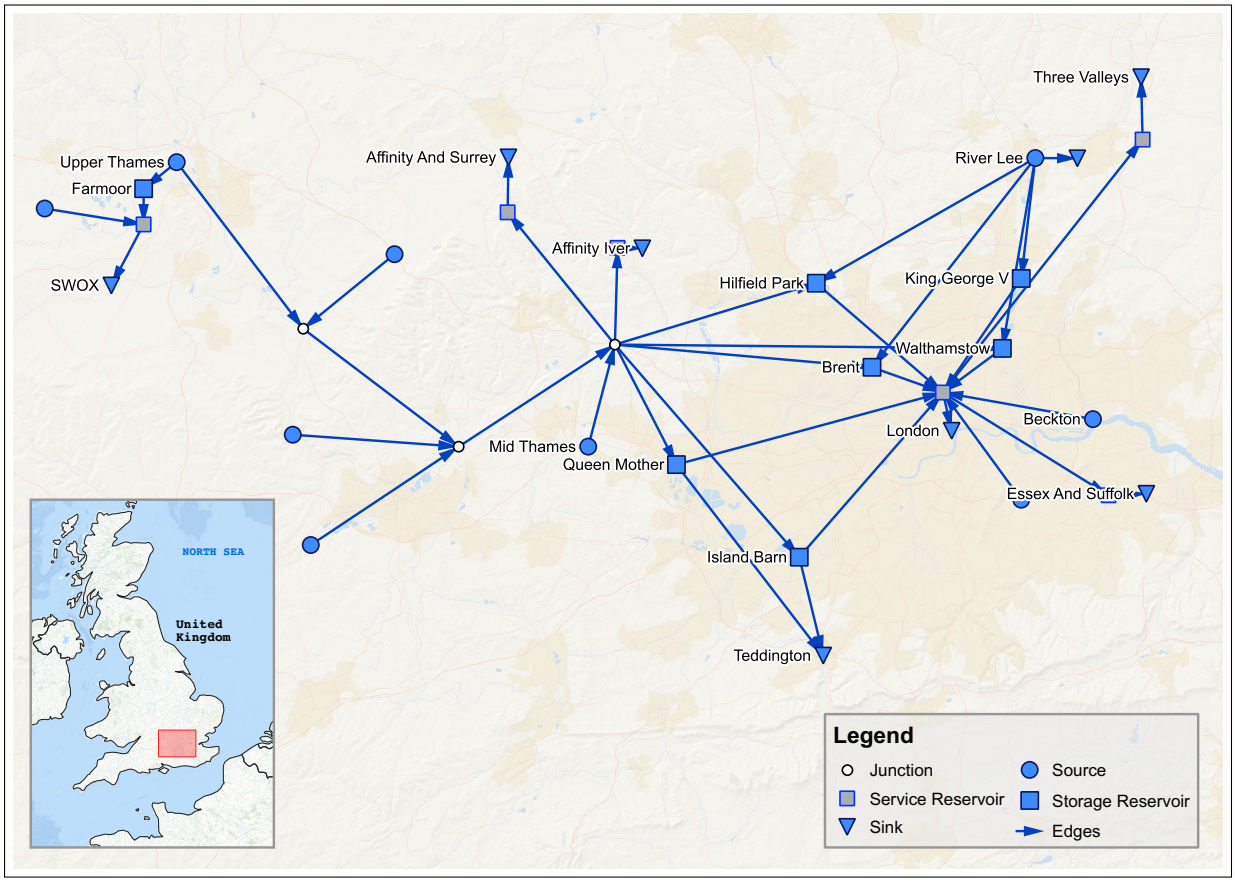


Figure B.3: Schematic of the TWUL model (TWmod) as modelled within the WATHNET. The black boundaries show the spatial domain of TWUL's water resource zones. TWmod aggregates operations within the TWUL system by water resource zones.

tween nodes was assigned an energy-intensity e_i value in kilowatt hours per megalitre of flow (kWh/ML). This includes both existing arcs and the arcs associated with potential infrastructure supply expansions. The electricity consumption could then be computed as the product of the flow through the arc and the energy intensity. The value for e_i represents the electricity requirements to abstract, pump, and treat per unit of water supplied.

One of the water supply options considered in the planning case-study is an indirect effluent reuse scheme in which treated wastewater could be pumped into storage reservoirs during periods of drought (option 4). The assumed e_i for such a reuse scheme can normally be as high as 1500 kWh/ML given that part of the throughput of a wastewater treatment facility is further

processed to be reused. However, since our simulation model does not incorporate TWUL's wastewater treatment process, we only use the e_i for the additional treatment needed after secondary treatment (without removal of nitrogen and phosphorus removal). Hence, the assumed e_i for indirect effluent reuse (as shown by Table B.1) is lower than has previously been reported.

Finally, since the age of a water supply network is one of the most important factors in its energy requirements (Coelho et al. 2014), e_i was also assumed to increase at a rate of 0.1% per year based on empirical data (Gay et al. 2012). The assumed e_i values are given by Table B.1.

Table B.1: An overview of the energy-intensity values used to model the energy requirements of different arcs in the system.

Operation	Energy-intensity (kWh/ML)	Data source
Abstraction		
Ground water pumping	300	(Plappally et al. 2012)
Treatment		
Conventional treatment	500	(Majid et al. 2020)
Indirect potable reuse	1140	(Sim et al. 2021)
Brackish water desalination	2450	(Plappally et al. 2012)
Seawater desalination	3400	(Plappally et al. 2012)
Network		
Distributional pumping (per km)	5	(Plappally et al. 2012)

B.3.3 Renewable energy modelling

Energy self-generation within the TWUL system was computed as the function of outputs from solar, wind, and biogas assets within their network (Equation 5.1). Output from solar assets was computed as a function of the net short-wave radiation from the synthetic weather data, as well as the assumed characteristic of solar panel arrays, such that:

$$E_{PV} = ArH\eta \tag{B.4}$$

where A is the total solar panel area (m^2), r is the solar panel efficiency (assumed as 15%), H is the net short-wave radiation for the day (W/m^2 per day), and η is the weather corrected performance coefficient for losses (assumed as 84% (Dierauf et al. 2013)).

Electricity output from wind turbines vary significantly based on the design characteristics of the turbine selected. The standard design procedure to estimate the electrical energy output (kWh) from a given wind turbine is to use a power curve supplied by the manufacturer. In this work, we assume only one type of turbine can be selected in the planning process: The Vestas V120-2.2 MW turbine^{TM}. This specific turbine was selected as its specifications closely match those currently used by TWUL; for example, at the Crossness Treatment Plant. Based on the average wind speed from the weather@home2 scenario, we estimate the daily electricity production using the supplied power curve for the turbine (see (Vestas 2020)). As observed, the wind energy output is a function of the daily mean wind speed and influenced by the cut-in and cut-out speeds of the turbine.

The electricity generation from biogas plants within the TWUL network were computed as fixed function of their rated capacity. Since we do not model the wastewater cycle of TWUL's operations in this paper, we do not capture the variability within biogas generation owing to seasonal and random variability within wastewater resources. This represents a significant limitation within the modelling process.

B.4 Decision module setup

B.4.1 Objectives

A multi-objective optimisation problem with two objectives was formulated. The first objective was to minimise the total capital and operational expenditure associated with each option across all future states of the world (scenarios). This was defined as:

$$\min f_1 = \frac{\sum_{n=1}^{N} \sum_{t=1}^{T} \frac{C_t}{(1+r)^t} + R_t}{N} \tag{B.5}$$

where t represents the specific year of the simulation and T is the total number of years across which the simulation is taking place. N refers to the total number of scenarios being considered in the simulation. Whereas r is the discount rate defined as 4.5% in this study. The term R_t is the costs associated with electricity use computed as the product of net energy use and the electricity price at each time step. Though there are additional operational expenditures associated with water supply (*e.g.* asset maintenance costs), the dominant portion of operational expenditures in TWUL's system are for electricity, and so we ignore all other factors.

The second objective was to minimise the total economic costs associated with imposing restrictions on water uses. Figure B.4 shows the Lower Thames reservoir control curve, which expresses the relationship between water storage volumes and restrictions L of severity $i \in \{1, 2, 3, 4\}$ in the water supply system. Reservoir levels decrease during periods of lower river flows and droughts and hence restrictions on water use may need to be imposed. The simulation model evaluates the control curve shown to calculate the number of restrictions implemented throughout the simulation period, as well as the economic costs associated with

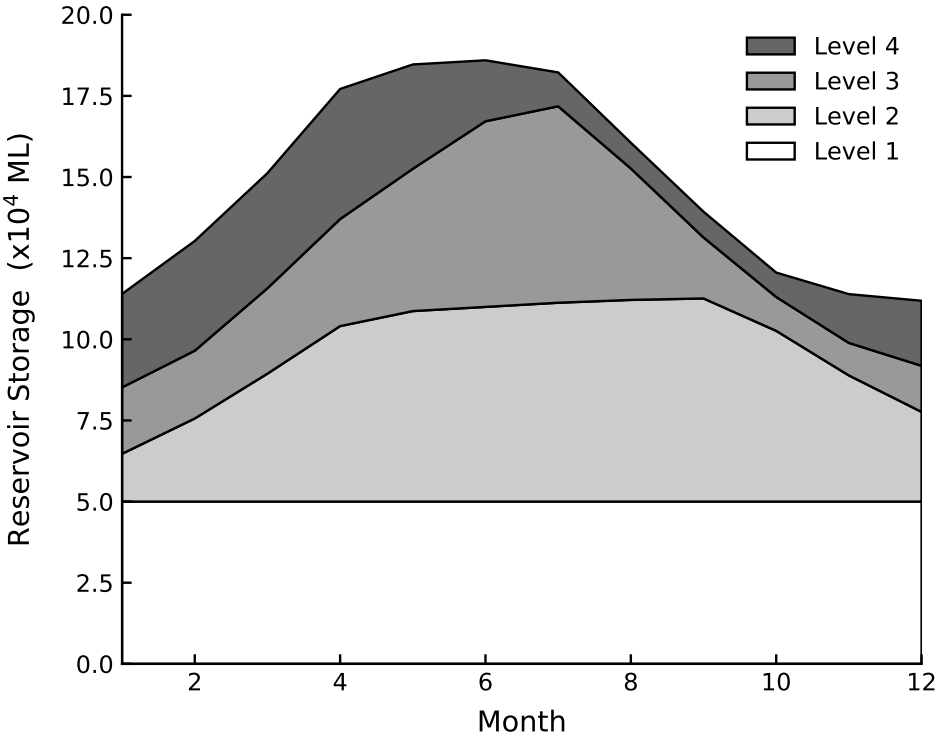


Figure B.4: Lower Thames reservoir storage control curve (Thames Water 2014).

this. Details of water restrictions in terms of their consequences, expected frequency, and the planned response are shown by Table B.2. Following Borgomeo et al. (2018), we computed f_2 as a function of L_3 and L_4 such that:

$$\min f_2 = \frac{\sum_{n=1}^{N} \sum_{t=1}^{T} \sum_{i=3,4}^{i} \epsilon[C_i]_t}{N} \tag{B.6}$$

where $\epsilon[C_i]$ is the expected annual economic cost of water use restrictions of severity i imposed in year t. This function is a proxy risk metric, in that the risk of imposing costly restrictions on water usage are being minimised.

Table B.2: Costs, measures, expected frequency, and demand reduction associated with levels of water use restrictions of severity 1–4 (Borgomeo et al. 2018).

Restriction severity	Measures for customers	Expected frequency (year)	Expected demand reduction (%)	Expected daily economic losses (million GBP)
Level 1	Media campaign about drought	1 in 5	2.2	Not available
Level 2	Partial hosepipe ban	1 in 10	9.1	Not available
Level 3	Full sprinkler hosepipe ban	1 in 20	13.3	6.2
Level 4	Ban on all usage	"Never"	31.3	282

B.4.2 ϵ–MOEA Setup

A dual objective ϵ-dominance multi-objective optimisation (ϵ–MOEA) was used to derive the Pareto frontiers. We conducted six experiments in this work that considered the three energy strategies outlined in Table 5.2 across the baseline (BL) and near-future (NF) climate scenarios (5.2). As such, six separate optimisations were conducted for each experiment.

The optimisation was ran with the following parameters: (1) probability of crossover $= 1.0$, (2) probability of mutation $= 0.005$, (3) probability of inversion $= 0.005$, (4) probability of diagonal swap $= 0.2$, (5) tournament size $= 3$, (6) initial population size $= 180$. These parameters were used following a number of previous studies on efficient ϵ–MOEA model design (e.g. Mortazavi et al. 2012; Mortazavi-Naeini et al. 2014; Mortazavi-Naeini et al. 2015). The minimum and maximum number of generations were set to 10,000 and 200,000 respectively. The optimisation was terminated if the model reached the maximum number of iterations or if no changes were observed in the Pareto frontier for 500 iterations.

In order to ensure the convergence of the ϵ–MOEA and to filter the uncertainty in the initial operators used by the algorithm, we conducted five repetitions of the optimisation with varying seed numbers for each of the six experiments. Therefore, a total of 30 optimisations

Table B.3: Assigned parameters in the ϵ-multi-objective optimisation algorithm.

Parameter	Value
$\epsilon(f_1)$	0.1
$\epsilon(f_2)$	0.01
Minimum generations	10,000
Maximum generations	200,000
Initial population	180
Tournament size	3
Probability of crossover	1.0
Probability of mutation	0.005
Probability of inversion	0.005
Probability of diagonal swap	0.2

were conducted. Each of the 30 runs terminated at around 20,000 generations and hence prior to reaching the maximum number of iterations, thus indicating that the maximum number of iterations set was sufficient. For each experiment, the results from the five repetitions were combined to generate a single non-dominated Pareto frontier (duplicates solutions dropped) as presented within the main body of this paper.

The ϵ–MOEA was carried out on the University of Oxford's Advanced Research Computing (ARC) high-performance computing suite. Each optimisation run was conducted using 10 CPU based computing nodes, each with 16 cores, for a maximum run-time of 24 hours.

B.5 Results

B.5.1 Computing true Pareto frontier

The non-dominated solution sets were derived by combining the results from five optimisation repetitions for each of the six experiments. This process provides the *approximate* Pareto frontier as shown by the blue markers in Figure B.5. In order to estimate the *true* Pareto frontier for each of the six experiments (Deb 2011), a power law curve was fitted on

Table B.4: Overview of the experiments conducted in the study. An optimisation was ran for each experiment to generate a unique Pareto frontier for each case.

Experiment	Total solutions	Non-dominated solutions
BL-IMP	16,276	27
BL-PRO	26,575	19
BL-BAL	16,878	24
NF-IMP	18,152	30
NF-PRO	29,620	27
NF-BAL	15,997	21

the non-dominated Pareto optimal solution set. In each case, fitted curve demonstrated a high coefficient of determination ($R^2 \geq 0.95$) indicating a good-fit. The curves shown by Figure 5.4 are the *true* Pareto frontiers as estimated by the fitted power law curves.

B.5.2 Non-dominated solution sets

The complete non-dominated solution set for each of the six experiments are shown by Figure B.5. These were generated from the five repetitions of the six experiments. Table B.4 provides a breakdown of the total number of solutions in each set. The blue markers in Figure B.5 are the non-dominated solutions that were generated by combining the Pareto optimal solutions from each repetition. The total number of non-dominated solutions for each of the six experiments are also given by Table B.4.

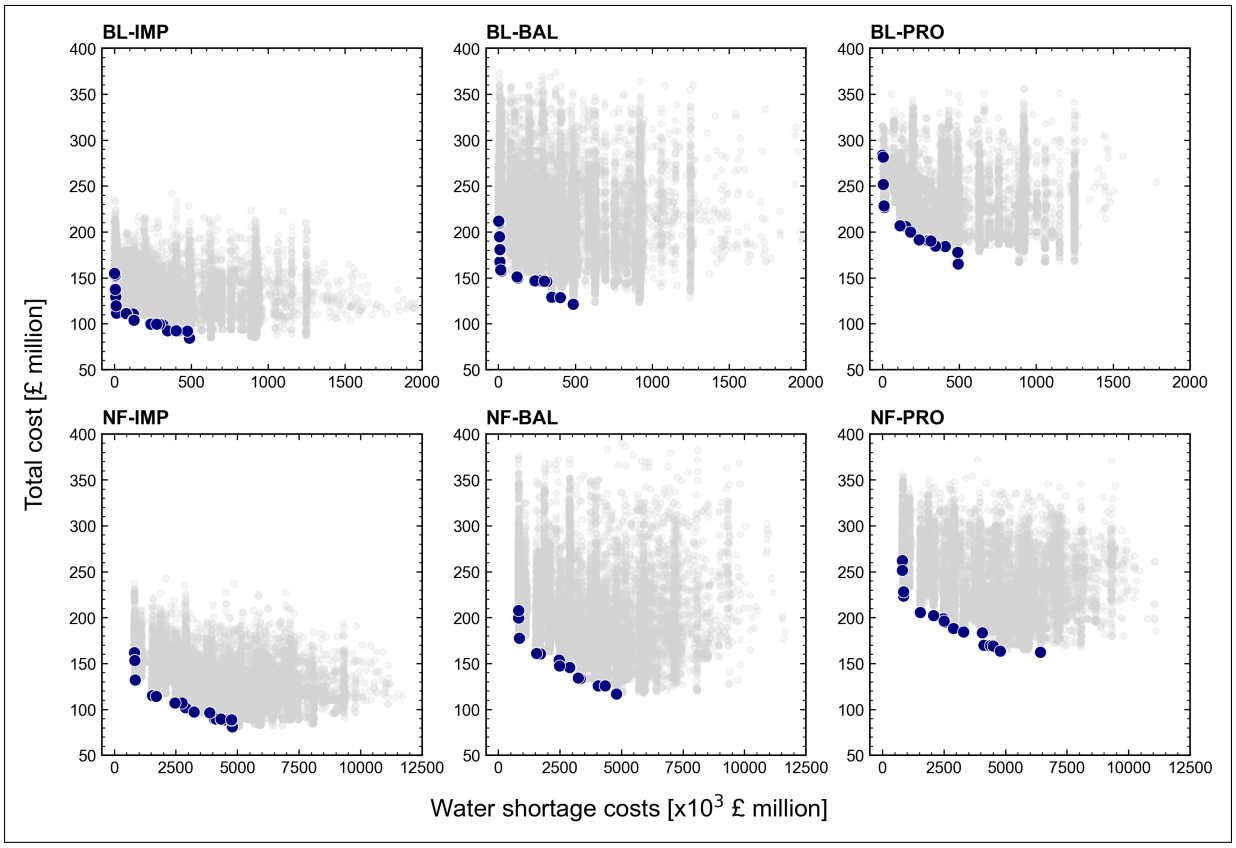


Figure B.5: Non-dominated Pareto optimal solutions (blue) along with the complete dominated solution set (grey) for all six experiments: BL-IMP, BL-BAL, BL-PRO, NF-IMP, NF-BAL, and NF-PRO.

References

Borgomeo, E., Mortazavi-Naeini, M., Hall, J. W., & Guillod, B. P. (2018). Risk, Robustness and Water Resources Planning Under Uncertainty. *Earth's Future*, *6*(3), 468–487. https://doi.org/10.1002/2017EF000730

Coelho, B., & Andrade-Campos, A. (2014). Efficiency achievement in water supply systems - A review. *Renewable and Sustainable Energy Reviews*, *30*, 59–84. https://doi.org/10.1016/j.rser.2013.09.010

Deb, K. (2011). Multi-objective Optimisation Using Evolutionary Algorithms: An Introduction, In *Multi-objective evolutionary optimisation for product design and manufacturing*. https://doi.org/10.1007/978-0-85729-652-8{_}1

Dierauf, T., Growitz, A., Kurtz, S., & Hansen, C. (2013). *Weather-Corrected Performance Ratio* (tech. rep. April).

Gay, L. F., & Sinha, S. K. (2012). Measuring Energy Efficiency in Urban Water Systems Using a Mechanistic Approach. *Journal of Infrastructure Systems*, *18*(2), 139–145. https://doi.org/10.1061/(ASCE)IS.1943-555X.0000072

Hall, J. W., Mortazavi-naeini, M., Borgomeo, E., Baker, B., Gavin, H., Gough, M., Harou, J. J., Hunt, D., Lambert, C., Piper, B., Richardson, N., & Watts, G. (2019). Risk-based water resources planning in practice : a blueprint for the water industry in England, *0*, 1–14. https://doi.org/10.1111/wej.12479

Kuczera, G. (1992). Water supply headworks simulation using network linear programming. *Advances in Engineering Software*. https://doi.org/10.1016/0965-9978(92)90084-S

Majid, A., Cardenes, I., Zorn, C., Russell, T., Colquhoun, K., Bañares-Alcantara, R., & Hall, J. W. (2020). An Analysis of Electricity Consumption Patterns in the Water and Wastewater Sectors in South East England, UK. *Water*, *12*(1), 225. https://doi.org/10.3390/w12010225

Mortazavi, M., Kuczera, G., & Cui, L. (2012). Multiobjective optimization of urban water resources: Moving toward more practical solutions. *Water Resources Research*, *48*(3). https://doi.org/10.1029/2011WR010866

Mortazavi-Naeini, M., Kuczera, G., & Cui, L. (2014). Application of multiobjective optimization to scheduling capacity expansion of urban water resource systems. *Water Resources Research*, *50*(6), 4624–4642. https://doi.org/10.1002/2013WR014569

Mortazavi-Naeini, M., Kuczera, G., & Cui, L. (2015). Efficient multi-objective optimization methods for computationally intensive urban water resources models. *Journal of Hydroinformatics*, *17*(1), 36–55. https://doi.org/10.2166/hydro.2014.204

Plappally, A. K., & Lienhard, J. H. V. (2012). Energy requirements for water production, treatment, end use, reclamation ,and disposal. *Renewable and Sustainable Energy Reviews*, *16*(7), 4818–4848. https://doi.org/10.1016/j.rser.2012.05.022

Sim, A., & Mauter, M. S. (2021). Environmental Science reuse systems †, 748–761. https://doi.org/10.1039/d1ew00017a

Thames Water. (2019). Facts and figures. https://corporate.thameswater.co.uk/media/Facts-and-figures

Thames Water. (2014). *Water Resources Management Plan 2014 (WRMP 14)* (tech. rep. June). Reading.

Vestas. (2020). V120-2.2 MW2122 at a glance. https://www.vestas.com/en/products/2%20mw%20platform/v120%2022_mw

Wurbs, R. A. (1993). Reservoir-system simulation and optimization models. *Journal of Water Resources Planning and Management*, *119*(4), 455–472.

Glossary

Capital cost Fixed initial costs incurred in financing an infrastructure project to purchase land, buildings, construction, and equipment. xii, 30

Constraint-based linked model A central sector model that introduces parameters or constraints related to another sector. 41, 42

Demand-side response A short-term change in a user's normal electricity use in response to a market signal in order to better match demand with available supplies. xv, 6, 68, 69, 74, 90–92, 94, 98, 100, 101

Flexibility The ability to temporally shift energy generation or consumption patterns in response to a market signal. ix, xiii, 68, 71, 73–75, 80, 86, 87, 90, 91, 93–99, 144

Hard-linked model A model of two or more sectors where mathematical expressions are shared and usually formulated within the same software or code. 41–44

InfraSim An open-source software used to model interconnected water, wastewater, and electricity networks. xii, 5, 6, 38, 40, 46, 50–54, 59, 61, 144, 146

InfraSim.Thames A water, wastewater, and energy model of the Thames Water Utilities Ltd. (TWUL) system using the InfraSim software.. xii, xiii, 38, 43, 47, 48, 51, 53–56, 58, 59, 61

Integrated models Models that capture interactions between two or more sectors (*e.g.* energy-water models). Also referred to as *linked* models. 2

Operational cost On-going expenses associated with the operation of infrastructure equipment and facilities. 31, 32

Pareto frontier A set of Pareto efficient solutions. x, 122–124, 163–165

Pareto optimal A solution where none of the objectives can be improved without degrading the performance of another. xiv, 122, 125, 126, 165, 166

Prosumer A combined producer and consumer of a commodity (*e.g.* electricity). 143, 146

Simulation model A parameterised dynamic computer model of a real-world infrastructure network. 5

Soft-linked model A model of two or more sectors where mathematical expressions are shared and usually formulated within the same software or code. 41, 42

Systems-of-systems Large-scale distributed infrastructure systems the components of which are complex systems themselves. 2, 5

Water resource zone The largest area of a water company's supply system where all customers have the same supply risk. xvi, 20, 21, 32

Water-related energy Electricity use associated with processes in the water and wastewater sectors. 2, 3, 5, 13, 14